



MASTERARBEIT

Titel der Masterarbeit

„Synthesis of mono- and disaccharide ligands related to the secondary cell wall polymer of *Paenibacillus alvei* containing pyruvate-substituted β -D-mannosamine residues“

verfasst von

Gudrun Martinz BSc

angestrebter akademischer Grad

Master of Science (MSc)

Wien, Jänner 2015

Studienkennzahl lt. Studienblatt: A 066 862

Studienrichtung lt. Studienblatt: Masterstudium Chemie

Betreut von: Ass.-Prof. Dipl.-Chem. Dr. Lothar Brecker, Privatdoz.



MASTER THESIS

Title of the Thesis

„Synthesis of mono- and disaccharide ligands related to the secondary cell wall polymer of *Paenibacillus alvei* containing pyruvate-substituted β -D-mannosamine residues“

written by

Gudrun Martinz BSc

Submitted in partial fulfilment of the requirements for the degree

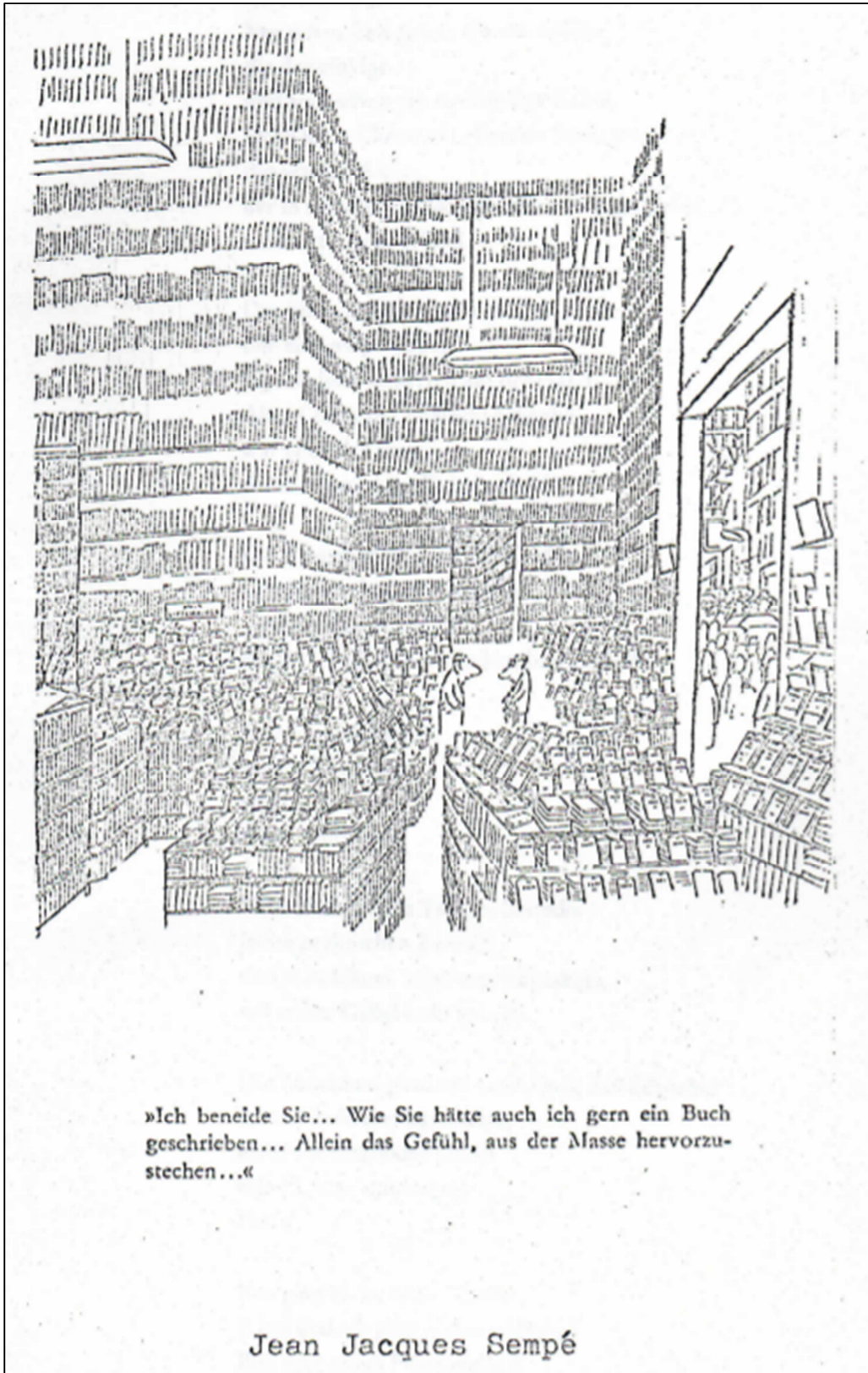
Master of Science (MSc)

Vienna, January 2015

Studienkennzahl lt. Studienblatt: A 066 862

Supervisor (formal): Ass.-Prof. Dipl.-Chem. Dr. Lothar Brecker, Privatdoz.

Supervisor (external): Univ.Prof. Dipl.-Ing. Dr.techn. Paul Kosma



In liebevoller Erinnerung an meinen Papa

Dr. Hans-Peter Martinz

Acknowledgements

First of all I would like to thank Prof. Paul Kosma for giving me the opportunity to work on this interesting topic in his group. I really appreciate his constant support, his ongoing motivation and helpful ideas during this thesis.

I also thank Prof. Lothar Brecker for being my formal supervisor and his kind support concerning the STD-NMR experiments.

A big thank you goes to Dr.rer.nat. Jean-Baptiste Farcet, Prof. Andreas Hofinger and Dipl.-Ing. Barbara Pokorny for recording my NMR and mass spectra and for their scientific advices whenever I needed some.

Furthermore I would like to thank Arturo López-Guzmán, MSc. from the Department of Nanobiotechnology for constructive cooperation and the performance of the ITC measurements. Moreover I have to thank Ryan J. Blackler from the group of Stephen V. Evans at the University of Victoria in Canada for executing the cocrystallization experiments.

I'm very thankful for helpful suggestions and the comfortable and friendly working atmosphere provided by all the employees in the organic chemistry department. In particular, I want to thank Dipl.-Ing. Angelika Derler, Ernst Maybachl, MSc. and Alessio Borio, MSc. for constructive conversations and interpretations as well as Maria Hobel for her technical support.

A special thanks goes to my friends for their support and presence over years. I'm deeply grateful to Max for helping me to keep the balance between work and relaxation and to Nicole for encouraging and exhilarative talks.

Last but not least I want to give my warmest thanks to my family including my parents, my sisters with their families and my grandparents who steadily supported me financially and mentally along the time of my study.

Abstract

Pyruvate-substituted glycans present in secondary cell wall polymers (SCWP) are supposed to act as mediators for the noncovalent attachment of surface-layer (S-layer) glycoproteins to the peptidoglycan (PG) meshwork of several Gram-positive bacteria. SpaA is a 106 kDa S-layer glycoprotein that occurs in the cell-wall of *Paenibacillus alvei* CCM 2051^T and shows the special ability to self-assemble into 2-D crystalline lattices. S-layer homology (SLH)-domains at the N-terminal part of the protein are known to play an important role in the anchoring mechanism to the pyruvate-substituted SCWP of *P. alvei* CCM 2051^T. The SCWP is covalently linked to the PG layer and is composed of $\rightarrow 3$)-4,6-O-Pyr- β -D-ManNAc-(1 \rightarrow 4)- β -D-GlcNAc-(1 \rightarrow disaccharide units.

This master thesis describes a synthetic route for the preparation of the related monosaccharide 4,6-Pyr- β -D-ManNAcOMe within 7 or 8 steps providing the basis for the following 3-step-synthesis of the disaccharide β -D-GlcNAc-(1 \rightarrow 3)-4,6-(S)-Pyr- β -D-ManNAcOMe. The glycosylation reaction was done using the pyruvylated β -D-N-acetyl-mannosamine as acceptor and an N-Troc-protected trichloroacetimidate donor. After global deprotection, different experiments involving the model saccharides and truncated, SLH-domains containing SpaA protein were performed. The binding contribution of the pyruvic acid acetal was confirmed by Saturation Transfer Difference (STD)-NMR and shown in a ligand-bound crystal structure. Isothermal Titration Calorimetry (ITC) gave useful information about the ligands' binding affinity to the protein.

Kurzfassung

Pyruvat-substituierte Glykane, welche in sekundären Zellwandpolymeren (SCWP) vorkommen, spielen vermutlich eine wichtige Rolle bei der nichtkovalenten Bindung von S-Schicht (surface-layer) Proteinen an das Peptidoglykan (PG) Netzwerk. SpaA ist ein 106 kDa großes S-Schicht Glykoprotein, welches in dem grampositiven Bakterium *Paenibacillus alvei* CCM 2051^T vorkommt und die Eigenschaft zur Selbstorganisation in regelmäßige, kristalline 2-D Gitter besitzt. Die SLH (S-layer homology)-Domänen am N-Terminus des Proteins sind beteiligt am Mechanismus zur Bindung an die mit Pyruvatgruppen substituierten SCWP von *P. alvei* CCM 2051^T. Das SCWP, welches kovalent an die PG-Schicht gebunden ist, besteht aus $\rightarrow 3$ -4,6-O-Pyr- β -D-ManNAc-(1 \rightarrow 4)- β -D-GlcNAc-(1 \rightarrow) Disaccharid-Bausteinen.

Diese Masterarbeit beschreibt die 7- bzw. 8-schrittige Synthese des Monosaccharids 4,6-Pyr- β -D-ManNAcOMe, welches die Grundlage für die darauffolgende 3-schrittige Synthese zum Disaccharids β -D-GlcNAc-(1 \rightarrow 3)-4,6-(S)-Pyr- β -D-ManNAcOMe bildet. Die entsprechende Glykosylierung wurde mit dem pyruvilierten β -D-N-Acetyl-mannosamin als Akzeptor und einem N-Troc geschützten Trichloracetimidat Donor durchgeführt. Nach Entfernung der Schutzgruppen wurden die synthetischen Saccharide für verschiedene Experimente mit einem verkürzten SpaA Protein, welches die SLH-Domänen enthält, verwendet. Der Beitrag am Bindungsprozess durch die Pyruvatgruppe konnte mittels Saturation Transfer Difference (STD)-NMR bestätigt und anhand von Ligand-gebundenen Kristallstrukturen gezeigt werden. Die Ergebnisse der Isothermen Titrations-kalorimetrie (ITC) gaben außerdem Auskunft über die Bindungsaffinität der Liganden zum Protein.

Abbreviations

aa	Amino acid
ACN	Acetonitrile
Ac ₂ O	Acetic anhydride
BF ₃	Boron trifluoride etherate
COSY	Correlated Spectroscopy
DCM	Dichloromethane
DMAP	4-Dimethylaminopyridine
DMF	Dimethylformamide
Et ₃ N	Triethylamine
EtOAc	Ethylacetate
HCl	Hydrochloric acid
HEPES	4-(2-hydroxyethyl)-1-piperazineethanesulfonic acid
HMBC	Heteronuclear multiple-bond correlation spectroscopy
HPTLC	High performance thin layer chromatography
HR MS	High resolution mass spectroscopy
HSQC	Heteronuclear single quantum coherence
MeOH	Methanol
MgSO ₄	Magnesium sulfate
Na ₂ SO ₄	Sodium sulfate
NaHCO ₃	Sodium hydrogen carbonate
NaOH	Sodium hydroxide
NaOMe	Sodium methoxide
NMR	Nuclear magnetic resonance
NOE	Nuclear Overhauser effect
OAc	O-acetyl group
OBn	O-benzyl group
OMe	O-methyl group
PhCH(OMe) ₂	Benzaldehyde dimethyl acetal
p-TsOH	p-Toluenesulfonic acid monohydrate
RT	Room temperature
TfOH	Trifluoromethanesulfonic acid
TLC	Thin layer chromatography
TMS	Tetramethylsilane
TMSOTf	Trifluoromethanesulfonic acid trimethylsilylester
THF	Tetrahydrofuran
TOCSY	Total correlation spectroscopy
Troc	2,2,2-Trichloroethoxycarbonyl

Content

Acknowledgements	I
Abstract	III
Kurzfassung	IV
Abbreviations	V
1. Introduction	1
1.1. Bacterial Cell Envelopes	1
1.2. S-Layer (Glyco)proteins	2
1.3. Secondary Cell Wall Polymers	4
1.4. Interaction of Pyruvate-Substituted SCWPs with S-Layers	5
1.5. Synthesis of Pyruvate-Substituted Saccharides	7
2. Aim	8
3. Results and Discussion	9
3.1. Overview of the Synthetic Routes	9
3.1.1. Monosaccharide	9
3.1.2. Disaccharide	10
3.2. Synthesis of the Monosaccharide	11
3.2.1. Introduction of the Protecting Groups	11
3.2.2. Inversion of the Configuration	12
3.2.3. Staudinger-Type Reactions	13
3.2.4. Benzylidene Removal and Methyl Pyruvate Introduction	16
3.2.5. Deprotection and Saponification	20
3.3. Synthesis of the Disaccharide	21
3.3.1. Glycosylation	21
3.3.2. Troc-Removal followed by Acetylation	23
3.3.3. Complete Deprotection and Saponification	23
3.4. Experiments involving SpaA protein	27
3.4.1. CocrySTALLIZATION Experiments	27
3.4.2. Isothermal Titration Calorimetry (ITC)	29
3.4.3. Saturation Transfer Difference (STD) - NMR	30

1. Introduction

1.1. Bacterial Cell Envelopes

Gram-positive and gram-negative bacteria can be distinguished on the basis of a special staining procedure using the dark-blue iodine gentian violet dye complex. Due to the difference in the construction of their cell envelope the bacteria either remain colored (gram-positive) or not (gram-negative) after staining and ethanol extraction. Gram-positive bacteria consist of a cytoplasmic membrane, a multilayered peptidoglycan (murein) shell and surface-located compounds as outermost part. The cell envelopes of gram-negative bacteria show an additional bilayer (outer membrane) which is located between their very thin murein and their surface-situated compounds ¹. Surface-located compounds are mostly glycoconjugates such as lipopolysaccharides, capsular polysaccharides or glycoproteins. Cell surface layer (S-layer) glycoproteins represent a type of special interest. In gram-positive bacteria they are anchored to secondary cell wall polymers (SCWPs) - another species of glycans that occurs in bacterial cell envelopes and is covalently linked to the murein layer ². Figure 1 shows the cellular location of these components in gram-positive bacteria.

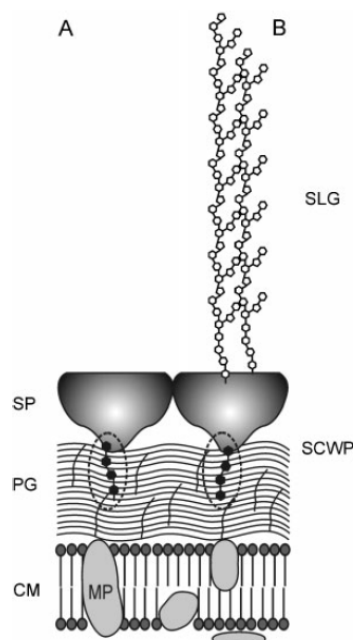


Figure 1: Cell wall profile of (A) S-layer-protein- and (B) S-layer-glycoprotein-carrying gram-positive bacteria. CM: Cytoplasmic membrane, MP: Membrane protein, PG: Peptidoglycan, SP: S-layer protein, SLG: S-layer glycoprotein, SCWP: Secondary cell wall polymer ³

1.2. S-Layer (Glyco)proteins

S-Layer proteins occur in all types of prokaryotic organisms (archaea and bacteria). Although glycosylation is their major modification they are not necessarily glycosylated. They have the special ability to self-assemble into 2-D crystalline lattices that show periodicity at the nanometer scale ². S-Layer lattices can be found with hexagonal, square or oblique symmetry (see Figure 2) and are 5-25 nm thick. S-Layers form pores with identical size and morphology as they consist of identical subunits. In most cases one single protein or glycoprotein species with a molecular weight of 40 to 200 kDa represents this subunit ⁴. Some organisms, for example *Bacillus anthracis*, are known to exhibit S-layers with a defined lattice out of two types of proteins ⁵.

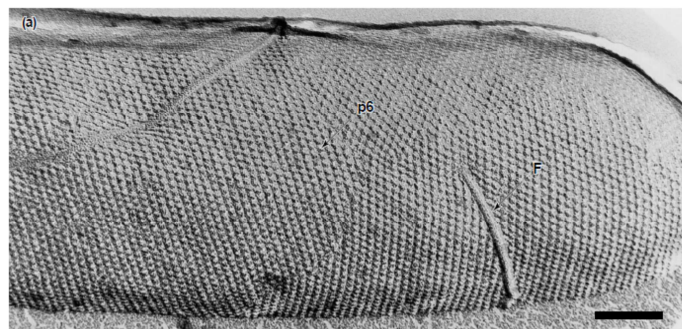


Figure 2: Electron micrograph of freeze-etched preparations of intact cells of *Thermoanaerobacter thermohydrosulfuricus* L111 showing a hexagonal (p6) surface lattice. Scale bars = 100 nm ⁶.

Concerning the biological function of S-layer (glyco)proteins only little is known. It is assumed that they play a role in protective coating of the cell, surface recognition, cell adhesion to substrates, receptor-substrate interaction, template fine-grain mineralization and in the mediation of pathogenicity-related phenomena ². Due to their property of self-assembly on cell surfaces isolated S-layer (glyco)proteins show application potential in the field of molecular nanotechnology and biomimetics. The isolated proteins can be used to create a regular array in suspension or on suitable surfaces (metals, polymers) or interfaces (liposomes, lipid films) ⁴. S-Layer proteins of two strains of *Bacillus stearothermophilus*, members of the family of *Bacillaceae*, were appropriate for the production of molecular sieves ⁷. A lot of investigations were already done on the S-layers (glycol)proteins of the gram-positive bacteria family *Bacillaceae*. One mesophilic bacteria of this family that was originally isolated from honeybee hives is *Paenibacillus* (former *Bacillus*) *alvei* ². The glycan structure of *P. alvei* CCM 2051^T is schematically shown in Figure 3 ⁸.

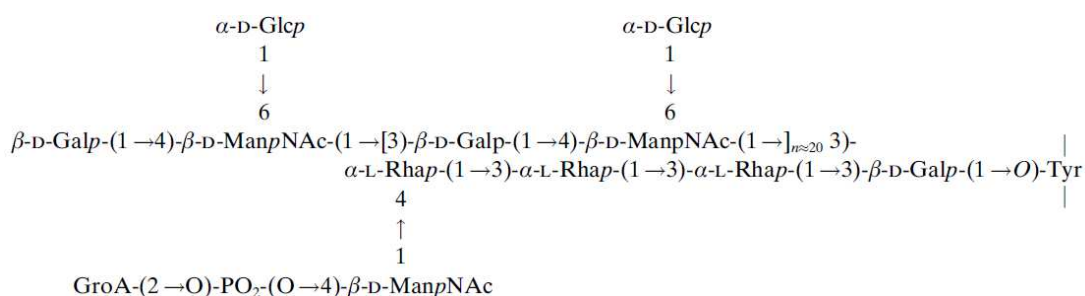


Figure 3: Schematic representation of the S-layer glycan structure of *P. alvei* CCM 2051^T ⁸

An O-glycosidic linkage to a tyrosin residue connects the S-layer glycan with the S-layer protein of *P. alvei* CCM 2051^T ². This S-layer protein is encoded by the gene *spaA* and consists of 983 amino acids of which 24 belong to the signal peptide. The mature SpaA protein shows a theoretical molecular mass of 105.95 kDa and a calculated pI of 5.83 ⁹.

In general, S-layer proteins can be divided into two functional regions: the N-terminal part containing in most cases the cell-wall-targeting domain and the C-terminus with the self-assembly domain. This cell-wall-targeting domain is called SLH (S-layer homology) and consists of about 55 amino acids with 10-15 residues. The SLH-domains are usually made up of one to three modules and do also occur in other surface-associated proteins ². Three SLH-domains can also be found at the amino-terminal region (aa 25-181) of the SpaA protein. Recently a truncated form of the SpaA protein (19.88 kDa) containing the cell-wall binding sites was crystallized for X-ray analysis (see Figure 4) [S. Evans, C. Schäffer, unpublished results].



Figure 4: SpaA protein (*Paenibacillus alvei* CCM 2051^T) in blue, Sap protein (*Bacillus anthracis*) in orange [S. Evans, C. Schäffer, unpublished results]

In 2011, the crystal structure of the S-layer protein Sap from *Bacillus anthracis*, a pathogen gram-positive bacteria strain, was published. The structure showed the three SLH-domains looking like a three-prong spindle ¹⁰. As obvious in Figure 4, the SpaA protein (blue) of *P. alvei* CCM 2051^T shows similarities to the Sap protein (orange) of *B. anthracis* concerning the helix bundles but differs concerning the loops that are connecting the helices. An amino acid sequence comparison between the amino-terminal region of SpaA and Sap (aa 1-200) gave 22.6 % identity and 36.7 % similarity ⁹. More detailed information about the SLH-domains and their binding function is given in chapter 1.4.

1.3. Secondary Cell Wall Polymers

Secondary cell wall polymers (SCWPs) are covalently linked to the peptidoglycan layer of gram-positive bacteria. SCWPs can be categorized into three classes based on their structural characteristics: (i) teichoic acids, (ii) teichuronic acids and (iii) other neutral or acidic polysaccharides which cannot be assigned to the two former types. While the first two types (classical SCWPs) are known to play important roles in normal cell functions, another group, the non-classical SCWPs, is of special interest due to the identification as mediators for the noncovalent attachment of S-layers to the peptidoglycan meshwork ². These non-classical SCWPs that are present in S-layer-carrying *Bacillaceae* organisms can be assigned to group (iii) defined by Araki and Ito ¹¹.

Non-classical SCWPs are glycans made of heteropolysaccharides that can possibly be modified with non-carbohydrate groups (pyruvate, phosphate, acetate) which lead to either a negative or neutral charge. They show a content of 7-15 % (by weight) in the peptidoglycan layer. Another common feature of investigated SCWPs is the α -configuration of the glucose residue linked to the peptidoglycan-bridging phosphate residue. According to their structural composition non-classical SCWPs from S-layer-carrying *Bacillaceae* that were investigated until now can be summarized into three groups. While the repeating units of the second and the third groups are of more complexity and variety, SCWPs of the first group all show the following general repeating unit: $[\rightarrow 3)\text{-}\beta\text{-D-ManpNAc-(1}\rightarrow 4)\text{-}\beta\text{-D-GlcpNAc-(1}\rightarrow]$ ³. In the case of the SCWP that occurs in *Paenibacillus alvei* CCM 2051^T the repeating disaccharide is substituted with 4,6-linked pyruvic acid residues that lead to an overall anionic character (see Figure 5).

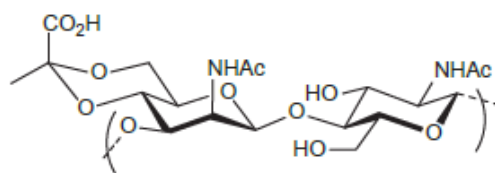


Figure 5: Repeating unit of the SCWP that occurs in *P. alvei* CCM 2051^{T 2}

Considerable loss of the pyruvate residues of the polymer can occur under acidic conditions. Based on biochemical and analytical experiments the following pyrophosphate containing linkage unit to the C-6 of the muramic acid residues of the peptidoglycan layer was proposed: α -D-Glc_pNAc-(1→O)-PO₂⁻-PO₂⁻-(O→6)-MurNAc¹². A schematic representation of the complete glycan structure is shown in Figure 6.

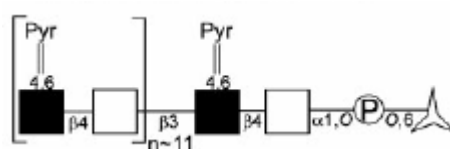


Figure 6: Schematic structure of the SCWP of *Paenibacillus alvei* CCM 2051^T (black box: *N*-acetylmannosamine, white box: *N*-acetylglucosamine, \blacktriangle : *N*-acetylmuramic acid, \textcircled{P} : phosphate-containing linker group)³

It was reported that two other S-layer-carrying organisms (*L. sphaericus* CCM 2177¹³ and *B. anthracis*¹⁴) contain pyruvate-substituted SCWPs as well. Although information is neither available on their full structures nor their linkage to the peptidoglycan layer it was demonstrated that the pyruvate transferase CsaB is involved in adding pyruvate to polysaccharides that are associated to the peptidoglycan layer. This enzyme can be found in several bacterial species, among them also *B. anthracis* and *P. alvei* CCM 2051^{T 14}.

1.4. Interaction of Pyruvate-Substituted SCWPs with S-Layers

The involvement of pyruvate-substituted SCWPs in the interaction with SLH-domains of S-Layer (glyco)proteins was first observed in *B. anthracis*¹⁴. In the gram-negative bacteria *T. Thermophilus* it was shown that pyruvylation of the SCWP is required for attachment of the SLH-domains containing S-layer¹⁵. It is known that the conserved four amino acid motif

TRAE that is located in SLH-domains plays an important role in the binding function to SCWPs¹⁶. This amino acid motif and similar motifs were also identified in the SLH-domains of the Sap protein (*B.anthraxis*). It is assumed that some of the positively charged residues (Arg, Lys) in the inter-prong grooves of the SLH-domains enable binding to the negatively charged pyruvate-substituted SCWPs¹⁰.

The SpaA protein of *P. alvei* CCM 2051^T exhibits three SLH-domains, one with the conserved amino acid motif TRAE and two with variations thereof (TVEE and TRAQ). The location of the three motifs, that are all critical for the binding function of SLH-domains, can be seen in Figure 7. Within *in vivo* and *in vitro* experiments it was shown that two functional motifs are sufficient for cell-wall binding, regardless of the domain location. Additionally a dual-recognition function of the SLH-domains for SCWP and the peptidoglycan layer was reported¹⁷. Inactivation of the *csaB* gene that encodes the pyruvyltransferase led to a lethal phenotype of *P. alvei* CCM 2051^T and also inactivation of the gene *spaA* was impossible (B. Janesch, unpublished results). Therefore intact cell envelopes seem to be substantial for the viability of *P. alvei* CCM 2051^T.

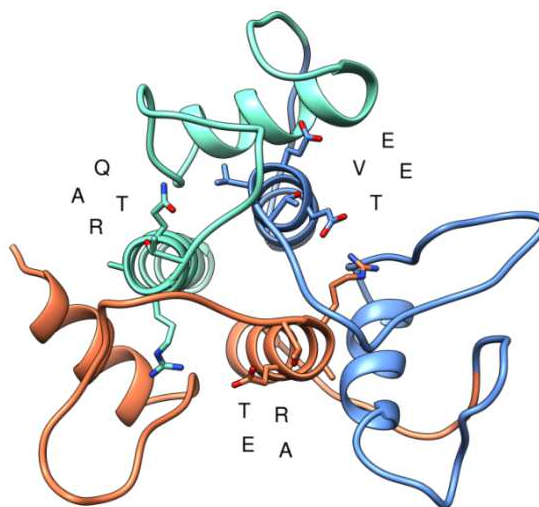


Figure 7: Truncated SpaA protein with its three SLH domains that are involved in the binding function
[S. Evans, C. Schäffer, unpublished results]

It is noteworthy that none of the SCWPs of organisms that possess S-layer proteins without SLH domains show pyruvate-modification but some have a net-neutral charge. This indicates that beside the involvement of pyruvate groups other mechanisms are responsible for binding S-layer proteins to the peptidoglycan layer³.

1.5. Synthesis of Pyruvate-Substituted Saccharides

The synthesis of pyruvylated glycosides is of special interest as pyruvic acid acetals occur in many bacterial oligo- and polysaccharides where they affect the saccharides' properties due to their negative charge and their chiral center. Pyruvate-substitution in the 4,6-*O*-position can be found in D-Glcp, D-Manp, D-GlcNAcp and D-ManNAcp in the (S)-configuration and in D-Galp (R)-configured. Additionally D-Galp and L-Rhap represent 3,4-*O*-pyruvic acid acetals while 2,3-*O*-pyruvate-substitution occurs in D-Galp and D-GlcA¹⁸.

Previously synthetic ways for pyruvate substitution of various pyranosides involving 1-acetoxy-2-propanone followed by deacetylation and oxidation were reported with very low yields and a mixture of the diastereomeric products^{19,20}. Alternatively pyranosides in the diol form were converted into the related pyruvic acetals using methyl pyruvate dithioacetal and an activating reagent like methyl triflate²¹. Another pyruvylation-method involving methyl aryl and furan-2-yl ketone dimethyl acetals and diols followed by oxidation and esterification was published in 1989²².

The formation of β -D-mannopyranosides with a pyruvic acid acetal in the 4,6-*O*-position was first described by Jansson *et al.* in 1993²³. The synthesis was based on a method in which 4,6-diols were trimethylsilylated and then treated with ethyl pyruvate and TMS triflate to give an (R)-(S)-isomeric product mixture²⁴.

The first direct condensation of sugar diols with alkyl pyruvate catalysed by a Lewis acid (BF₃-etherate) was published by Ziegler *et al.* in 1992¹⁸. The resulting 4,6-*O*-acetals showed one diastereomeric form (dependant on the type of saccharide) that could be determined by ¹³C-NMR spectroscopy²⁰. Ziegler *et al.* have published a number of synthetic routes for pyruvate-substituted oligosaccharides that are related to carbohydrate-components of various bacteria^{25,26,27}.

2. Aim

The aim of this thesis was the synthesis of mono- and disaccharide ligands related to pyruvate-substituted β -D-ManNAc residues that are present in the secondary cell wall polymer (SCWP) of *Paenibacillus alvei* CCM 2051^T. Starting from a methyl β -D-glucopyranoside that is converted into the corresponding *N*-acetyl-mannopyranoside the pyruvate introduction should be tried at different synthesis steps using the Lewis acid catalysed direct condensation method. The pyruvylated monosaccharide should also be used as acceptor for a glycosylation reaction to form a disaccharide that is related to the SCWP repeating unit [\rightarrow 3)- β -D-Man ρ NAc-(1 \rightarrow 4)- β -D-Glc ρ NAc-(1 \rightarrow)].

The interaction of the SCWP in *P. alvei* CCM 2051^T with its self-assembling S-layer glycoprotein SpaA is not fully understood so far. The model saccharides should act as a helpful tool to obtain more information about their binding contribution. Therefore experiments including the truncated SpaA protein either in solution or in a ligand-bound crystal form should be performed with the synthetic ligands.

3. Results and Discussion

3.1. Overview of the Synthetic Routes

3.1.1. Monosaccharide

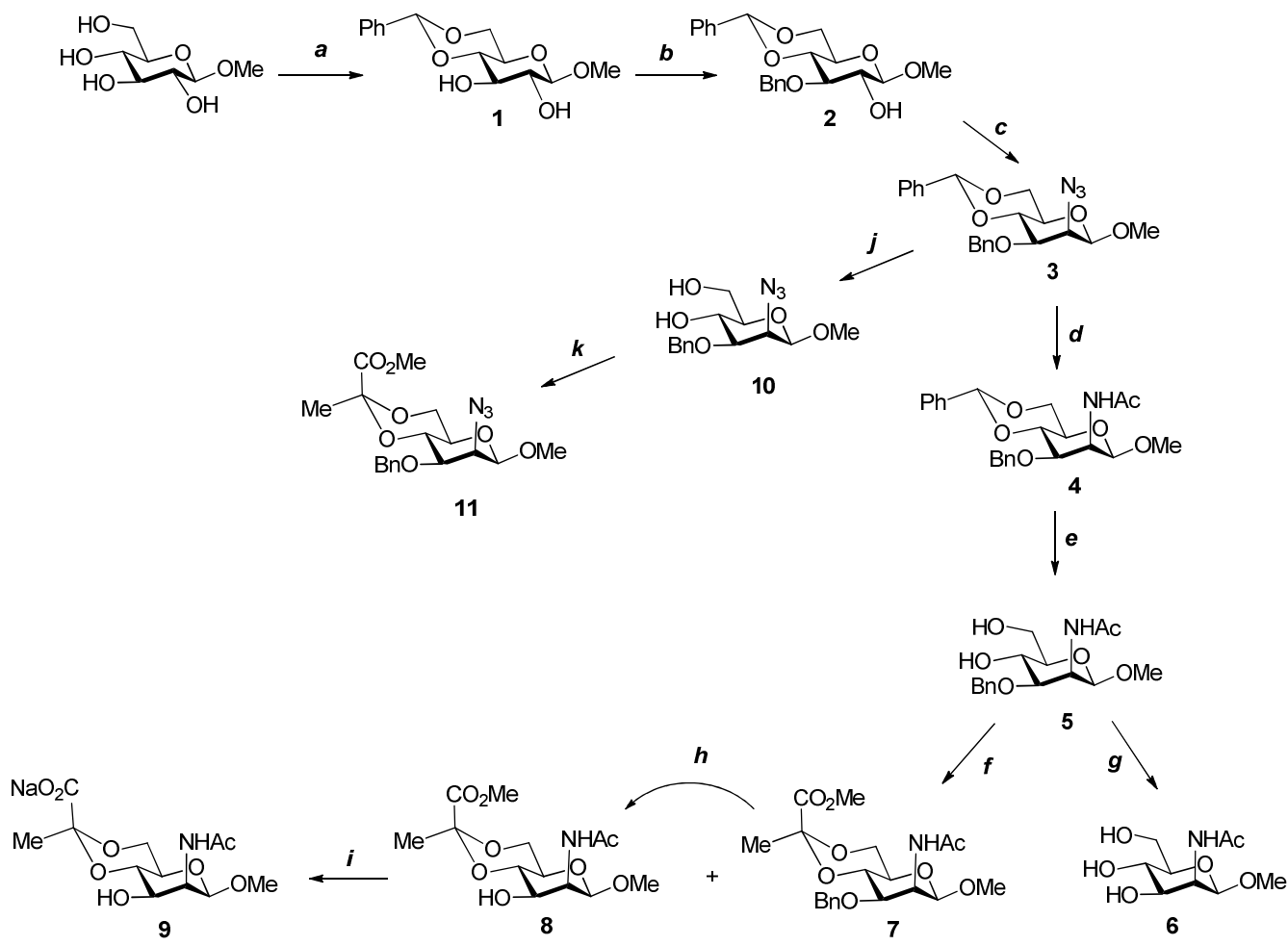


Figure 8: (a) $\text{PhCH}(\text{OMe})_2$, TsOH, 1,4-Dioxane; (b) Bu_2SnO , BnBr, Bu_4NI , Toluene; (c) Tf_2O , DCM/Pyr; NaN_3 , DMF; (d) PPh_3 , AcCl, DCM; Ac_2O , Pyr; (e) TFA, DCM; (f) H_2 , Pd-C, MeOH; (g) MeCOCO_2Me , TMSOTf, CH_3CN ; (h) H_2 , Pd-C, MeOH; (i) 0.2 M NaOH

The synthesis of the pyruvate-substituted monosaccharide starts with the commercially available Methyl β -D-glucopyranoside that first undergoes an acetal formation resulting in the 4,6-O-protected compound **1**. Benzylation is carried out within a two-step reaction using dibutyltin oxide and benzyl bromide to obtain the main product (**2**) and the corresponding 2-O-benzylated side product in a ratio of 3:2²⁸. The following conversion to the protected

Methyl 2-azido-2-deoxy- β -D-mannopyranoside (**3**) is carried out in two steps ²⁹. After activation with the triflic anhydride the carbon at position 2 is substituted by the azide stereoselectively. Considering the shorter synthetic route the next step is the acidic removal of the benzylidene group. The resulting azide-containing diol (**10**) is treated with a Lewis acid and methyl pyruvate in order to give the pyruvylated Methyl 2-azido-2-deoxy- β -D-mannopyranoside (**11**) in very low yields. Following the longer synthetic route, the azide (**3**) is reduced via a Staudinger-type reaction followed by a standard acetylation procedure to give the fully protected β -D-mannosamine (**4**). In the next step the acetal is opened with trifluoroacetic acid which leads to compound **5**. The benzylated β -D-mannosamine (**5**) is either completely deprotected with palladium catalysed hydrogenation to obtain the Methyl 2-acetamido-2-deoxy- β -D-mannopyranoside (**6**) or is subjected to the conditions for the introduction of the pyruvate. Treatment with TMS-triflate as Lewis acid and methyl pyruvate leads to the formation of the benzyl protected pyruvylated product (**7**) and to the 3-hydroxy pyruvate-substituted product (**8**). The benzyl group of **7** is removed by hydrogenation to get compound **8** as well. The last step is the saponification of the methyl ester in sodium hydroxide solution that leads to the final sodium salt product (**9**).

The single steps of the synthetic route are further discussed in chapter 3.2.

3.1.2. Disaccharide

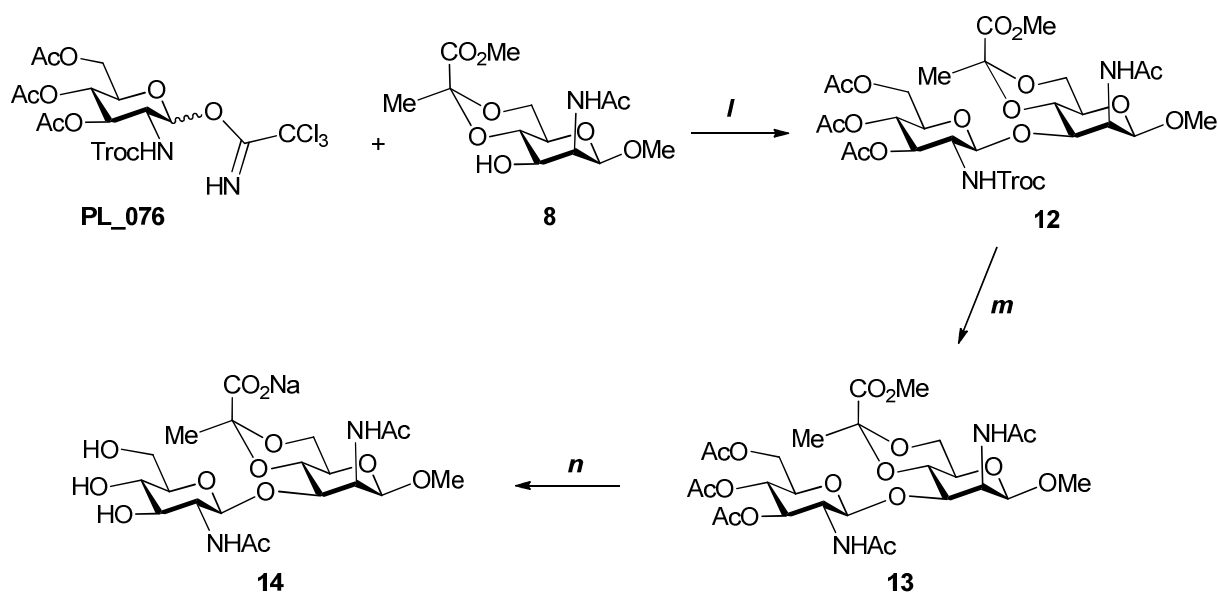


Figure 9: (l) TMSOTf, 4Å acid washed MS, ACN; (m) Zn, AcOH; Ac₂O, Pyr; (n) 0.1 M NaOMe, MeOH; 0.2 M NaOH

The pyruvate-substituted β -linked disaccharide (**12**) is formed via the TMS-triflate activated glycosylation between a glucopyranosyl donor (**PL_076**) and the pyruvylated mannopyranoside acceptor (**8**). In the next step the Troc-protecting group is removed under reductive acidic conditions before the resulting primary amine gets acetylated to give compound **13**. The final disaccharide in its sodium salt form (**14**) is afforded after Zemplén deacetylation followed by saponification of the methyl ester.

In chapter 3.3 the single steps are described in more detail.

3.2. Synthesis of the Monosaccharide

3.2.1. Introduction of the Protecting Groups

Benzylidene acetals as well as isopropylidene acetals are most frequently used for 4,6-O-protection in hexopyranosides. The most common methods for benzylidene introduction are the protic acid and the Lewis acid catalyzed reaction of a diol with benzaldehyde. The first method and the transacetalation normally promote the most thermodynamically stable product while the second method involving a Lewis acid is known to give the kinetically controlled product³⁰. 4,6-O-Benzylidene introduction is carried out after a method described by Yoneda *et al.*³¹ using 1.4 equivalents of benzaldehyde dimethyl acetal in two portions and a catalytic amount of *p*-toluenesulfonic acid. To keep the transacetalation reaction ongoing, the released methanol has to be removed by a current argon flow (here) or under diminished pressure on the rotary evaporator^{31,32}. As crystallization of the product occurs after solvent evaporation, no further purification is needed.

Due to free hydroxyl groups at position 2 and 3, a method for selective benzyl-etherification is required in the next step. Benzylation of the 3-hydroxy group is first tried after a Williamson-type procedure using 4 equivalents of sodium hydride and 1 equivalent of copper(II)chloride before adding 1.5 equivalents of benzyl bromide and 0.2 equivalents of tetrabutylammonium iodide²⁹. The slow reaction ends with the selectively formed 3-O-benzyl product in very low yields (11 %). Therefore the reaction is carried out according to another method published by Murphy *et al.*²⁸. Compound **1** is treated with 1.2 equivalents of dibutyltin oxide in toluene to form the dibutylstannylene acetal as intermediate under azeotropic water separation. 2.2 Equivalents of benzyl bromide (in two portions) and 1.1 equivalent of tetrabutylammonium iodide are added to form the more reactive benzyl iodide that gets attacked by the nucleophilic oxygens. The reaction yields the 3-O-benzylated product (**2**) with

61 % and the 2-O-benzyl side product with 39 % although in the described procedure 85 % of the main product are reported ²⁸. The same method without the usage of the added nucleophile (Bu_4NI) leads to a 1:1 mixture of 2- and 3-O-benzylated β -D-glucopyranoside ³³. Benzyl ethers, along with allyl ethers, are the most frequently used ether protecting groups in carbohydrate chemistry. They can be very beneficial in synthetic pathways due to their resistance to strong basic and acidic conditions ³². Removal of the benzyl group is partly observed under the pyruvylation conditions involving trimethylsilyl trifluoromethanesulfonate as a strong Lewis acid (see chapter 0).

3.2.2. Inversion of the Configuration

The conversion of the glucopyranoside into the mannopyranoside is performed after a two-step synthesis reported by Classon *et al* ²⁹. In the first step the 3-O-benzyl-4,6-O-benzylidene- β -D-glucopyranoside (**2**) reacts with 2.6 equivalents of triflic anhydride that is activated by pyridine. Water-free conditions are compulsive to maintain the reactivity of the anhydride and are achieved in dry dichloromethane under argon atmosphere. After a short work-up the trifluoromethanesulfonate derivative is treated with 5 equivalents of sodium azide in *N,N*-dimethylformamide. Within a $\text{S}_{\text{N}}2$ -reaction the 2-azido-2-deoxy-mannopyranoside is formed in good yields (85 %). Figure 10 shows the mechanism of the reaction. Azides can be seen as masked amino groups during the synthetic routes of carbohydrates as they are stable against various reaction conditions ³⁴. It is advantageous that the conversion to the mannopyranoside and the introduction of an amino group precursor is achieved at on go.

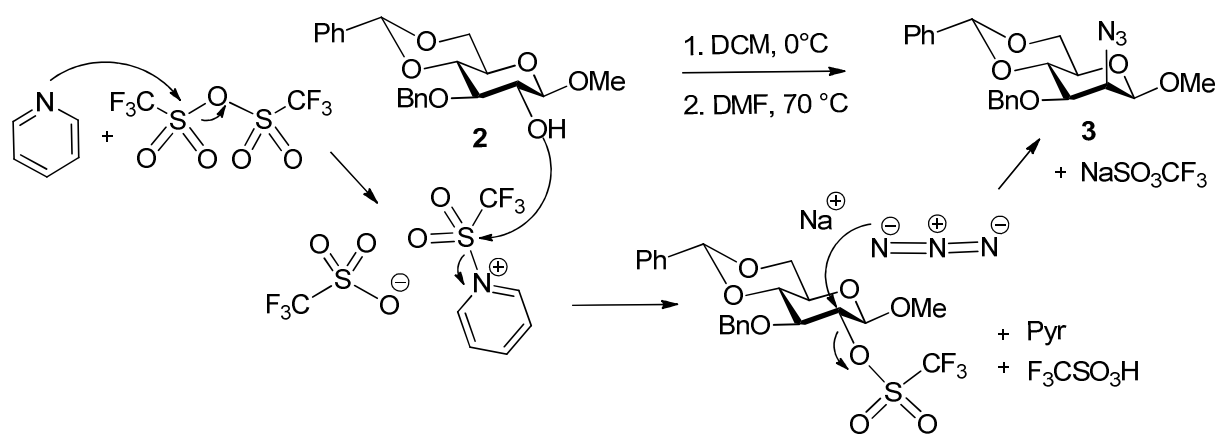


Figure 10: Reaction mechanism of the azide introduction

Within the inversion of the configuration the hydrogen at position 2 changes its axial position to equatorial which leads to a far smaller 3J -coupling with the axially located H-1. Additionally H-2 underlies a downfield shift due to the neighbouring azide group with its pseudohalogenic character that causes a stronger electron-withdrawing effect (see Figure 11).

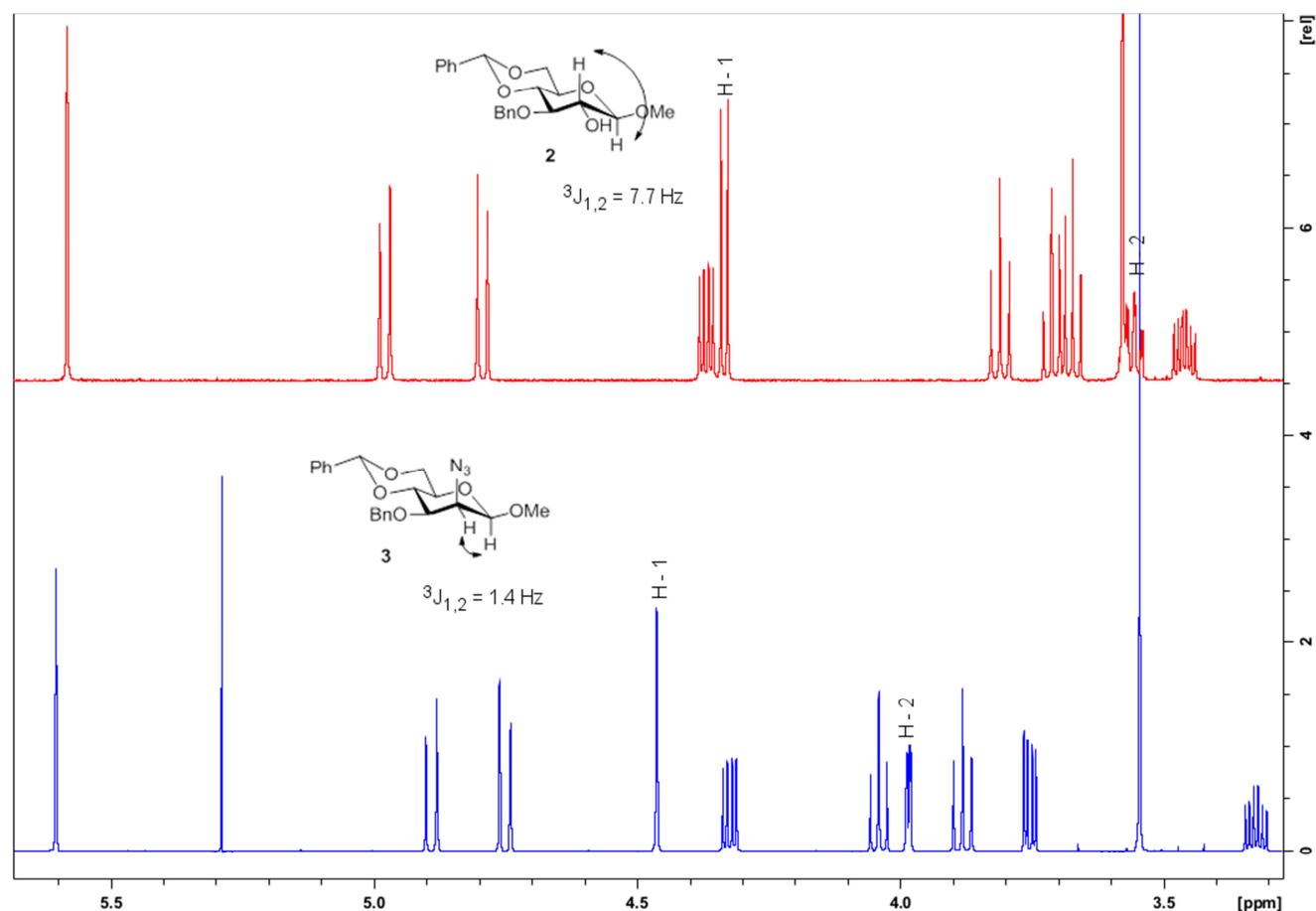


Figure 11: Expansion plot of the $^1\text{H-NMR}$ spectra (600 MHz, CDCl_3) of compound 2 (red) and 3 (blue) by comparison

3.2.3. Staudinger-Type Reactions

Different methods are known to perform the reduction from an azide to a primary amine. In this case hydrogenation is not possible due to the lability of the benzyl-protecting group under these reaction conditions. Several approaches based on the Staudinger reaction, a common tool for amine formation, are carried out and yield more or less satisfying results. The approaches that are listed in Table 1 differ concerning the type of the used phosphane-compound and the way of the following *N*-acetylation.

The 1st approach is performed after a method described by Maunier *et al.*³⁵ where β -glycopyranosyl azides are converted to the corresponding amides in a one-pot synthesis. Compound **3** is therefore treated with 1.8 equivalents of triphenylphosphine and 3.2 equivalents of acetyl chloride followed by the addition of acetic anhydride and pyridine to obtain complete *N*-acetylation. The method is unfavorable due to the formation of the 2-chloro-2-deoxy side product and the difficulty concerning the removal of residual PPh₃ that is only possible by HPLC purification. To prevent that problem in the 2nd approach acetyl chloride and polymer bound PPh₃ (1.6 mmol/g resin), easily removable by filtration, is used. Further acetylation is not necessary in this case but the chloro-substituted side product is formed in far higher yields (62 %) than the desired product (22.3 %). For the 3rd approach the phosphane-reagent was changed into trimethylphosphine that can be separated within an aqueous work up. Beside the primary amine intermediate (**4'**) another very polar compound was also detectable with the ninhydrin dip. That side product doesn't seem to be converted during the standard acetylation conditions using acetic anhydride in pyridine but is removed within the work up. Low yield (33.4 %) and side product formation render this method as inefficient. Although in the 4th approach that is involving polymer bound PPh₃ (1.6 mmol/g resin) the *N*-acetylation is carried out in a separate reaction step to prevent the formation of the chloro-derivate, a low amount of desired product is obtained (34.0 %). Insufficient water equivalents which are necessary for hydrolytic separation from the polymer could be responsible for the unfavorable results. Conversion of the azide to the amine using 3 mmol/g resin polymer bound PPh₃ is slow and not complete. The 5th approach that involves a hydrolytic step using 10 equivalents of H₂O in tetrahydrofuran finally shows satisfying yields and no side product formation. Fusion of parts 1) and 2) in THF might also be possible.

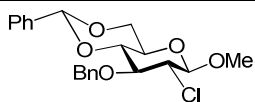
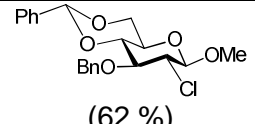
Approach	Reduction Condition	Acetylation Condition	Yield	Side Product
1 st	PPh ₃ , AcCl, DCM	Ac ₂ O, Pyr	118.2 % (containing residual PPh ₃)	
2 nd	PPh ₃ polymer bound (1.6 mmol/g), AcCl, DCM		22.3 %	 (62 %)
3 rd	PMe ₃ , H ₂ O, DCM	Ac ₂ O, Pyr	33.4 %	very polar compound
4 th	PPh ₃ polymer bound (1.6 mmol/g), DCM	Ac ₂ O, Pyr	34.0 %	-
5 th	1) PPh ₃ polymer bound (1.6 mmol/g), DCM 2) THF, 10 equ. H ₂ O, 55°C	Ac ₂ O, Pyr	75.1 %	-

Table 1: Approaches of the Staudinger-type reactions by comparison

The mechanism for a Staudinger reaction involving polymer bound triphenylphosphine is shown in Figure 12 and shows the need of hydrolysis to remove the compound from the polymer. After the attachment of the polymeric PPh_3 to the azide group a ring is formed. Within the ring opening nitrogen is split off and the phosphanimine intermediate that is still bound to the polymer is formed. Hydrolysis then leads to the free amine ($4'$) and triphenylphosphine oxide.

Usage of acetyl chloride for the one-pot Staudinger-type reaction might induce a different mechanistic behavior. Maunier *et al.*³⁵ report an acylation mechanism via imidoyl chloride intermediates that are hydrolyzed to the corresponding amides. Formation of possible N- or C-phosponium salts³⁶ could explain the equatorial attachment of the chloride anion at position 2 and therefore the formation of the chloro-side product in the 1st and the 2nd approach.

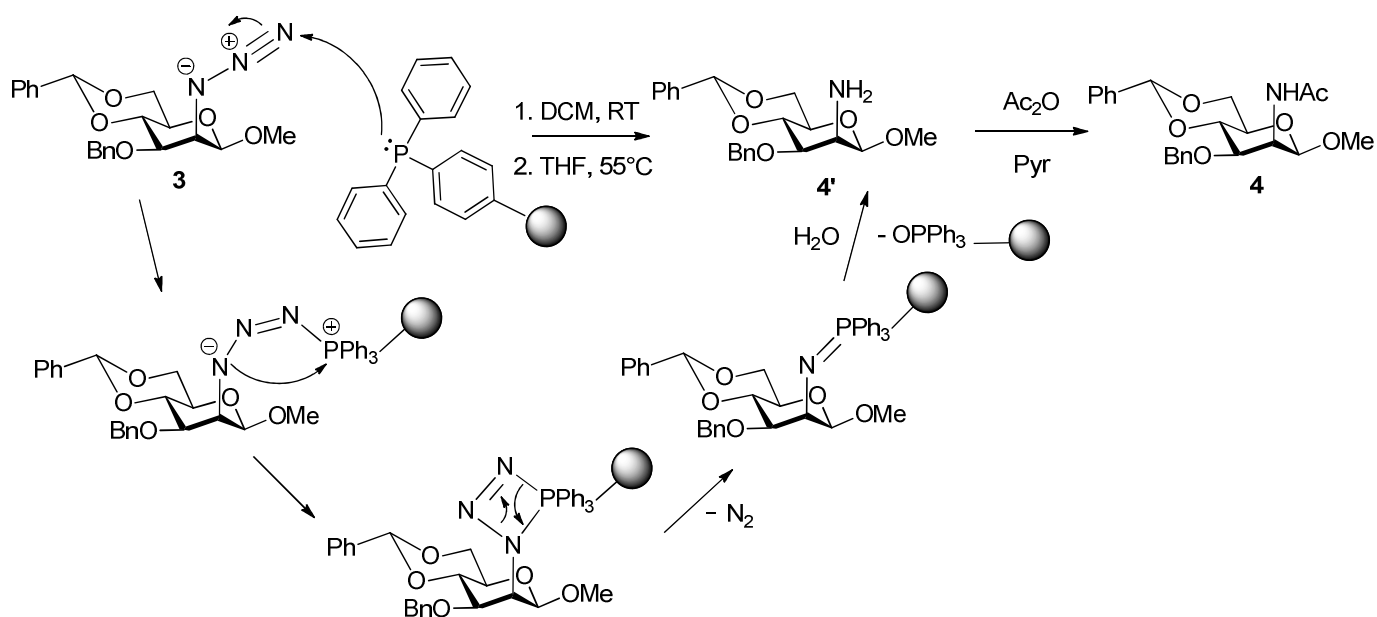


Figure 12: Reaction mechanism for a Staudinger reaction with polymer bound PPh_3 followed by *N*-acetylation

Beside the modified Staudinger reactions two other methods were tried. Neither by using the reducing reagent dithiothreitol in DMF/ H_2O nor thioacetic acid and 2,6-lutidine in DCM, a method that should directly result in the amide compound, leads to the formation of the desired product.

3.2.4. Benzylidene Removal and Methyl Pyruvate Introduction

Complete removal of the 4,6-O-benzylidene group was carried out under harsh acidic conditions at 0 °C using trifluoroacetic acid (99 %) in excess. Although this standard reaction is fast and efficient monitoring via TLC is difficult due to the strong acid and may lead to a premature termination of the reaction. Maybe addition of H₂O could improve the reaction process as the reaction-type is a matter of acidic hydrolysis.

The following used method for pyruvylation of the 4,6-diol is modified after a procedure reported by Ziegler *et al*²⁵. As no product formation was observed by using 2.3 equivalents of methyl pyruvate and 2.3 equivalents of boron trifluoride diethyl etherate the Lewis acid is changed into trimethylsilyl trifluoromethanesulfonate. These reaction conditions lead to the diastereoselective formation of the desired product (**7**) and a side product (**8**). Induced by the Lewis acid the carbocation is formed and attacked by the nucleophilic 6-OH group. Water elimination is followed by the ring closure to obtain the cyclic ketal (see Figure 13). A path wherein the 4-hydroxy group first reacts with the methyl pyruvate might also occur.

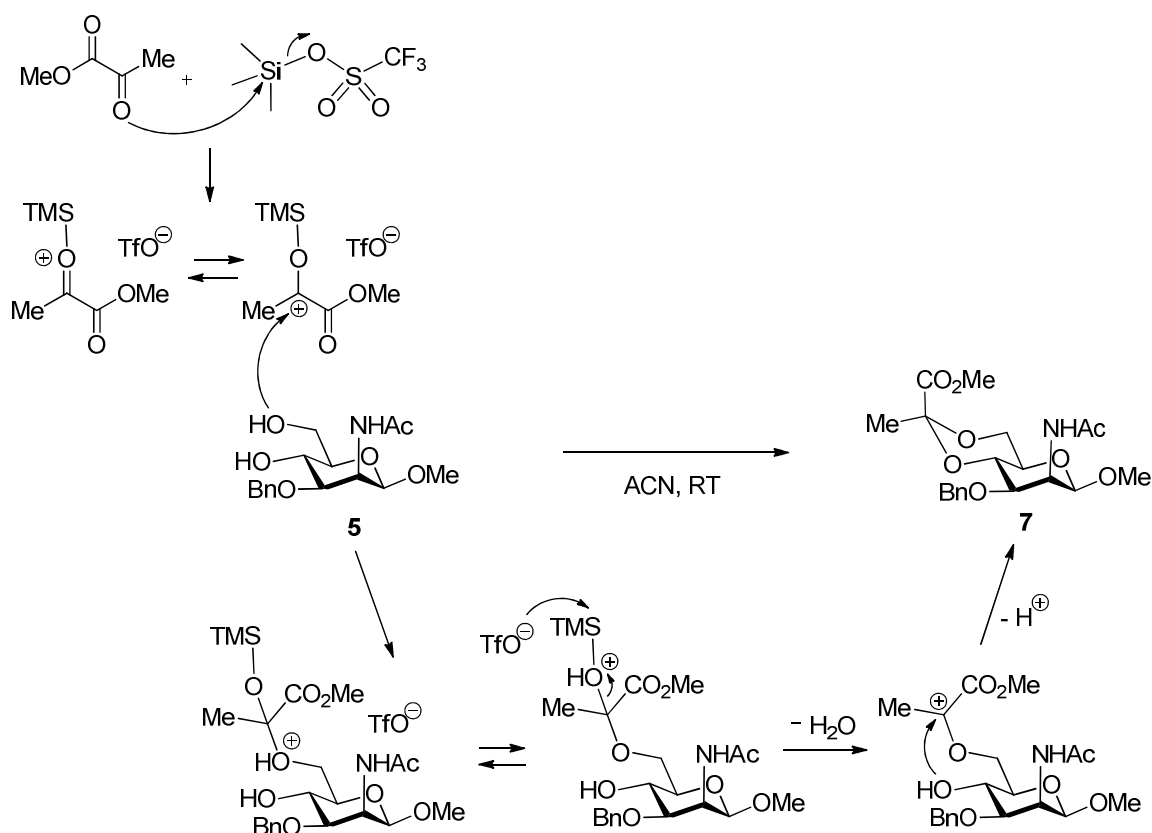


Figure 13: Proposed mechanism for the methyl pyruvate introduction

The strong Lewis acid (TMS-triflate) might also be responsible for the removal of the 3-O-benzyl group and therefore for the formation of the side product (**8**). Due to high similarity concerning the TLC-retention factors of the starting material (**5**) and compound **8** identification has to be carried out by NMR analysis. As the next synthesis step involves the deprotection of the 3-O-benzyl group the formation of compound **8** is advantageous. Figure 14 shows the ^1H -NMR spectra of the two compounds (**5** and **8**). The additional signals arising from the introduced methyl pyruvate group are highlighted in colour. The aromatic as well as the aliphatic signals belonging to the benzyl protecting group are obviously absent in the lower spectrum.

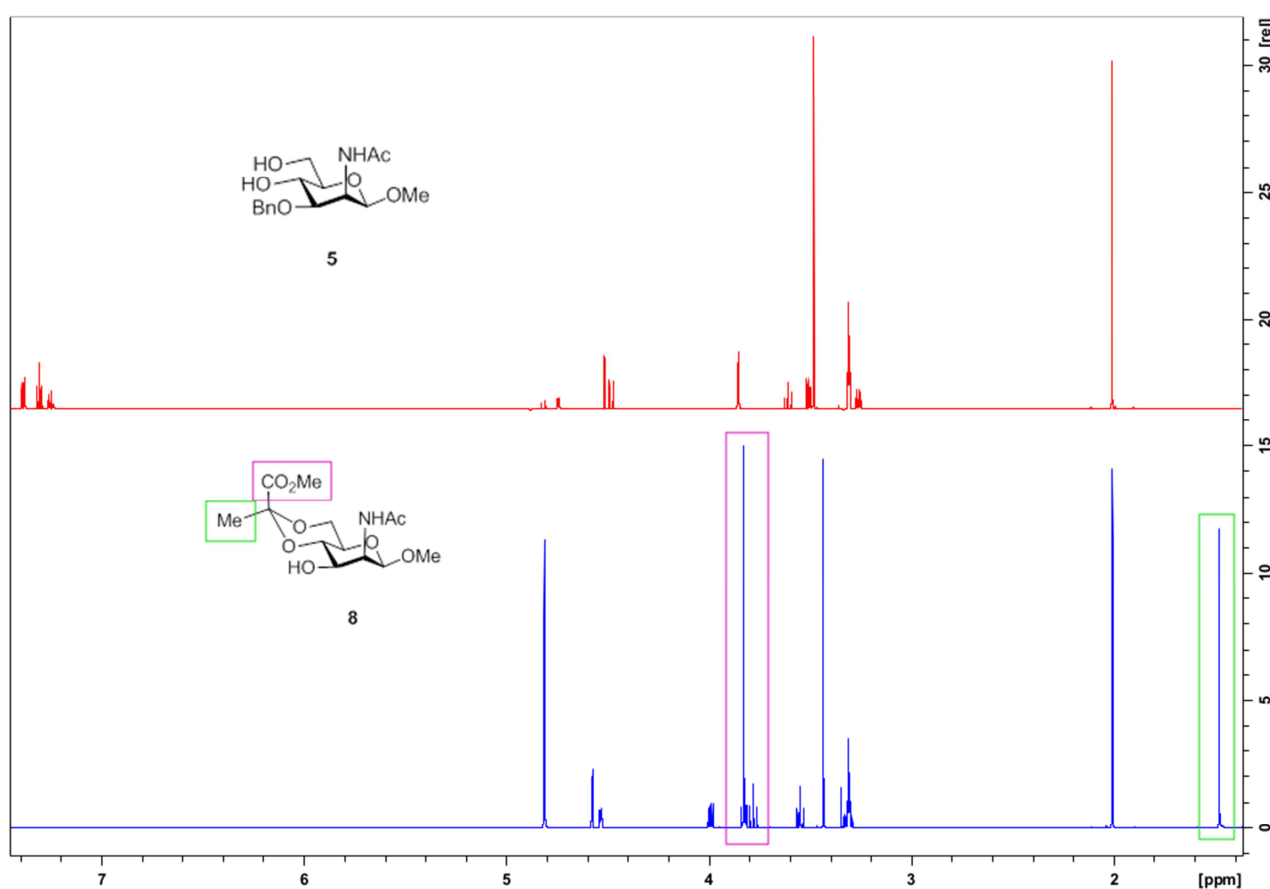


Figure 14: ^1H -NMR spectra (600 MHz, $\text{MeOH-}d_4$) of compound **5** (red) and **8** (blue) by comparison

The diastereoselectivity of the reaction is proven by the ^1H - and ^{13}C -NMR shifts of the methyl group. In Table 1 Table 2 experimental ^1H - and ^{13}C -NMR shifts of the final compound **9** and shifts of similar pyruvate-substituted mannopyranosides that are reported in literature^{18,23} are listed. By comparison of the shifts, product (**9**) can be identified as (*S*)-configured with an equatorially arranged methyl group.

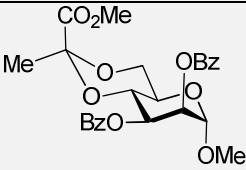
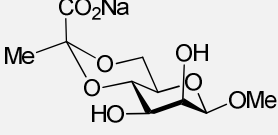
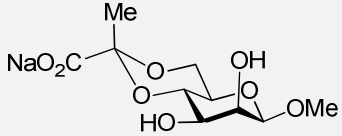
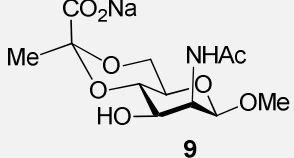
Compound	δ (Me) $^1\text{H-NMR}$ [ppm]	δ (Me) $^{13}\text{C-NMR}$ [ppm]
	not stated	24-26 ¹⁸
	1.47 ²³	25.62 ²³
	1.63 ²³	17.78 ²³
	1.44	25.30

Table 2: Literature reported and experimental ^1H - and ^{13}C -NMR shifts of the methyl group of pyruvate-substituted mannosides

Pyruvylation is also tried starting from the 2-azido-2-deoxy compound (**3**) whose benzylidene group is first removed by strong acidic conditions. Introduction of the pyruvate group is performed as described above with 2.3 equivalents of methyl pyruvate and 2.0 equivalents of TMS-triflate in acetonitrile. The reaction yields in the formation of the pyruvylated product (**11**) in very low yields (12 %) and two side products of which one might be the debenzylated compound. Probably the azide group affects the reaction process although it is known to be a non-participating group in glycosylation reactions. Therefore pyruvate introduction at the step of the *N*-acetylated mannopyranoside (**5**) seems to be more efficient as only product (**7**) and useful side product (**8**) are formed in moderate yields.

Interesting observations are obtained concerning the used methyl pyruvate reagent. NMR measurements show the presence of a cyclic ketal that might be formed in an equilibrium reaction. Through the HMBC-NMR spectrum the correlations within the two systems (red and blue) are observed and enable the assignment of the ^1H - and ^{13}C -NMR shifts (see Figure 16 and Figure 16). During the reaction conditions involving the strong Lewis acid the methyl pyruvate might remain in its non-cyclic form and is therefore able to react as shown in Figure 13.

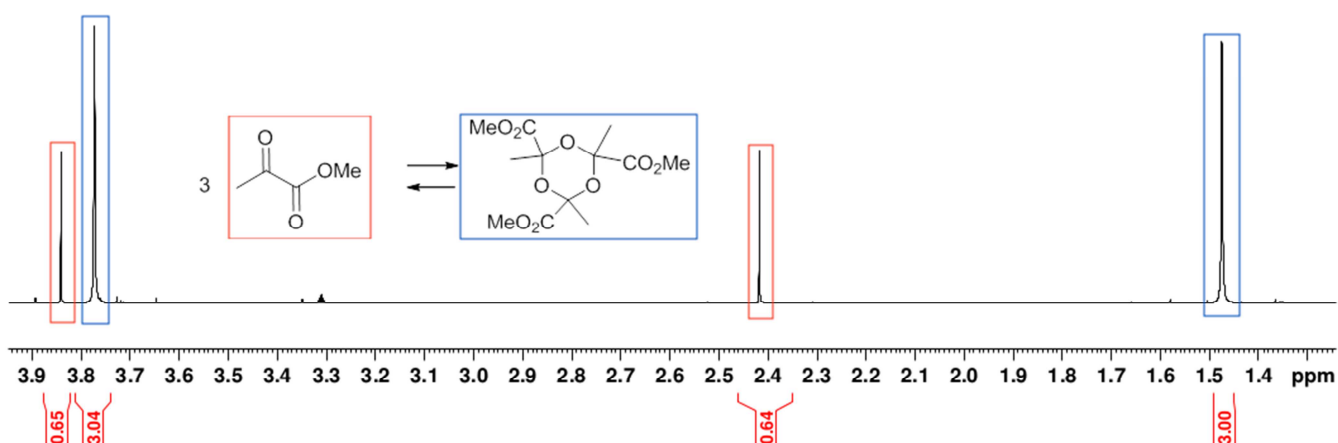


Figure 15: ^1H -NMR spectrum (600 MHz, $\text{MeOH-}d_4$) of the methyl pyruvate reagent

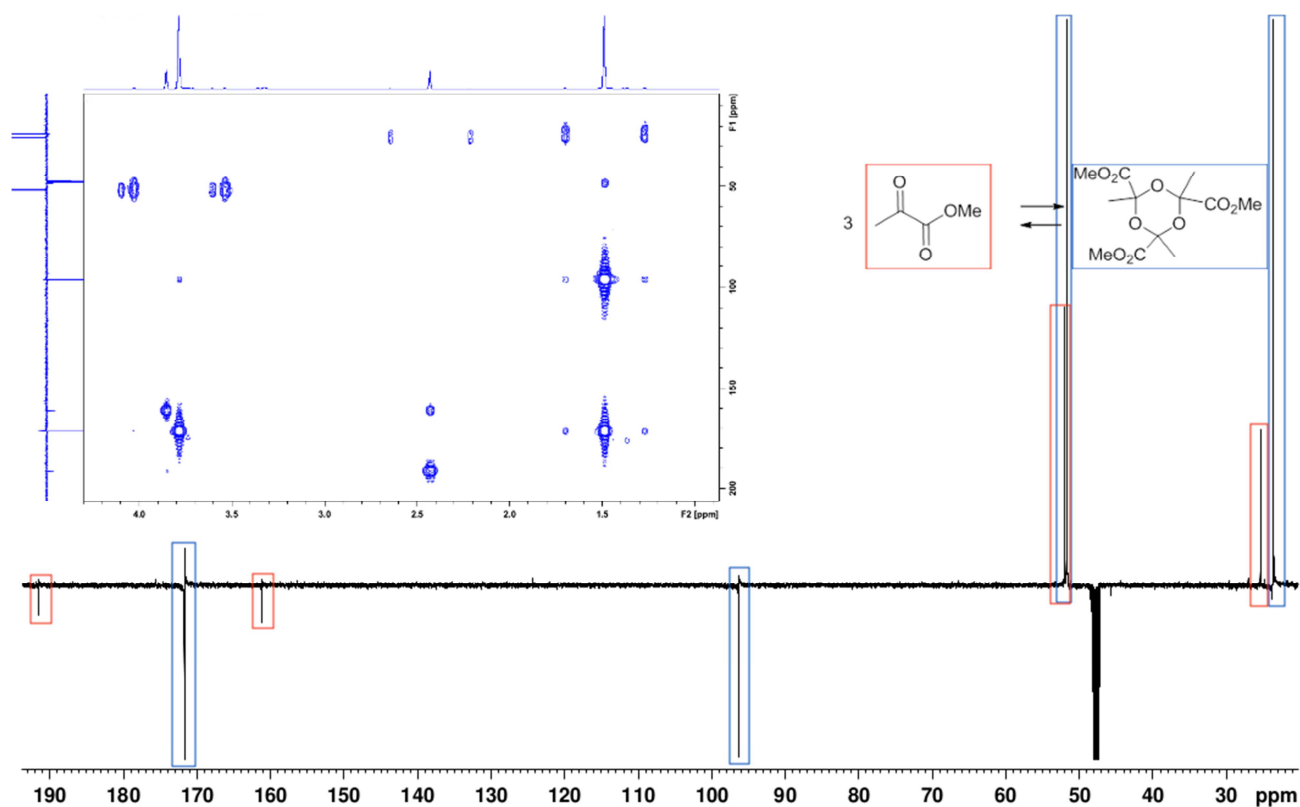


Figure 16: ^{13}C -NMR (600 MHz, $\text{MeOH-}d_4$) and HMBC-NMR spectrum (300 MHz, $\text{MeOH-}d_4$) of the methyl pyruvate reagent

3.2.5. Deprotection and Saponification

Removal of the benzyl protecting group is carried out by catalytic hydrogenation with palladium on carbon (10 %) in methanol. The 1st approach to obtain product **8** fulfills the expectations of a quantitative reaction that requires no purification. In the 2nd approach, where compound **8** is partly crystallized, formation of a side product occurs. Purification of the residual syrup by column chromatography leads to unexpected but reproducible loss of substance. A 2D-TLC experiment and treatment of compound **8** with silica gel shows no decomposition under the weak acidic conditions.

The non-pyruvylated *N*-acetyl mannosamine compound (**6**) is obtained by Pd/C-catalyzed hydrogenation as well. After the high-yielding reaction (90 %) beside a PD-10 desalting column no further purification is required. An approach to introduce the pyruvate group enzymatically to compound **6** fails.

Saponification of the methyl ester represents the last step of the monosaccharide synthesis. The quantitative reaction is carried out in 0.2 molar aqueous sodium hydroxide solution. The pH-value is adjusted to 7.5 to obtain the product in the sodium salt form. Removal of remaining suspended solids is achieved via size exclusion chromatography and leads to the pure final compound **9** (see Figure 17 and Figure 18).

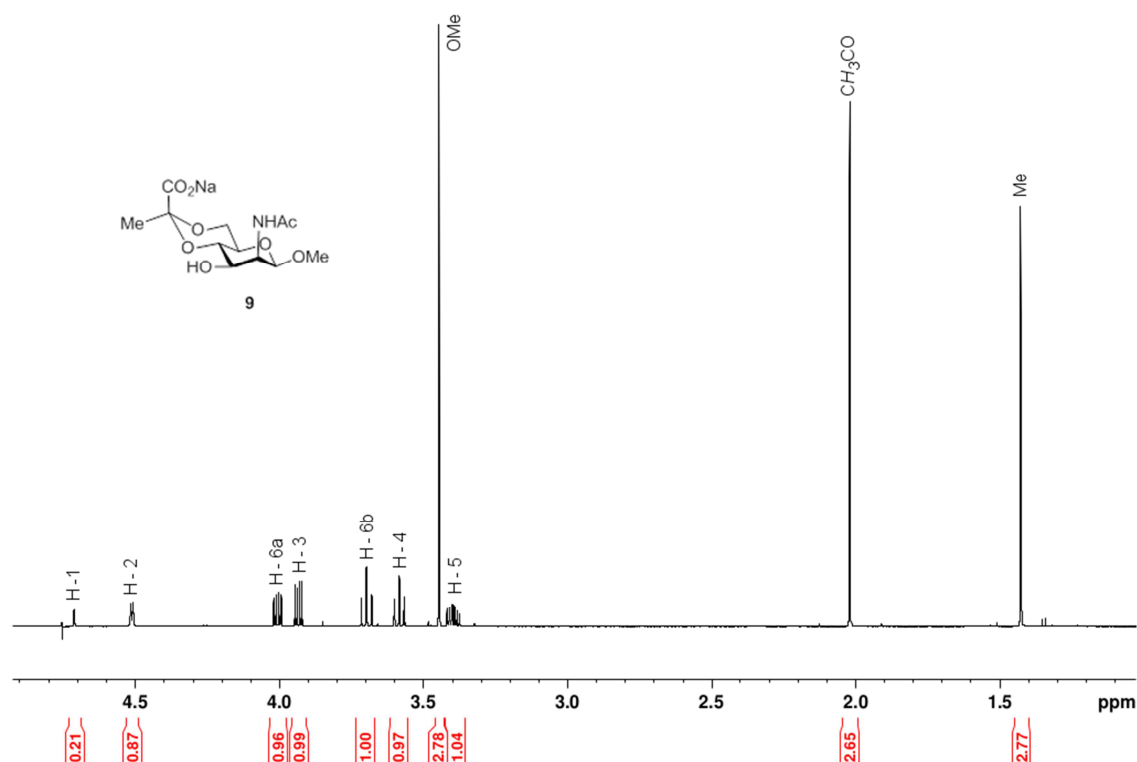


Figure 17: ¹H-NMR spectrum (600 MHz, D₂O) of the final monosaccharide compound (**9**)

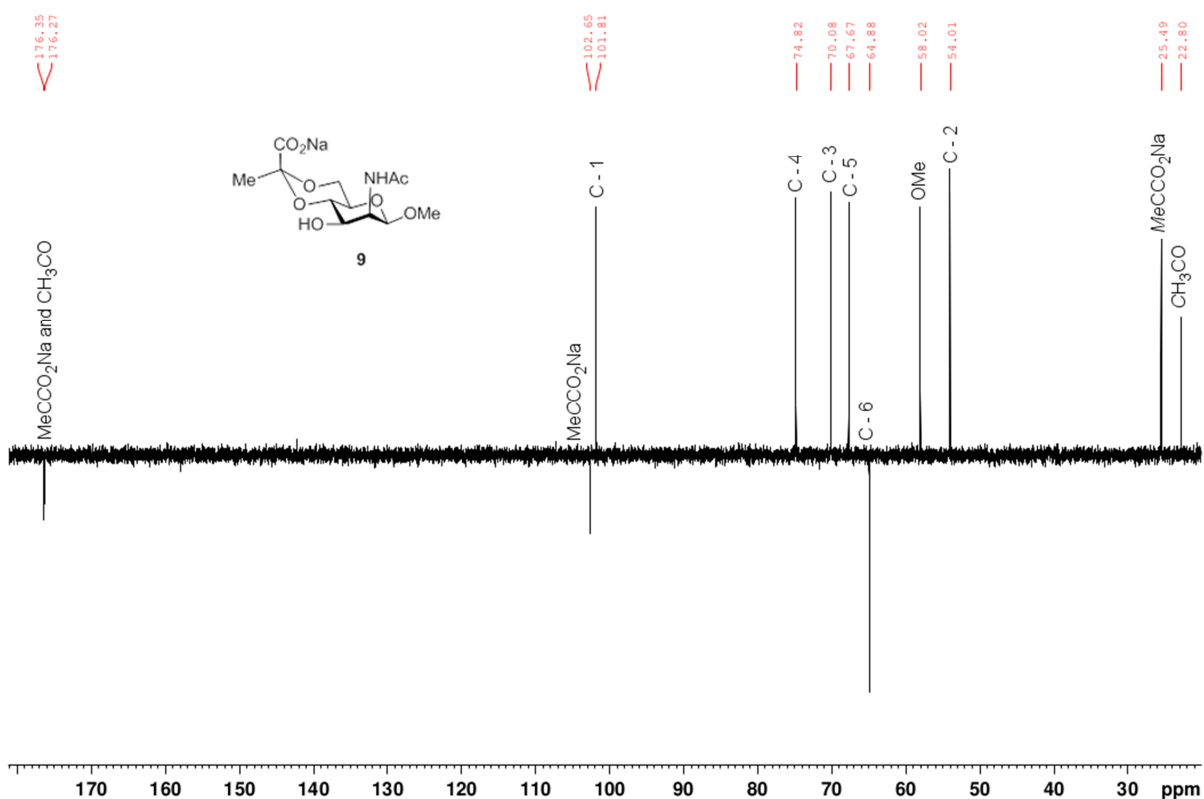


Figure 18: ¹³C-NMR spectrum (150 MHz, D₂O) of the final monosaccharide compound (9)

3.3. Synthesis of the Disaccharide

3.3.1. Glycosylation

O-Glycosyl trichloroacetimidates are advantageous compared to glycosyl bromides as they are stable at low temperatures for many months. Additionally they are known to act as strong glycosyl donors under relatively mild acid catalysis whereby ester protected trichloroacetimidates are less reactive than the ether protected ones. Rearrangement of the trichloroacetimidate to the corresponding trichloroacetamide might occur in case of an unreactive acceptor resulting in lower yields of the oligosaccharide³².

Anomeric stereocontrol leading to the 1,2-*trans* glycoside is usually given through neighbouring group participation of the protecting group at position 2. As the *N*-Troc (2,2,2-trichloroethoxycarbonyl) protecting group is known to induce the selective formation of the corresponding β-glycosides it is used here³⁷.

1,2-*Trans* glycosidation is performed via the Lewis acid catalyzed trichloroacetimidate method where the corresponding dissolved donor (**PL_076**) is added in 2 equivalents excess to a solution of the pyruvate-substituted acceptor (**8**). Stepwise addition of overall 0.2 equivalents trimethylsilyl trifluoromethanesulfonate using a stock solution activates the trichloroacetimidate leaving group and leads to the formation of the oxocarbenium ion. The desired β -linked disaccharide is formed within the nucleophilic attack of the 3-hydroxy group of the acceptor at the carbocation located at the anomeric position of the donor (see Figure 19). Reaction progress is only observed after warming the reaction mixture up to room temperature. The acceptor is not consumed completely despite long reaction time and is partly recycled by column chromatography. The formed side product is identified as the 3-*O*-trimethylsilyl-substituted acceptor compound. Acetonitrile as inert solvent gives the disaccharide in moderate yields ($\sim 30\%$). Difficulties with the preparation of dry acetonitrile results in side products due to hydrolysis of the donor compound. Usage of dry dichloromethane leads to less hydrolytic side product formation but a lower yield of the desired disaccharide (17%). The acid washed (AW) molecular sieve might help to retain the promoters activating property.

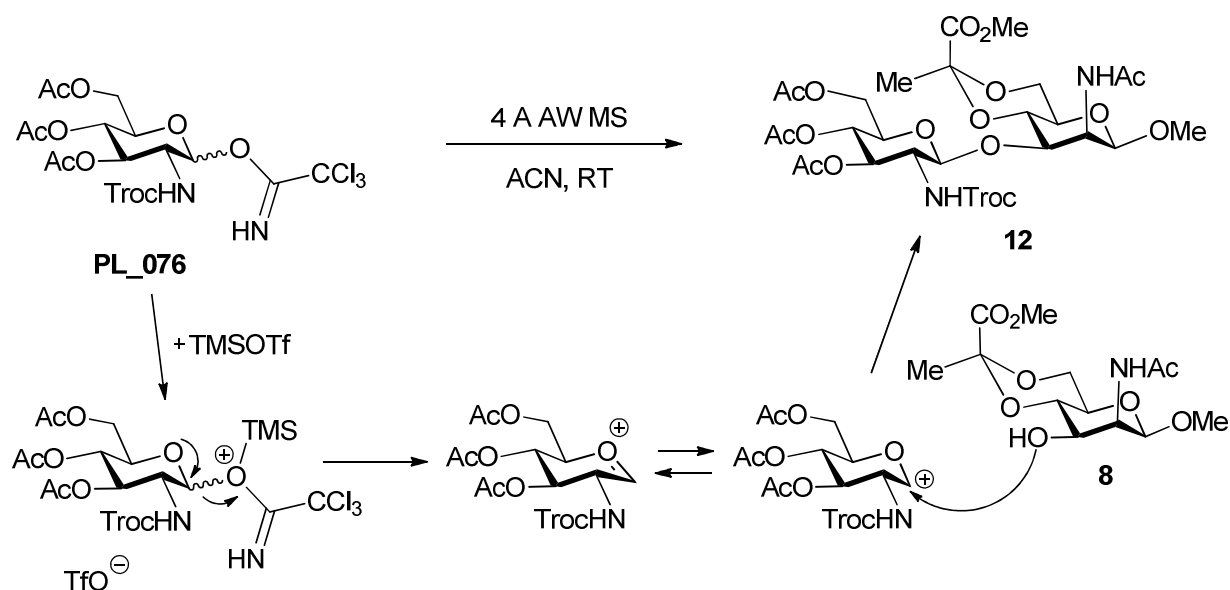


Figure 19: Mechanism for the glycosylation reaction between donor (**PL_076**) and acceptor (**8**)

Ziegler *et al.*²⁵ report that glycosylation reactions using various pyruvylated acceptors failed due to low reactivity of position 3. Maybe usage of pyruvylated donors or introduction of the pyruvate on the disaccharide stage would increase the yielding amounts of the desired pyruvate-substituted compound.

3.3.2. Troc-Removal followed by Acetylation

The *N*-Troc (2,2,2-trichloroethoxycarbonyl) protecting group is removed within reductive cleavage using 50 equivalents of zinc powder in glacial acetic acid. To obtain the 2-acetamido-2-deoxy sugar in good yields (83 %) the amine intermediate compound is directly acetylated under standard conditions with pyridine and acetic anhydride in the ratio 2:1. Use of a zinc-copper-couple instead of pure zinc powder doesn't improve the reaction progress.

Although not visible on TLC, ¹H-NMR analysis of the product shows about 12 % of an unidentified saccharide impurity. Loss of the pyruvate group under the reductive acidic conditions is improbable according to literature^{25,38}. Another possible side reaction would be the reduction of the methyl ester group to the corresponding primary alcohol that gets acetylated afterwards. This theory is not in agreement with the ¹H-NMR shifts that are observable for the impurity. Due to comigration on silica gel the desired compound (**13**) cannot be separated from the impurity by flash column chromatography or HPLC although using different solvent systems.

3.3.3. Complete Deprotection and Saponification

Removal of the *O*-acetyl protecting groups is carried out according to a standard-procedure in basic medium first described by G. Zemlén³⁹. Only catalytic amounts of sodium methoxide (0.1 molar solution) in dry methanol are required to execute the transesterification. After neutralization and removal of the methyl acetate by evaporation the deacetylated product can be directly used for the following saponification of the methyl ester. This step is carried out like described for the monosaccharide synthesis with 0.2 molar aqueous sodium hydroxide solution. A satisfying yield (87 %) is reached over the two steps.

Impure compound **13** is used in order to get rid of the impurity within these final steps. Although after purification with a Biogel-P2-column the final compound (**14**) looks pure on TLC, ¹H-NMR analysis shows again impurity signals. The signals might arise from the same saccharide impurity that is observed in compound **13**. Maybe the impurity compound is also converted under the given reaction conditions. Under the supposition that the compound with the reduced carboxylate ester is present, purification using AG 1x8 anion exchanger (HCO₃⁻ form) is tried but without success. The ¹H- and ¹³C-NMR spectra of the final compound containing about 8 % impurity are shown in Figure 20 and Figure 21. Calculation of the impurity is related to the multiplet signal at 4.25 ppm that is assumed to arise from a single proton.

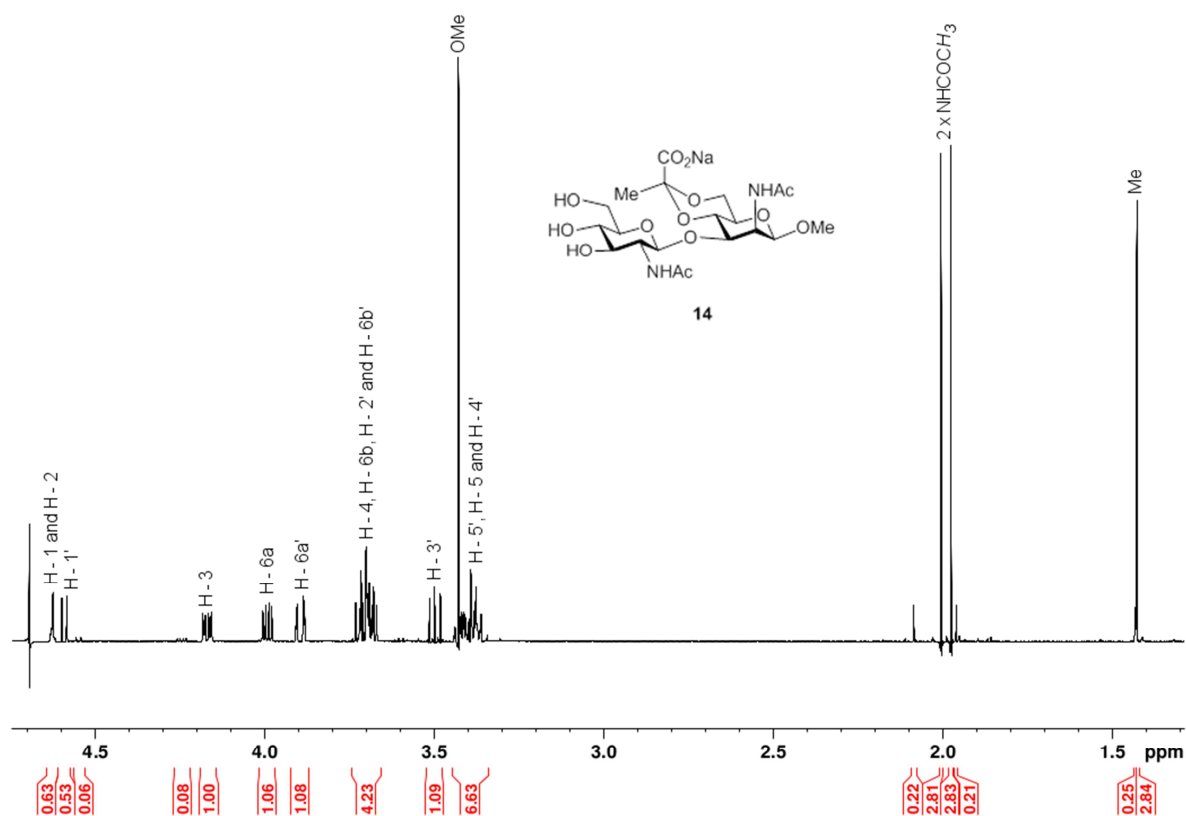


Figure 20: $^1\text{H-NMR}$ spectrum (600 MHz, D_2O) of the final disaccharide compound (14) containing about 8 % impurity

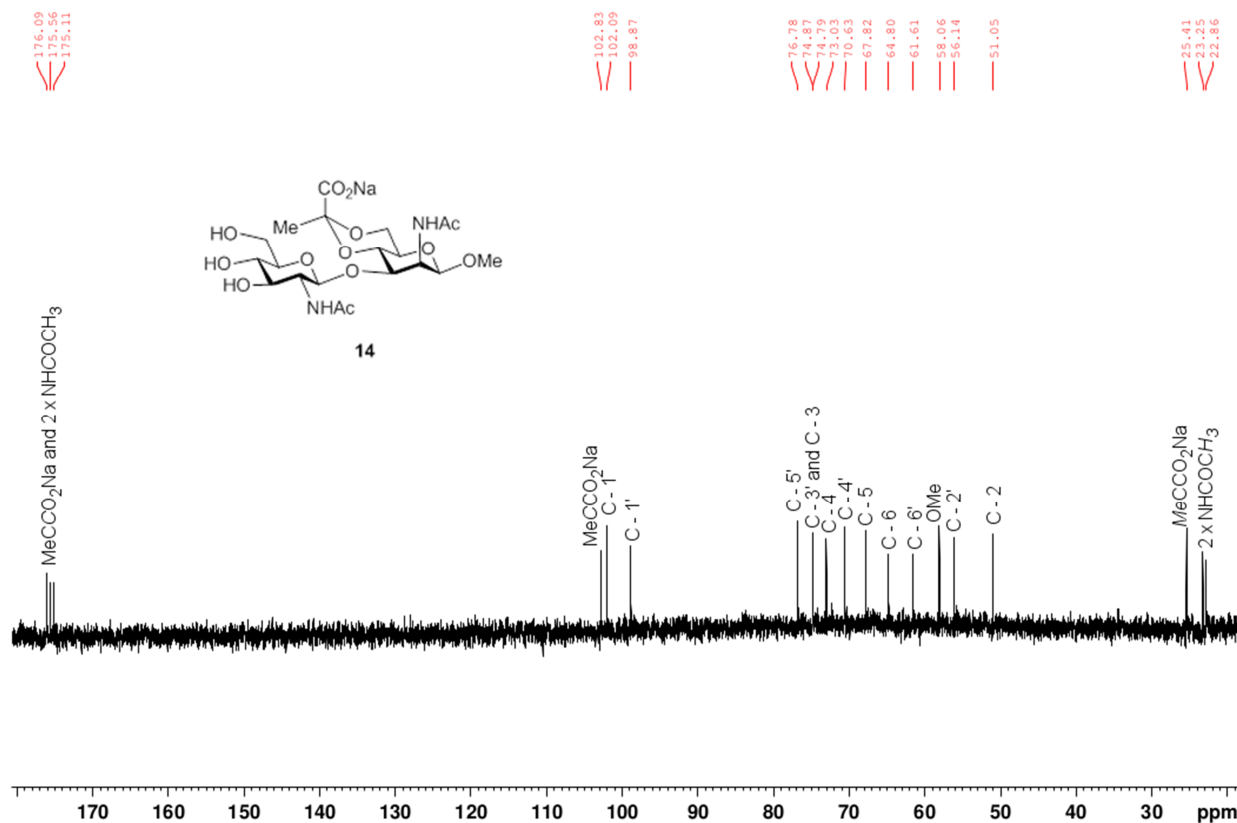


Figure 21: $^{13}\text{C-NMR}$ spectrum (600 MHz, D_2O) of the final disaccharide compound (14) containing about 8 % impurity

To simplify the assignment of the proton NMR signals of the final compound **14** a 2D TOCSY-NMR spectrum is recorded in addition to the usual 2D COSY-NMR. TOCSY-NMR enables the representation of correlations between not directly coupled spins, while through the COSY-NMR only correlations to neighboring nuclei are visible. Each of the two saccharide units can be seen as an isolated spin system whose scalar coupling network of protons can be displayed using the TOCSY experiment. The red cross peaks framed in green (see Figure 22) represent the couplings within the two spin systems as seen from the anomeric protons (mannopyranoside on the left, glucopyranoside on the right side).

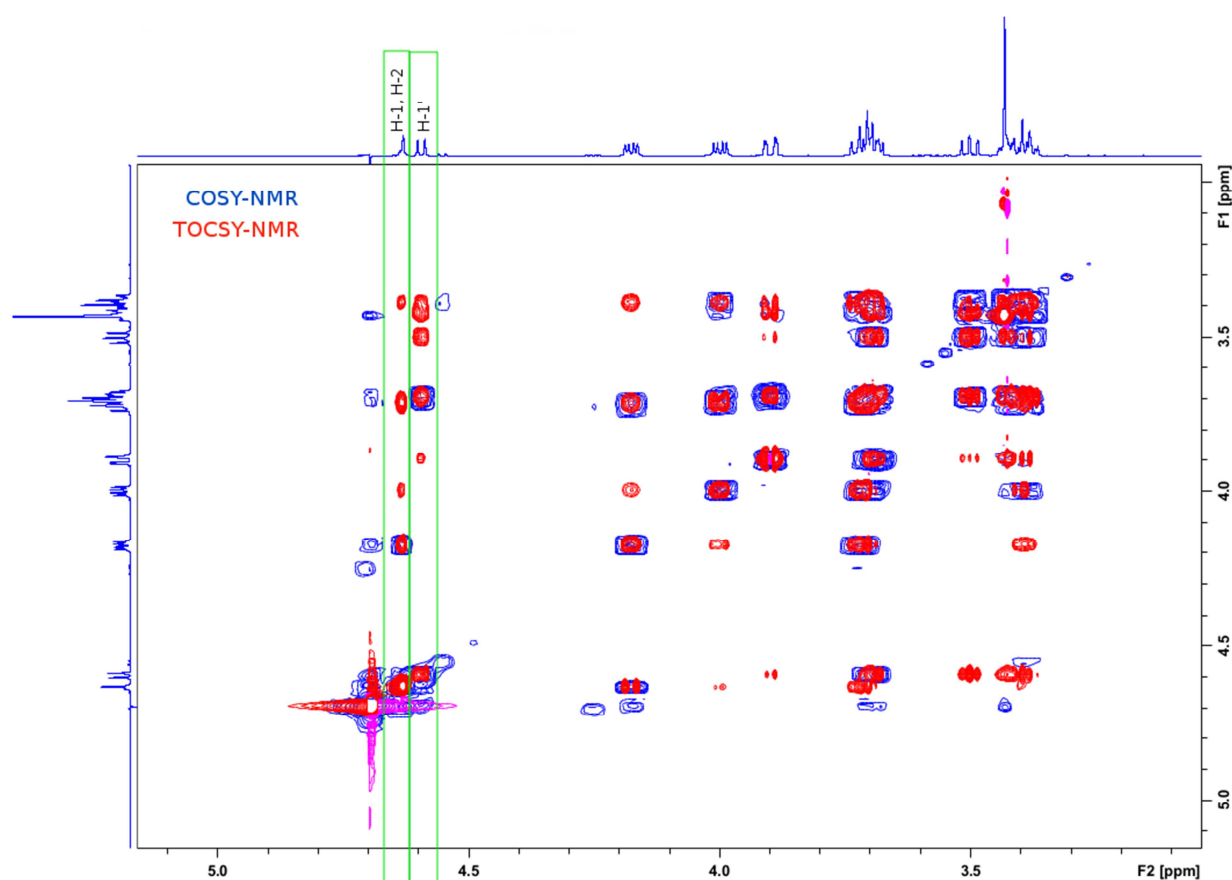


Figure 22: TOCSY-NMR (red) and COSY-NMR (blue) spectra of compound **14** (600 MHz, D₂O)

In order to find out whether the impurity signals observed in the ¹H-NMR spectrum are based on rotational isomerism a variable temperature (VT)-NMR study was performed with compound **14**. The phenomenon of rotamers occurs when rotation around a single bond (here the glycosidic linkage) is restricted by sterically unfavored substituents resulting in duplicity of NMR signals. VT-NMR makes identification of such equilibrating species possible as through increasing temperature the energy barrier for rotation can be overcome and leads to coalescence of the duplicity signals⁴⁰.

$^1\text{H-NMR}$ spectra of the sample (**14**) are recorded at six different temperatures ranging from 20 °C to 77 °C (see Figure 23 and Figure 24). Higher temperatures lead to signal broadening and a decrease in signal intensity. Regarding the framed impurity signals approaching to the signals of the main compound is not observed in this temperature range. Coalescence of the signals might be misinterpreted due to a general decrease in signal resolution.

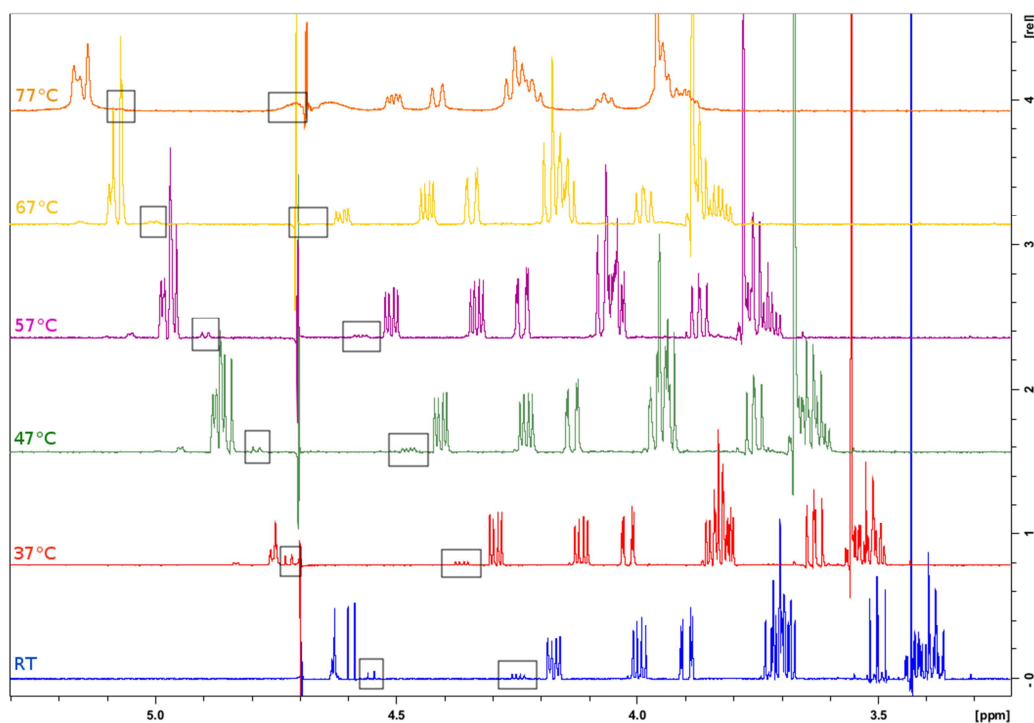


Figure 23: Expansion plot (5.3-3.2 ppm) showing the VT-NMR study of compound **14** (600 MHz, D_2O)

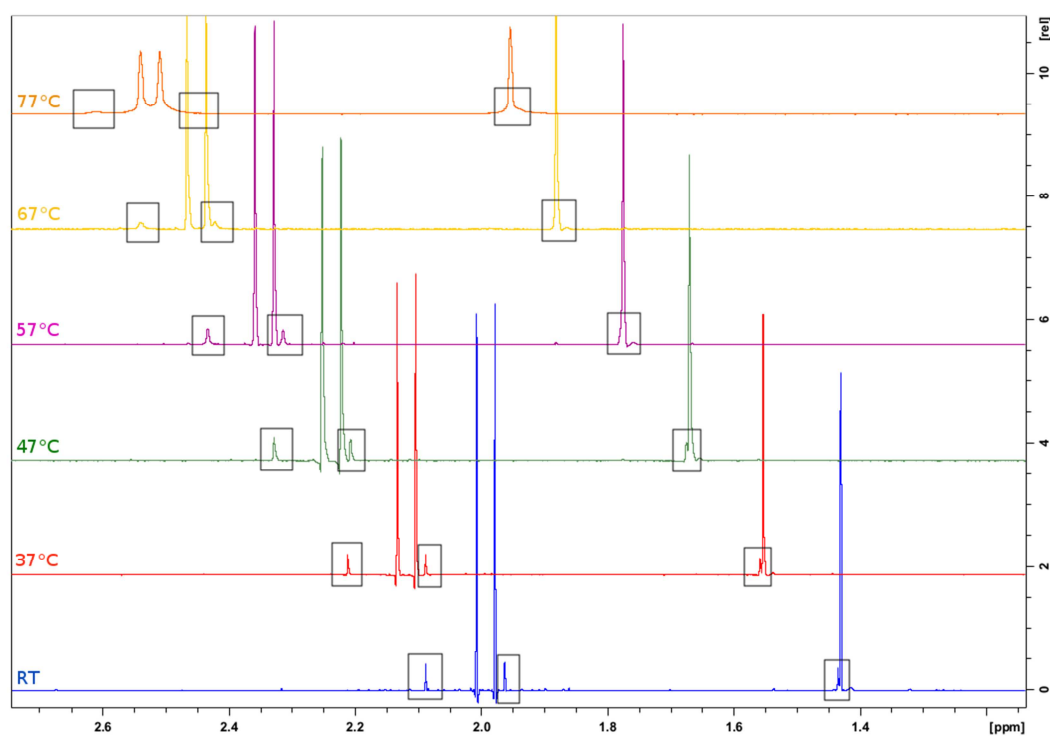


Figure 24: Expansion plot (2.7-1.2 ppm) showing the VT-NMR study of compound **14** (600 MHz, D_2O)

Another NMR method to prove the existence of rotamers is based on 1D selective chemical-exchange experiments⁴¹. Thereby two signals belonging to rotational isomers can be identified by creating a 1D NOE difference spectrum after irradiating selectively with the resonance frequency of one signal. As these NMR experiments give no useful results they are not shown and discussed in more detail.

3.4. Experiments involving SpaA protein

3.4.1. Cocrystallization Experiments

Cocrystallization experiments with the pyruvylated saccharides (**9** and **14**) and the truncated SpaA protein were performed successfully by the group of S. Evans *et al.* in Canada (University of Victoria, BC). The crystal structure of compound **9** is shown in Figure 25 and proves the (S)-configured diastereomer with the methyl group in equatorial position.

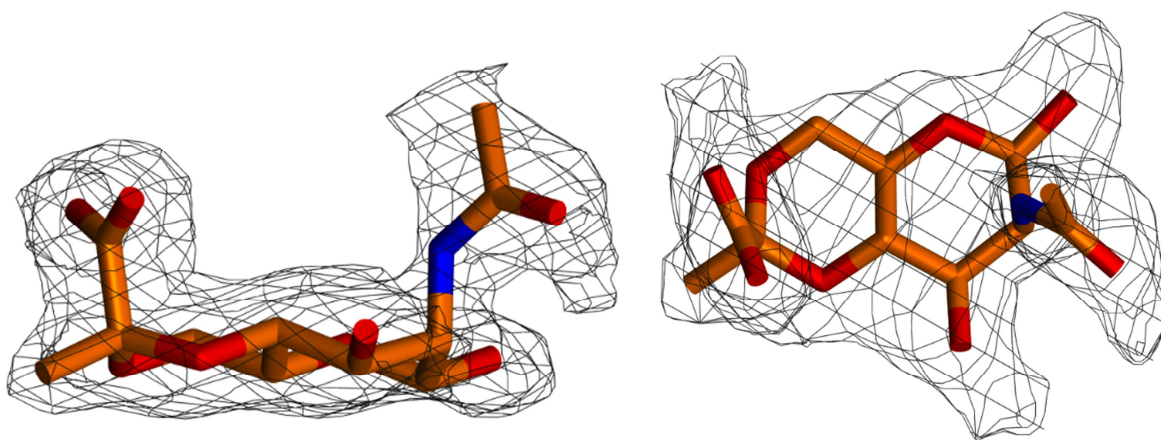


Figure 25: Crystal structures of the final monosaccharide compound (**9**) (S. Evans, unpublished results)

Figure 26 shows the ligand in the binding position of the truncated SpaA protein after successful cocrystallization. The amino acid residues that are in short distance to the ligand are illustrated separately. The pyruvic acid acetal group is surrounded by the basic amino acids arginine and lysine which might be involved in electrostatic interaction with the carboxyl group. The *N*-acetyl group seems to be in hydrophobic interaction with the leucine residue.

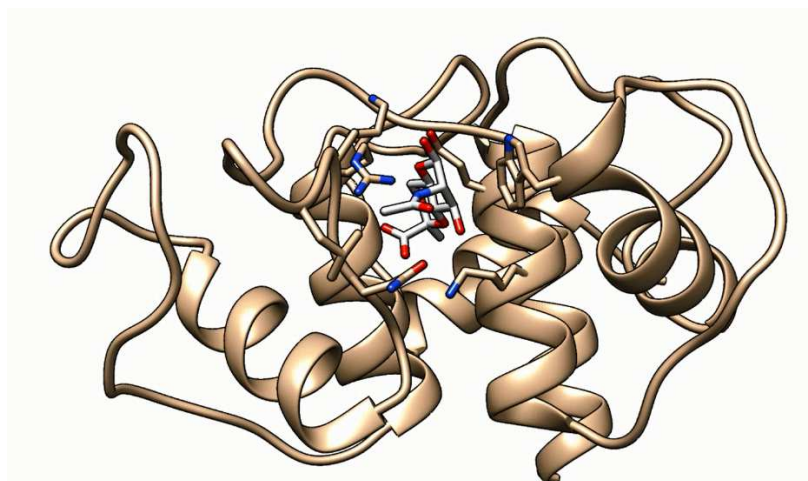


Figure 26: Ligand-bound crystal structure of truncated SpaA protein with ligand 9 (S. Evans, unpublished results)

The crystal structures of the pyruvate substituted disaccharide (**14**) are shown in Figure 27. In the course of the cocrystallization experiments disordering effects in certain regions of the protein are observed as the ligand binds in two different conformations. The ribbon diagram in Figure 28 displays the two conformations of the bound disaccharide. The conformation shown with light blue carbons corresponds with the left one in Figure 27 while the tan coloured binding conformation is given on the right side of Figure 27. The latter conformation causes disorder in the region of the dark blue coloured protein residues shown in Figure 28. Another interesting aspect is the possible intramolecular interaction between the two acetamido groups via a hydrogen bridge linkage.

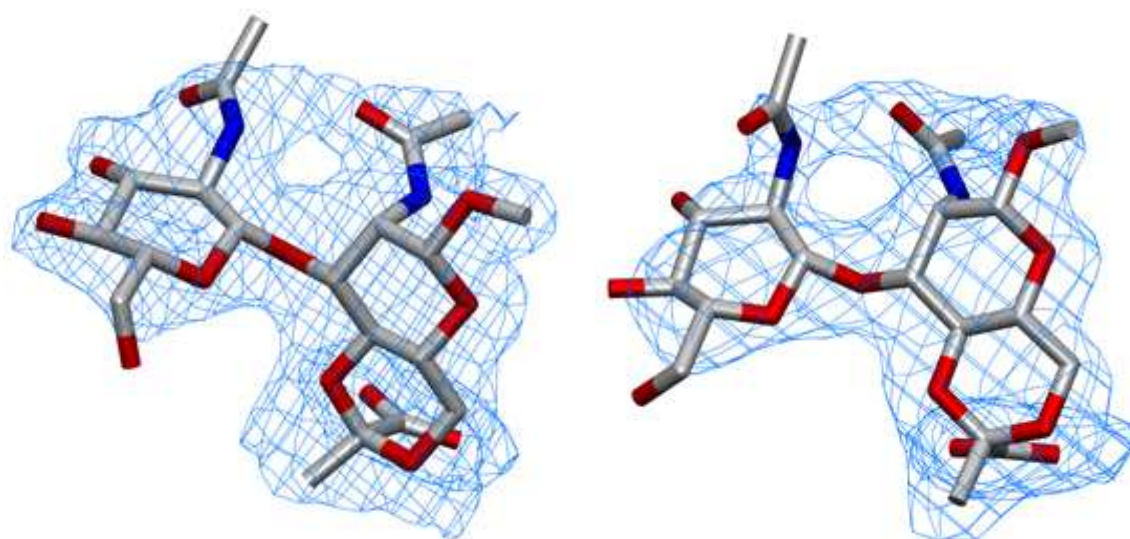


Figure 27: Crystal structures of the final disaccharide compound (14) showing the two different conformations (S. Evans, unpublished results)

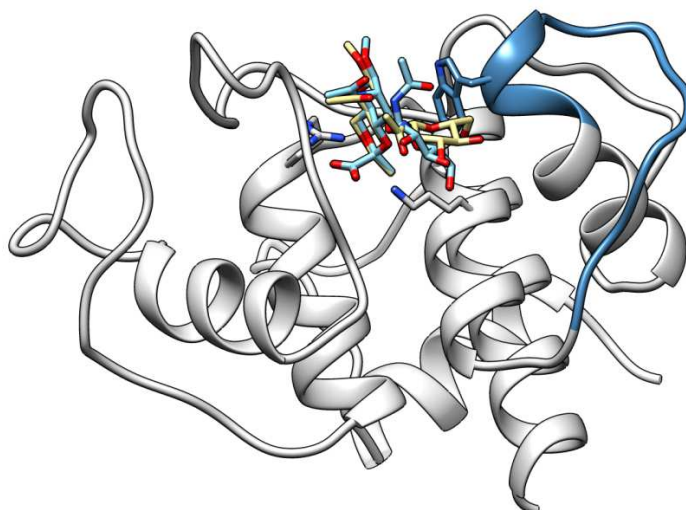


Figure 28: Ligand-bound crystal structure of truncated SpaA protein with ligand 14 showing two different binding conformations (S. Evans, unpublished results)

3.4.2. Isothermal Titration Calorimetry (ITC)

Isothermal titration calorimetry (ITC) is a common method for the thermodynamic characterization of biochemical association processes. In a typical ITC measurement a ligand solution is added to the protein solution in small portions. The released (exothermic reaction) or absorbed (endothermic reaction) heat resulting from the binding reaction is monitored by the ITC device after each addition. Through the given relation $\Delta G = -R \cdot T \cdot \ln K = \Delta H - T \cdot \Delta S$ further thermodynamic values which might provide useful information about the binding process can be calculated⁴².

All ITC measurements involving compound **6**, **9** and **14** are performed by Arturo López-Guzmán (Department of Nanobiotechnology, University of Natural Resources and Life Sciences, Vienna, unpublished results).

The resulting average thermodynamic parameters ($n=5$) for the pyruvate-substituted monosaccharide **9** are $2.65 \cdot 10^7$ l/mol for the binding constant (K_a) and -1.9194 cal/mol for the binding enthalpy (ΔH). The calculated values indicate a strong binding interaction that is probably caused by the presence of the pyruvic acid acetal.

ITC measurements involving the pyruvate-substituted disaccharide compound (**14**) and the non pyruvylated *N*-acetyl-mannosamine compound (**6**) are carried out as well. A very small release of binding enthalpy implies a low affinity of the ligands to the protein.

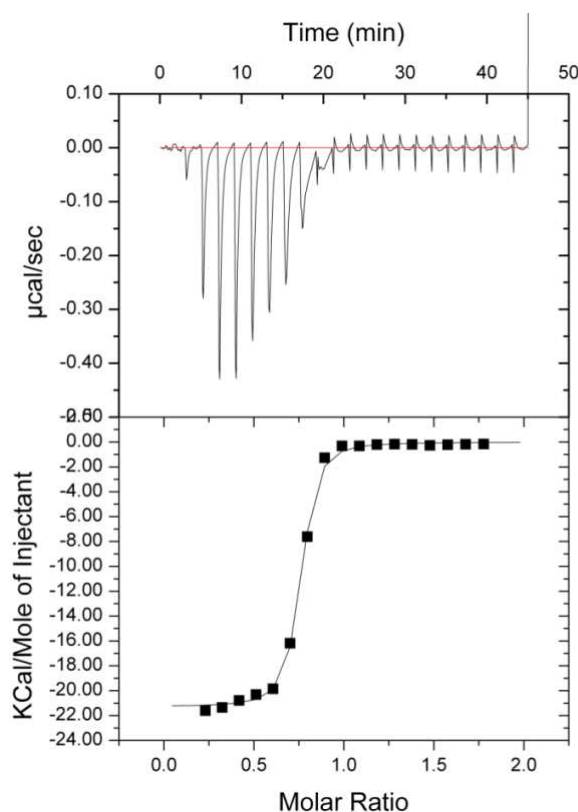


Figure 29: Example for resulting ITC diagrams (above: base line corrected raw data, below: titration curve) involving compound 9 and truncated SpaA protein (A. López-Guzmán, unpublished results)

3.4.3. Saturation Transfer Difference (STD) - NMR

STD-NMR is a popular technique to study protein-ligand interactions in solution. The experiment relies on the Nuclear Overhauser Effect (NOE) that is a matter of dipol-dipol-relaxation of two close nuclei in space. If one nuclei is saturated the other shows a change in NMR resonance intensity. For the NOE enhancement, which can be positive or negative, an approximate correlation with internuclear separation is given ⁴³.

In the case of STD-NMR the NOE between protein- and ligand-nuclei is of special interest. A weak binding interaction (dissociation constant K_D ranging from 10^{-8} M to 10^{-3} M) is required for the experiment to have an exchange between the bound and the free ligand state. In a typical STD experiment one measurement (on-resonance) is done involving the selective saturation of the protein by irradiating at a protein-characteristic region (around 0 ppm) where the ligand shows no signals while the other measurement (off-resonance) is carried out without protein saturation. By subtracting the signal intensities of the on-resonance-spectrum from the signal intensities of the off-resonance-spectrum the STD-spectrum is obtained (see

Figure 30). The difference spectrum shows only the signals of the ligand that received saturation transfer from the protein through the NOE. STD-NMR can be applied for identification of main structural conformations, determination of the ligand binding sites or ligand-based screening which is important for the drug-discovery process⁴⁴.

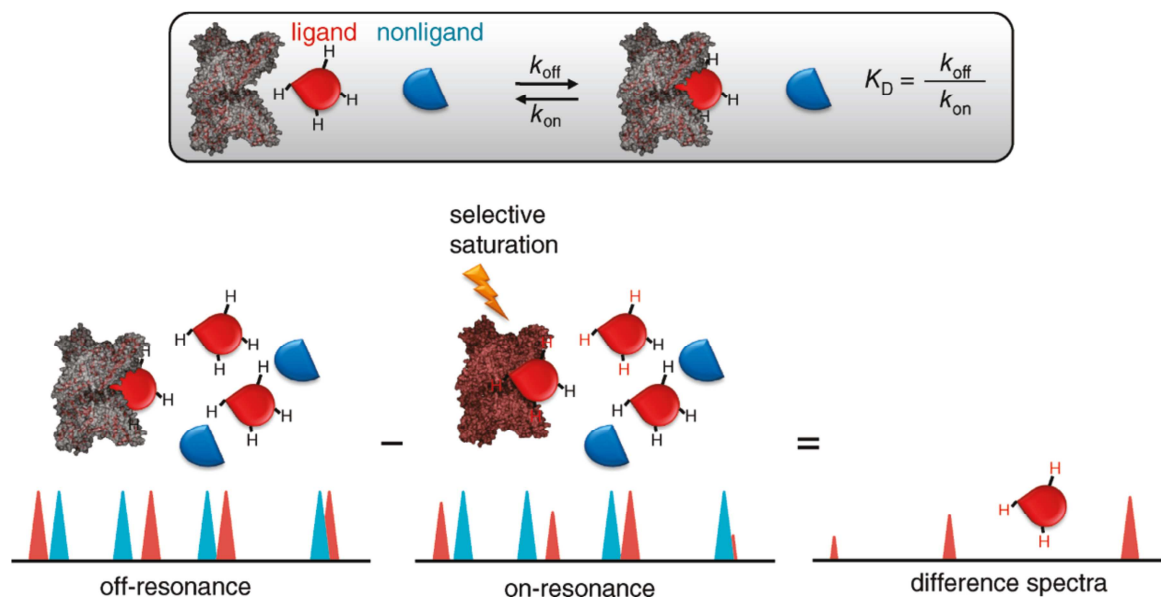


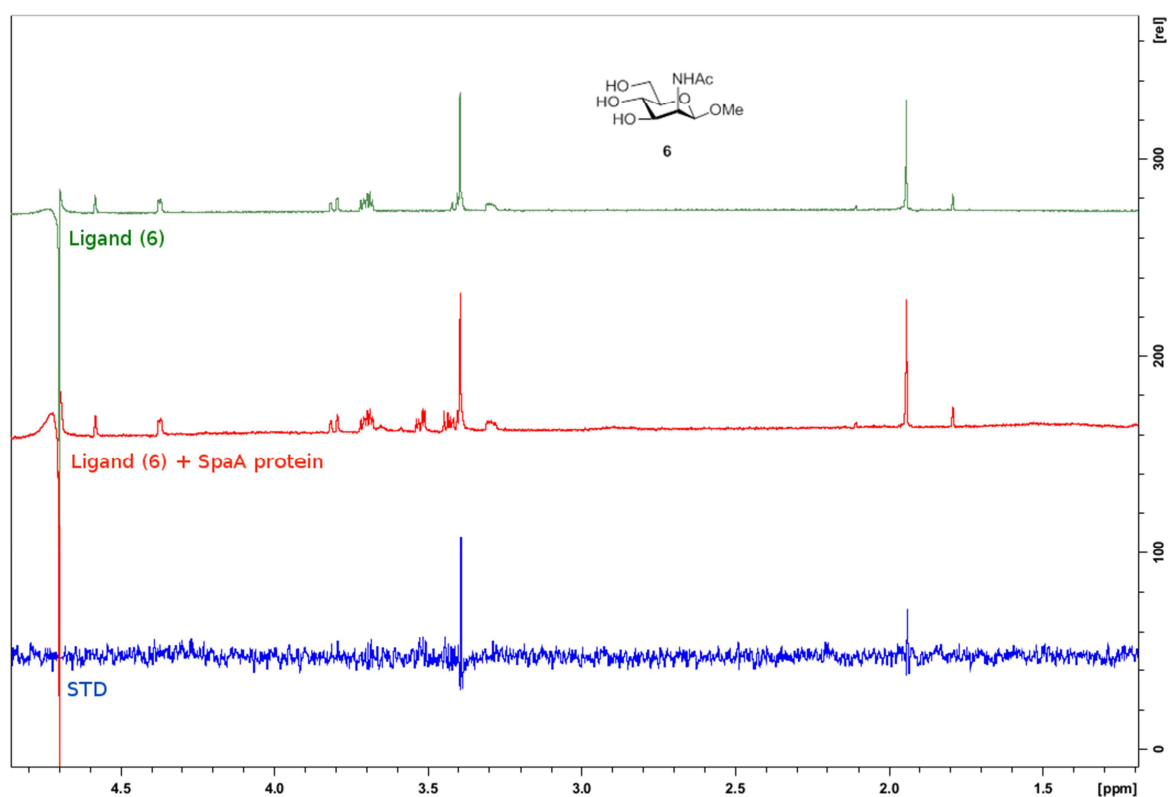
Figure 30: Scheme of the STD-NMR experiment⁴⁴

As usual for STD-NMR experiments the ligands are added in high excess (30 equivalents) to the protein. The experimental amounts for the STD-NMR experiment involving three different ligand compounds (**6**, **9** and **14**) and the truncated SpaA protein are given in Table 3. The general procedure starts with the preparation and measurement of the ligand solution in D₂O containing the desired amount of each ligand. In the next step the corresponding amount of protein is added using a stock solution in D₂O-phosphate buffer. After recording a standard ¹H-NMR spectrum of the mixture the STD measurement is done. For the STD-NMR experiment involving the ligand mixture (**6+9**) the prepared ligand solutions already containing the protein were mixed in a 1:1 ratio. The STD-NMR measurements are performed under the support of Lothar Brecker and Susanne Felsing (Institute of Organic Chemistry, University of Vienna).

	SpaA protein	Ligand 6	Ligand 9	Ligand 14
M [g/mol]	19884.4	235.11	327.09	530.17
m [μ g]	100	35.5	49.1	79.5
n [nmol]	5	150	150	150

Table 3: Experimental amounts for the STD-NMR experiments

According to the ITC results strong binding is expected for the pyruvylated monosaccharide (9) and very weak binding for the non pyruvylated monosaccharide (6) and the disaccharide (14). To obtain anyway acceptable STD signals under these binding conditions a high number of scans (160) and therefore long acquisition times (~ 13 h) are required. All STD-NMR experiments are performed with the same experimental parameters to keep the results comparable. The recorded spectra (ligand solution, mixture of ligand(s) and SpaA protein and STD) for each of the four NMR experiments are shown in Figure 31-Figure 34.

Figure 31: STD-NMR experiment recorded with compound 6 and SpaA protein (600 MHz, D₂O)

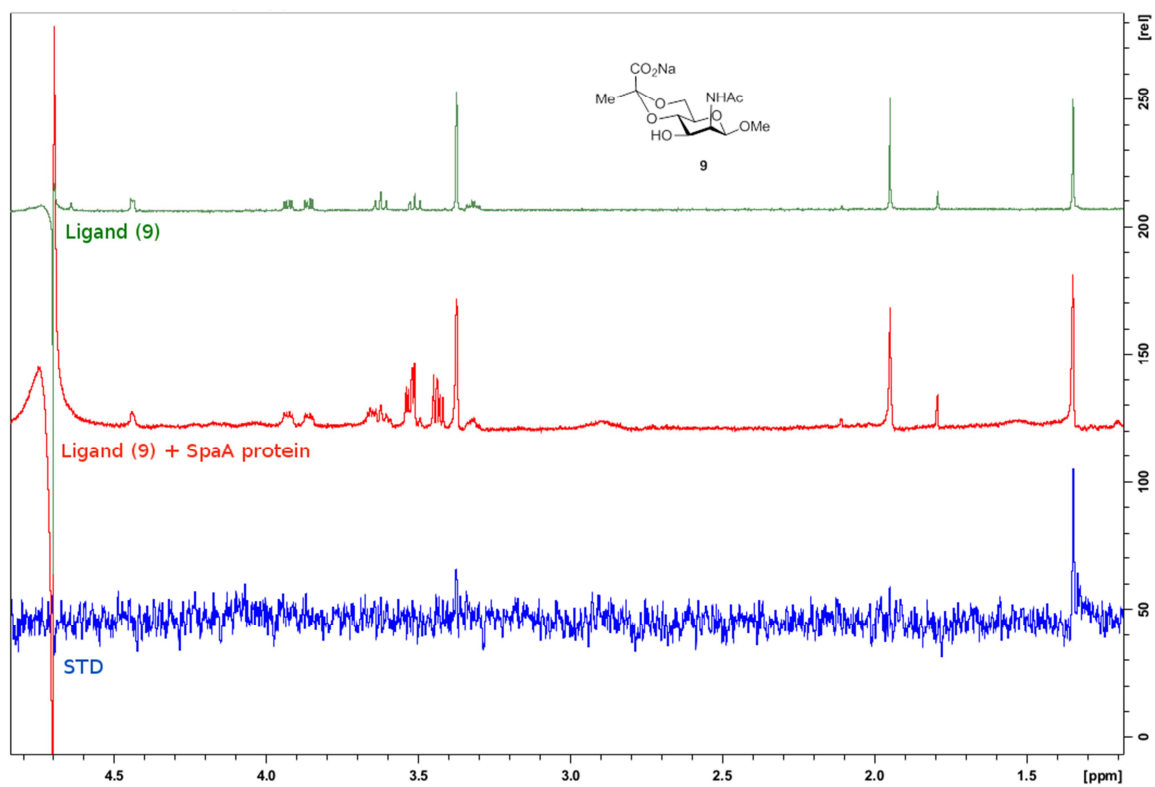


Figure 32: STD-NMR experiment recorded with compound 9 and SpaA protein (600 MHz, D₂O)

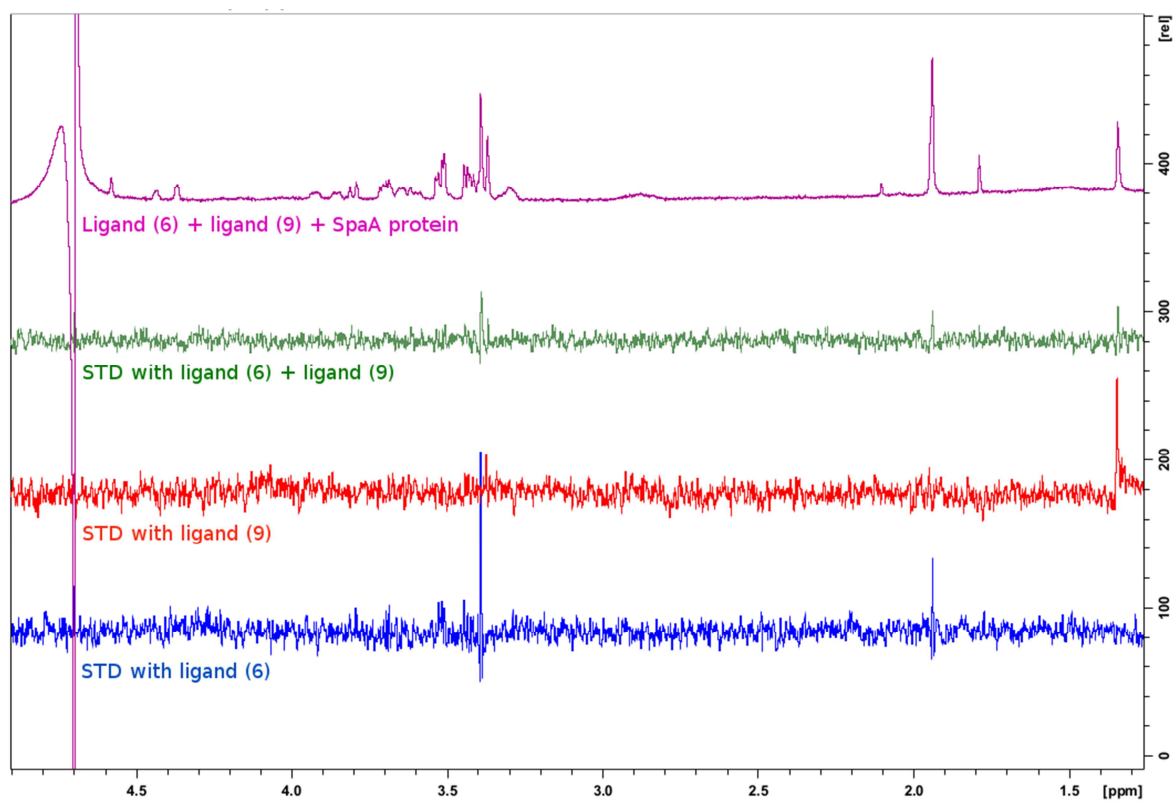


Figure 33: STD-NMR experiment recorded with compounds 6 + 9 and SpaA protein (600 MHz, D₂O)

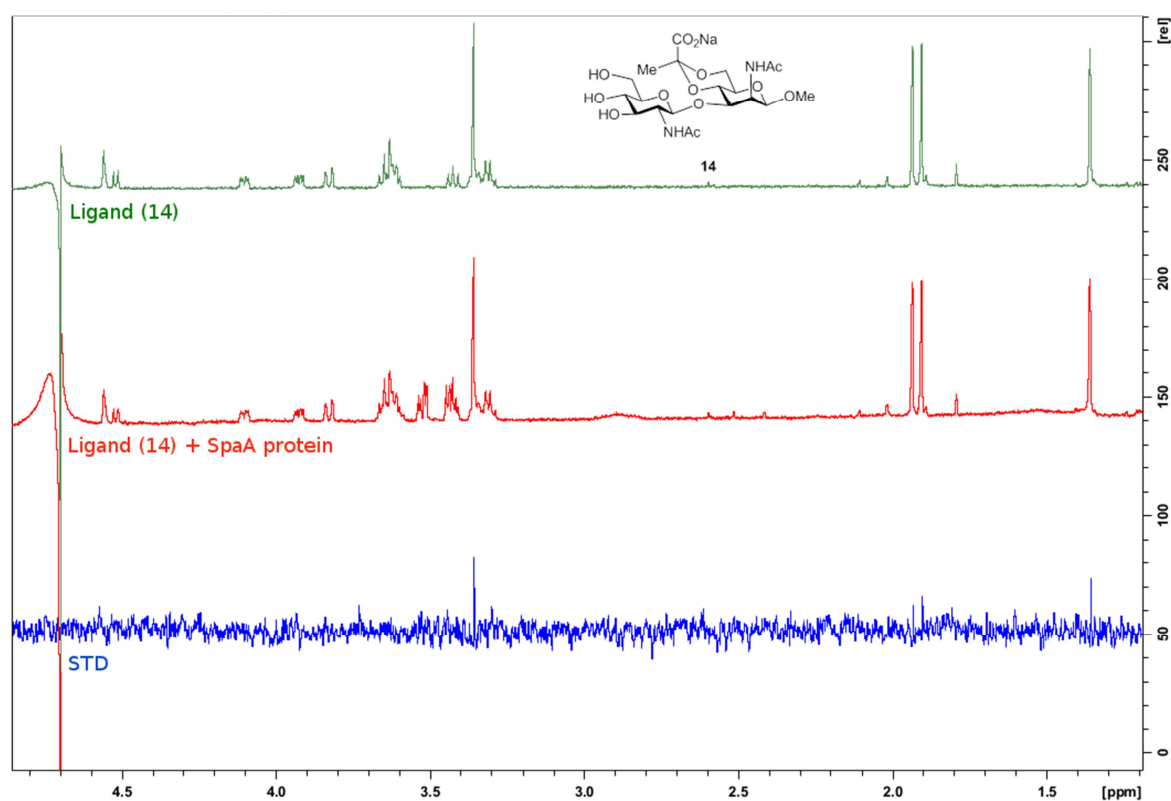


Figure 34: STD-NMR experiment recorded with compound 14 and SpaA protein (600 MHz, D₂O)

The resulting STD signals provide qualitative information about the ligand groups that are involved in the protein binding process. Quantitative analysis of the STD-NMR peaks is not possible due to the general weakness of the signals and the resulting signal to noise ratio.

Considering ligand **6** it can be seen in Figure 31 that magnetization transfer from the protein mainly happens via the 1-methoxy group and partly via the 2-*N*-acetyl group. The former might be due to unspecific binding which is obviously stronger than the specific binding of the latter. The binding behavior of ligand **6** observed in the STD-NMR experiment disagrees with the ITC measurements which have shown very weak binding. The STD spectrum of ligand **9** (see Figure 32) shows that the methyl group of the pyruvic acid acetal is mainly involved into the binding process. Additionally STD signals for the 1-methoxy group and a very weak one for the 2-*N*-acetyl group are observable. The pyruvate group is probably in competition with the *N*-acetyl group for binding the protein. According to the ligand-bound crystal structure of SpaA with ligand **9** (see Figure 26) STD-signals would have been expected also for the sugar ring hydrogens. Maybe longer acquisition times would be necessary to obtain visible signals representing also their binding contribution. Additionally a higher STD-effect would have been expected for the *N*-acetyl group due to its spatial proximity to a leucine residue.

The fact that STD-NMR is a dynamic process that takes place in solution might be responsible for the differences to the results of the cocrystallization experiment. The STD-NMR experiment involving both ligands **6** and **9** (see Figure 33) results in continuously weak signals for all methyl-containing groups. Displacement of one ligand through the other is therefore not noticeable although for the pyruvate-substituted monosaccharide (**9**) stronger and more selective binding would have been expected. For the disaccharide ligand **14** STD signals are observable (see Figure 34) although ITC measurements have predicted very low binding affinity. The 1-methoxy peak shows the highest intensity while the methyl peak is weaker and the two *N*-acetyl group peaks have the lowest intensity. The additional *N*-acetylglucopyranoside unit might cause another binding position than assumed for the monosaccharide.

Impurity signals around 3.5 ppm are observable in all experiments after addition of the protein. They might arise from residual HEPES (4-(2-hydroxyethyl)-1-piperazineethanesulfonic acid)-buffer in the used protein solution.

4. Experimental Part

4.1. General Methods

Thin layer chromatography (TLC) was performed using silica gel 60 F254 pre-coated glass plates (Merck) and for high performance thin layer chromatography (HPTLC) silica gel 60 F254 pre-coated glass plates with 2.5 cm concentration zone (Merck) were used. The compounds were detected using an anisaldehyde- H_2SO_4 -acetic acid reagent or a ninhydrin dip (for primary amines) followed by heating the plates up to 200-250 °C on a heating plate.

Column chromatography was performed with silica gel 60 (230-400 mesh, Merck). Glass columns with diameters ranging from 1 to 5 cm were used.

Size exclusion chromatography was performed on a Biogel-P2-column (polyacrylamide in water). For elution a prepared aqueous solution ($\text{H}_2\text{O} + 5\% \text{EtOH} + 8 \text{mg/l NaCl}$) was used.

Melting points were determined on a Kofler-type Reichert Thermovar micro hot stage microscope and are uncorrected.

Optical rotation was measured on a Perkin Elmer 143 B polarimeter. The concentrations are given in g/100ml.

High resolution mass analysis (HPLC-HRMS) was carried out from $\text{H}_2\text{O}/\text{CH}_3\text{CN}$ solutions (concentration 10-50 mg/l) using an HTC PAL system autosampler (CTC Analytics AG), an Agilent 1100/1200 HPLC with binary pumps, degasser and column thermostat (Agilent Technologies, Waldbronn, Germany) and Agilent 6210 ESI-TOF mass spectrometer (Agilent Technologies, Palo Alto, U.S.). Data analysis was done with Mass Hunter software (Agilent Technologies).

For lyophilisation Christ Beta 1-8 LD Freeze dryer was used.

Nuclear magnetic resonance (NMR) spectra were recorded either on a Bruker DPX 300 spectrometer or a Bruker Avance III 600 instrument. For spectra recorded in $\text{MeOH-}d_4$ the solvent peaks were used as reference signals (^1H : δ 3.31 ppm, ^{13}C : δ 49.00 ppm). Spectra recorded in CDCl_3 were either referenced to TMS (^1H : δ 0.00 ppm) or to the solvent peak (^{13}C : δ 77.16 ppm). For D_2O -spectra recently recorded reference spectra of DSS (^1H : δ 0.00 ppm) and 1,4-dioxane (^{13}C : δ 67.4 ppm) were used for calibration.

For NMR-data of the monosaccharides the ring-carbons and hydrogens were numbered from 1-6. In the NMR-spectra of the disaccharides the mannopyranoside-unit was numbered from 1-6 while the glucopyranoside-unit was numbered from 1'-6'. For the protecting groups the following abbreviations were used: Ph (Phenyl), Bn (Benzyl), Me (Methyl) and Ac (Acetyl).

Dry solvents (DCM, CH₃CN) were prepared on 3Å or 4Å-molecular sieves. Water content determination of the dry solvents was performed on a Mitsubishi Karl Fischer moisture meter model CA-21.

Regenerated Dowex 50W-X8 cation exchange resin (100-200 mesh) was used. Other solvents and chemicals were used as purchased from commercial suppliers unless otherwise noted.

Preparation of solutions:

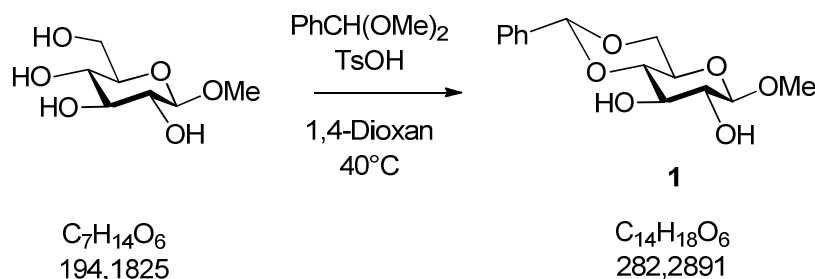
0.2 M NaOH: 160 mg NaOH were dissolved in 20 ml of distilled water.

0.1 TMS-triflate stock solution: 44 µl TMS-triflate were added to 956 µl of DCM.

0.1 M NaOMe-solution: Has already been prepared.

4.2. Synthesis of the Monosaccharide

4.2.1. Methyl 4,6-*O*-benzylidene- β -D-glucopyranoside (**1**)



The commercially available methyl pyranoside (5.48 g, 28.22 mmol) was dissolved in 1,4-dioxane (123 ml) in a twin-necked flask. A catalytic amount of *p*-TsOH monohydrate (53.7 mg, 0.282 mmol) as well as benzaldehyde dimethyl acetal (5.08 ml, 33.87 mmol) was added. The reaction mixture was stirred under reflux at 40 °C and was permanently flushed with argon. After 2 ½ hours another portion of benzaldehyde dimethyl acetal (847.1 μ l, 5.644 mmol) was added. The reaction was stopped after 4 hours. Dioxane was removed by evaporation and the remaining white solid (**1**) was treated with EtOAc. The suspension was filtered, the filtrate was concentrated and the remaining crystals were washed with cold H₂O and EtOAc. The residue obtained upon concentration of the filtrate was suspended in the washing liquor, the suspension was filtered and the crystals (**1**) were washed with hexane. Both products were air-dried.

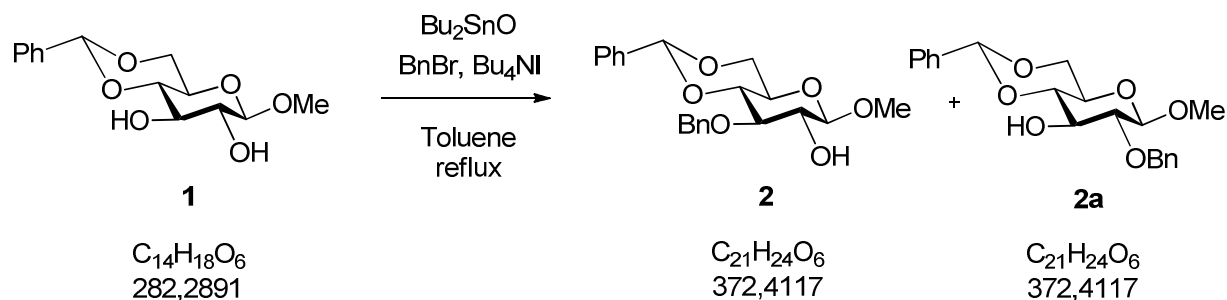
Yield: 6.68 g of white crystals (83.9 %)

R_f = 0.52 (EtOAc, TLC)

Melting Point: 195-197 °C (needle crystals), 189-191 °C (other crystals), lit. 199-200 °C⁴⁵
 After cooling down only the needle crystals were recrystallizing.

¹H-NMR (600 MHz, MeOH-*d*₄): δ 7.51-7.49 and 7.36-7.33 (m, 5H, *CHPh*), 5.58 (s, 1H, *CHPh*), 4.31 (d, 1H, ³J_{1,2}=7.7 Hz, H-1), 4.29 (dd, 1H, ³J_{5,6a}=4.7 Hz, ²J_{6a,6b}=10.4 Hz, H-6a), 3.77 (app. t, 1H, ³J_{5,6b}=²J_{6a,6b}=10.0 Hz, H-6b), 3.63 (app. t, 1H, ³J_{2,3}=³J_{3,4}=8.9 Hz, H-3), 3.53 (s, 3H, OMe), 3.46 (app. t, 1H, ³J_{3,4}=³J_{4,5}=9.1 Hz, H-4), 3.46-3.42 (m, 1H, H-5), 3.27 (dd, 1H, ³J_{1,2}=7.7 Hz, ³J_{2,3}=8.9 Hz, H-2) ppm

4.2.2. Methyl 3-O-benzyl-4,6-O-benzylidene-β-D-glucopyranosid (2)



Compound **1** (1.99 g, 7.053 mmol) and Bu_2SnO (2.14 g, 8.605 mmol) were dissolved in toluene (100 ml). The solution was boiled for 19 hours under reflux and azeotropic water removal using a water separator connected to the flask. The light yellow solution was reduced to half of the volume by evaporation. Benzyl bromide (0.986 ml, 7.547 mmol) and Bu_4NI (2.94 g, 7.970 mmol) were added before the reaction mixture was boiled under reflux for 8 hours. More benzyl bromide (0.986 ml, 7.547 mmol) was added to the reaction mixture as TLC still showed educt. The reaction was stopped after 4 ½ h and the brown solution was concentrated. The residue was treated with toluene: EtOAc 5:1, the remaining white solid (**2**) was filtered and dissolved in EtOAc. The first filtrate was concentrated and the procedure was repeated twice using pure toluene. The EtOAc solutions were combined and concentrated to dryness. The remaining crude mixture was purified by column chromatography (toluene: EtOAc 5:1 to toluene: EtOAc 3:1). The pink product fraction was washed with $\text{Na}_2\text{S}_2\text{O}_3$ to reduce the iodine. The light yellow organic phases were combined, dried over MgSO_4 , filtered and concentrated to obtain more of product **2**. The side product (**2a**) was collected and concentrated as well.

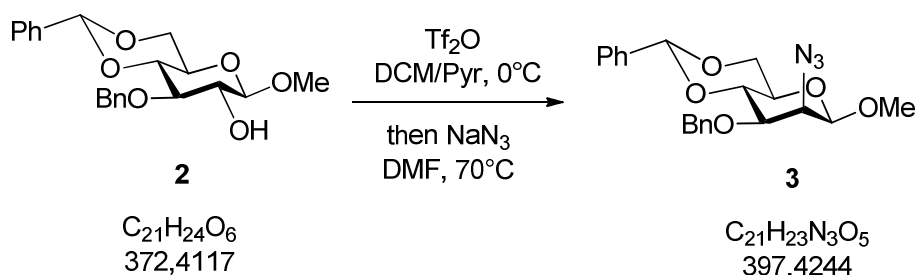
Yield: 1.59 g of a light yellow solid (**2**) (60.6 %), 1.02 g of an off-white solid (**2a**) (38.8 %)

R_f = 0.59 (toluene: EtOAc 1:1, TLC)

$^1\text{H-NMR}$ (600 MHz, CDCl_3): δ 7.50-7.48 and 7.41-7.28 (m, 10H, 1x CHPh and 1x OCH_2Ph), 5.58 (s, 1H, CHPh), 4.98 and 4.79 (2d, 2H, $^2J=11.6$ Hz, OCH_2Ph), 4.37 (dd, 1H, $^3J_{5,6a}=5.0$ Hz, $^2J_{6a,6b}=10.5$ Hz, H-6a), 4.33 (d, 1H, $^3J_{1,2}=7.7$ Hz, H-1), 3.81 (app. t, 1H, $^3J_{5,6b}=^2J_{6a,6b}=10.3$ Hz, H-6b), 3.71 (app. t, 1H, $^3J_{3,4}=^3J_{4,5}=9.1$ Hz, H-4), 3.67 (app. t, 1H, $^3J_{2,3}=^3J_{3,4}=8.9$ Hz, H-3), 3.58 (s, 3H, OMe), 3.58-3.54 (m, 1H, H-2), 3.46 (ddd, 1H, $^3J_{4,5}=9.1$ Hz, $^3J_{5,6a}=5.0$ Hz, $^3J_{5,6b}=10.1$ Hz, H-5), 2.44 (1H, $^3J_{2,2-\text{OH}}=2.2$ Hz, 2-OH) ppm

$^1\text{H-NMR}$ data is identical to the data published by van der Ven *et al.* ⁴⁶

4.2.3. Methyl 2-azido-3-O-benzyl-4,6-O-benzylidene-2-deoxy- β -D-mannopyranoside (**3**)



Compound **2** (298.0 mg, 0.800 mmol) was co-evaporated twice with toluene before dry DCM (5.14 ml) and pyridine (2.57 ml) were added. The solution was stirred on an ice-bath and under argon-atmosphere before triflic anhydride (0.326 ml, 1.936 mmol) was added. After 45 minutes additional triflic anhydride (0.050 ml, 0.297 mmol) was injected to the solution as TLC showed incomplete conversion of the educt. The reaction was stopped after 1 hour and 15 minutes. The mixture was diluted with DCM and was washed once with saturated aqueous NaHCO_3 solution. The yellowish organic phase was concentrated to dryness and the brown residue was dissolved in anhydrous DMF (8.57 ml). Sodium azide (260.1 mg, 4.001 mmol) was added and the reaction mixture was stirred under reflux for 2 hours at below 70 °C. Stirring was continued for another 19 hours at 70 °C. The off-white solid was removed by filtration of the reaction mixture over Celite. The still murky filtrate was concentrated and the residue was suspended in DCM. The suspension was filtered again over Celite and the clear yellow filtrate was concentrated. Purification of the crude product **3** was done by column chromatography (toluene: EtOAc 6:1).

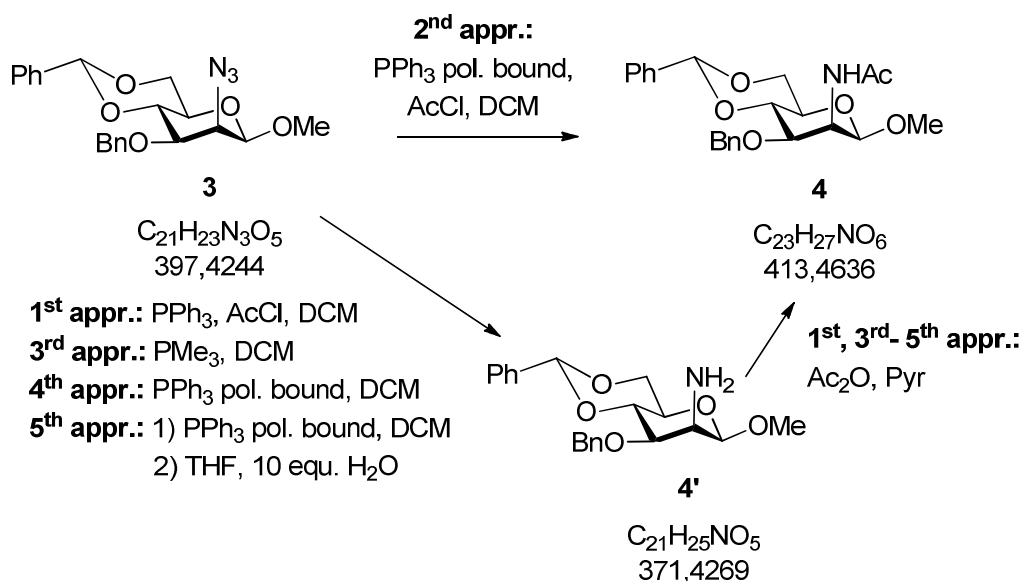
Yield: 269 mg of a light yellow syrup (84.7 %)

R_f = 0.61 (toluene: EtOAc 6:1, TLC)

$^1\text{H-NMR}$ (600 MHz, CDCl_3): δ 7.50-7.48 and 7.41-7.25 (m, 10H, 1xCHPh and 1xOCH₂Ph), 5.60 (s, 1H, CHPh), 4.89 and 4.75 (2d, 2H, $^2J=12.4$ Hz, OCH₂Ph), 4.46 (d, 1H, $^3J_{1,2}=1.4$ Hz, H-1), 4.32 (dd, 1H, $^3J_{5,6a}=5.0$ Hz, $^2J_{6a,6b}=10.5$ Hz, H-6a), 4.04 (app. t, 1H, $^3J_{3,4}=^3J_{4,5}=9.5$ Hz, H-4), 3.98 (dd, 1H, $^3J_{1,2}=1.4$ Hz, $^3J_{2,3}=3.7$ Hz, H-2), 3.88 (app. t, 1H, $^3J_{5,6b}=^2J_{6a,6b}=10.3$ Hz, H-6b), 3.75 (dd, 1H, $^3J_{2,3}=3.7$ Hz, $^3J_{3,4}=9.6$ Hz, H-3), 3.54 (s, 3H, OMe), 3.46 (ddd, 1H, $^3J_{4,5}=9.6$ Hz, $^3J_{5,6a}=5.0$ Hz, $^3J_{5,6b}=10.0$ Hz, H-5) ppm

The chemical shifts agree with the data given in Augé *et al.*⁴⁷

4.2.4. Methyl 2-acetamido-3-O-benzyl-4,6-O-benzylidene-2-deoxy- β -D-mannopyranoside (**4**)



1st approach:

Compound **3** (210.5 mg, 0.530 mmol), dissolved in dry DCM (7.26 ml), was stirred at RT under argon-atmosphere. Acetyl chloride (123 μ l, 1.727 mmol) and a solution of triphenylphosphine in DCM (245.9 mg, 0.938 mmol) were added. Stirring was continued under the same conditions for 18 hours. Pyridine (7.26 ml) and acetic anhydride (726 μ l) were added to acetylate remaining free amine. After another 3 hours of stirring at RT and under argon-atmosphere the reaction was quenched with dry MeOH (3.6 ml). The mixture was diluted with toluene and was concentrated carefully. The residue was co-evaporated for four times with toluene. Purification of the crude product was done by column chromatography (toluene: EtOAc 5:1 to EtOAc: toluene 3:1).

Yield: 258.9 mg of a yellowish syrup (118.2 %, containing residual PPh₃)

2nd approach:

To a solution of compound **3** (62.8 mg, 0.158 mmol) in dry DCM (3.0 ml) polymer bound PPh₃ suspended in DCM (1.6 mmol/g resin, 100-200 mesh, 197.5 mg, 0.316 mmol) and acetyl chloride (37 μ l, 0.515 mmol) were added. The reaction mixture was stirred at RT under argon-atmosphere for 22 hours. The mixture was diluted with DCM and cooled on ice before a few drops of Et₃N were added. After filtration toluene was added to the filtrate which was

then concentrated. The crude product was purified by column chromatography (toluene: EtOAc 1:1 to pure EtOAc).

Yield: 14.6 mg of a colourless syrup (**4**) (22.3 %), 39.4 mg of a white solid (side product) (63.8 %)

3rd approach:

Compound **3** (9.5 mg, 0.024 mmol) was dissolved in DCM (1.0 ml). The solution was stirred at RT under argon-atmosphere before PMe_3 (7 μl , 0.072 mmol) was added. After 45 minutes of stirring 2 drops of H_2O were added. Reaction was stopped after 2 ½ hours when TLC showed two products detectable with ninhydrin. The mixture was diluted with DCM and dried with MgSO_4 . After filtration the filtrate was concentrated and dried. The residue was dissolved in pyridine (1.0 ml) and acetic anhydride (9 μl , 0.024 mmol) was added. The mixture was stirred at RT under argon-atmosphere for 2 hours. A second portion of acetic anhydride (5 μl , 0.053 mmol) was injected and stirring was continued for another 24 hours. Although conversion was not complete the mixture was quenched with MeOH (100 μl). The mixture was concentrated in vacuo and the residue was co-evaporated twice with toluene. After dilution with DCM the solution was washed twice with saturated aqueous NaHCO_3 -solution. The organic phase was dried with MgSO_4 , was filtered and concentrated. Purification was done by column chromatography (EtOAc: toluene 3:1 to pure EtOAc).

Yield: 3.3 mg of a colourless syrup (33.4 %)

4th approach:

Compound **3** (16.4 mg, 0.041 mmol) and polymer bound PPh_3 (1.6 mmol/g resin, 100-200 mesh, 57.9 mg, 0.093 mmol) were treated with dry DCM (1.5 ml). The reaction mixture was stirred at RT under argon-atmosphere. After about 17 hours another portion of polymer PPh_3 (1.6 mmol/g resin, 100-200 mesh, 30.8 mg, 0.049 mmol) and more DCM (1.0 ml) was added. Stirring was continued and after 22 hours the mixture was filtered. The filtrate was concentrated to dryness and the oily residue was dried. The residue was dissolved in pyridine (1.5 ml) and acetic anhydride (15.6 μl) was added. Stirring at RT and under argon-atmosphere was performed for 16 hours until conversion was almost complete. Quenching with MeOH (200 μl) was followed by evaporation and two times co-evaporation with toluene. The yellow oily residue was diluted with DCM and washed once with saturated aqueous

NaHCO₃-solution. The organic phase was dried with MgSO₄, filtered and concentrated. The crude product **4** was purified by column chromatography (EtOAc: toluene 3:1 to pure EtOAc).

Yield: 5.8 mg of a yellowish syrup (34.0 %)

5th approach:

Compound **3** (787.0 mg, 1.980 mmol) and polymer bound PPh₃ (1.6 mmol/g resin, 100-200 mesh, 3.094 g, 4.951 mmol) were treated with dry DCM (26.0 ml). The mixture was stirred at RT and under argon-atmosphere for 18 hours. The polymer was filtered and washed several times with EtOAc, DCM and MeOH. The yield of **4'** obtained from the filtrate was very low (50 mg). The polymer was suspended with CH₃CN (20.0 ml), H₂O (600 µl, 33.3 mmol) was added and the mixture was stirred for 30 minutes at RT. After filtration and purging with EtOAc the filtrate was concentrated and showed low yield of **4'** again (20 mg). The polymer was treated with THF (20.0 ml) and H₂O (360 µl, 20.0 mmol). The reaction mixture was stirred 1 hour at 55 °C and another 15 hours at RT. The polymer was filtered and washed with EtOAc several times. Concentration of the filtrate gave a higher yield of **4'** (550 mg). Hydrolysis of the polymer was repeated with the same reagent conditions and stirring for 2 hours at 55 °C. After filtration and evaporation another amount of intermediate **4'** was obtained (120 mg). The first portion of **4'** (650 mg, 1.75 mmol) was dissolved in pyridine (2.0 ml) and the solution was treated with acetic anhydride (1.3 ml, 13.8 mmol). Acetylation was finished after stirring for 1 hour 45 minutes at RT and under argon-atmosphere. The mixture was concentrated and quenched with MeOH. It was again concentrated in vacuo and co-evaporated once with toluene. The second portion of the intermediate **4'** (122 mg, 0.328 mmol) was acetylated with pyridine (1.5 ml) and Ac₂O (0.5 ml, 5.29 mmol) as well. Reaction was complete after 30 minutes. The mixture was concentrated in vacuo, treated with MeOH and concentrated to dryness again. The combined acetylated crude products **4** were purified by MPLC (EtOAc: toluene 3:1 to pure EtOAc, flow rate: 60 to 50 ml/min).

Yield: 615 mg of a yellow syrup (75.1 %)

R_f = 0.42 (EtOAc, HPTLC)

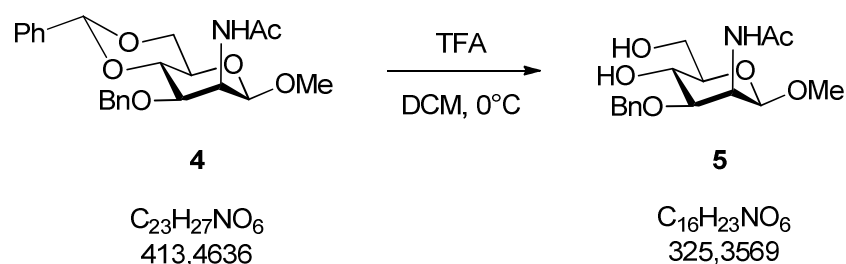
[α]_D²⁰ - 62.9° (c 1.0, CHCl₃)

¹H-NMR (600 MHz, CDCl₃): δ 7.50-7.48 and 7.41-7.29 (m, 10H, 1xCHPh and 1xOCH₂Ph), 5.76 (d, 1H, ³J_{NH,2}=9.6 Hz, NH), 5.59 (s, 1H, CHPh), 4.88 (ddd, 1H, ³J_{1,2}=1.9 Hz, ³J_{2,3}=4.1 Hz, ³J_{NH,2}=9.6 Hz, H-2), 4.81 and 4.66 (2d, 2H, ²J=12.2 Hz, OCH₂Ph), 4.53 (d, 1H, ³J_{1,2}=1.9 Hz, H-1), 4.35 (dd, 1H, ³J_{5,6a}=4.9 Hz, ²J_{6a,6b}=10.4 Hz, H-6a), 3.80 (app. t, 1H, ³J_{5,6b}=²J_{6a,6b}=10.3 Hz, H-6b), 3.79-3.75 (m, 2H, H-3 and H-4), 3.50 (s, 3H, OMe), 3.46 (dt, 1H, ³J_{4,5}=³J_{5,6b}=9.7 Hz, ³J_{5,6a}=4.9 Hz, H-5), 2.08 (s, 3H, CH₃CO) ppm

¹³C-NMR (150 MHz, CDCl₃): δ 170.83 (s, CH₃CO), 137.93 and 137.35 (2s, 1xCHPh and 1xOCH₂Ph), 129.16-126.18 (10d, 5xCHPh and 5xOCH₂Ph), 101.76 (d, CHPh), 101.48 (d, C-1), 79.06 and 75.63 (2d, C-3 and C-4), 71.80 (t, OCH₂Ph), 68.92 (t, C-6), 67.16 (d, C-5), 57.15 (q, OMe), 50.03 (q, CH₃CO) ppm

HR-MS: [M+Na]⁺ m/z (predicted) = 436.1731, m/z (found) = 436.1715, Δ = 3.77 ppm

4.2.5. Methyl 2-acetamido-3-O-benzyl-2-deoxy-β-D-mannopyranoside (5)



1st approach:

Compound **4** (224.9 mg, 0.544 mmol, containing residual PPh₃) in dry DCM (20 ml) was stirred on an ice-bath and under argon-atmosphere. Trifluoroacetic acid (4.5 ml, 58.411 mmol) was added and stirring was continued under the same conditions. The reaction was stopped after 40 minutes when conversion was almost complete. Solvent and excess of TFA was removed by concentration. Co-evaporation with toluene was done twice. The crude residue was purified by column chromatography (EtOAc: toluene 3:1 to EtOAc: 2-propanol 2:1).

Yield: 164 mg of a colourless syrup (95.2 % over two steps, containing residual PPh₃)

An aliquot was purified on HPLC which led to a complete removal of PPh₃ (EtOAc: ethanol 10:1, column: YMC 250x10, flow rate: 3ml/min).

2nd approach:

Compound **4** (605.9 mg, 1.465 mmol) was dissolved in dry DCM (20 ml). The solution was stirred at 0 °C and under argon-atmosphere before trifluoroacetic acid (12.1 ml, 157.32 mmol) was added. TLC interpretation was difficult due to the strong acidic reaction conditions. Stirring was continued on the ice-bath and under argon-atmosphere for 1 hour. The reaction mixture was concentrated carefully. The resulting brown residue was co-evaporated twice with toluene. Purification was done by column chromatography (EtOAc: toluene 3:1 to EtOAc: EtOH 4:1).

Yield: 296 mg (**5**) (62.0 %), 172.9 mg (**4**) (28.5 %)

R_f = 0.33 (EtOAc: EtOH 9:1, HPTLC)

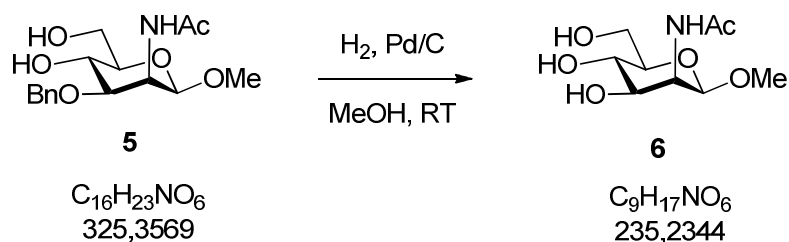
$[\alpha]_D^{23} - 44.6^\circ$ (c 0.75, MeOH)

¹H-NMR (600 MHz, MeOH-*d*₄): δ 7.40-7.38, 7.32-7.29 and 7.27-7.24 (m, 5H, OCH₂Ph), 4.82 and 4.48 (2d, 2H, ²J=11.1 Hz, OCH₂Ph), 4.74 (dd, 1H, ³J_{1,2}=1.5 Hz, ³J_{2,3}=4.2 Hz, H-2), 4.52 (d, 1H, ³J_{1,2}=1.6 Hz, H-1), 3.86 (app. d, 2H, ³J_{5,6a}=³J_{5,6b}=3.4 Hz, C-6a and C-6b), 3.61 (app. t, 1H, ³J_{3,4}=³J_{4,5}=9.7 Hz, H-4), 3.75 (dd, 1H, ³J_{2,3}=4.2 Hz, ³J_{3,4}=9.5 Hz, H-3), 3.48 (s, 3H, OMe), 3.26 (dt, 1H, ³J_{4,5}=9.8 Hz, ³J_{5,6a}=³J_{5,6b}=3.3 Hz, H-5), 2.01 (s, 3H, CH₃CO) ppm

¹³C-NMR (150 MHz, MeOH-*d*₄): 173.87 (s, CH₃CO), 139.64 (s, OCH₂Ph), 129.22 and 128.60 (5d, OCH₂Ph), 102.02 (d, C-1), 81.60 (d, C-3), 78.18 (d, C-5), 72.20 (t, OCH₂Ph), 67.04 (d, C-4), 61.95 (t, C-6), 57.00 (q, OMe), 50.88 (d, C-2), 22.60 (q, CH₃CO) ppm

HR-MS: [M+H]⁺ m/z (predicted) = 326.1598, m/z (found) = 326.1599, Δ = 0.31 ppm

[M+Na]⁺ m/z (predicted) = 348.1418, m/z (found) = 348.1420, Δ = 0.58 ppm

4.2.6. Methyl 2-acetamido-2-deoxy- β -D-mannopyranoside (**6**)

Compound **5** (13.6 mg, 0.042 mmol) was prepared in a flask connected to an Anschütz-extension. Pd/C (10 %, 4.4 mg, 0.041 mmol) was suspended in dry MeOH. The suspension was added to **5** and the vial was purged once with dry MeOH. The flask was evacuated (by water-jet pump) and flushed with H₂-gas twice while stirring vigorously. Stirring was continued and the reaction mixture was kept under H₂-atmosphere at RT until conversion was almost complete (after 22 ½ hours). The suspension was carefully filtered with Celite using only gravity force. Purification of the crude product **6** was performed with a PD-10 Desalting Column (GE Healthcare). After purging the column with dist. H₂O the product was added and eluted with dist. H₂O. Compound **6** was lyophilized.

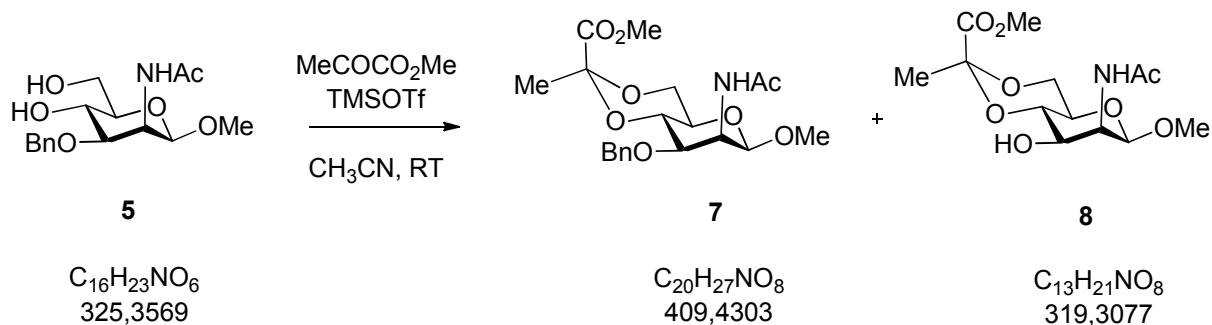
Yield: 8.8 mg of a white solid (89.5 %)

R_f = 0.67 (MeOH: CHCl₃: H₂O 10:10:3, TLC)

¹H-NMR (600 MHz, D₂O): 4.63 (d, 1H, ³J_{1,2}=1.6 Hz, H-1), 4.42 (dd, 1H, ³J_{1,2}=1.5 Hz, ³J_{2,3}=4.5 Hz, H-2), 3.85 (dd, 1H, ³J_{5,6a}=2.3 Hz, ²J_{6a,6b}=12.2 Hz, H-6a), 3.75 (dd, 1H, ³J_{5,6b}=5.2 Hz, ²J_{6a,6b}=12.5 Hz, H-6b), 3.74 (dd, 1H, ³J_{2,3}=4.4 Hz, ³J_{3,4}=9.6 Hz, H-3), 3.45 (app. t, 1H, ³J_{3,4}=³J_{4,5}=9.8 Hz, H-4), 3.44 (s, 3H, OMe), 3.34 (ddd, 1H, ³J_{4,5}=9.9 Hz, ³J_{5,6a}=2.3 Hz, ³J_{5,6b}=5.1 Hz, H-5), 1.99 (s, 3H, CH₃CO) ppm

¹H-NMR data is in agreement with the results of Kaji *et al.* ⁴⁸

4.2.7. Methyl 2-acetamido-3-O-benzyl-2-deoxy-4,6-O- [1-(methoxycarbonyl)ethylidene]- β -D-mannopyranoside (**7**)



1st approach:

Compound **5** (82.9 mg, 0.255 mmol, containing residual PPh_3) was dissolved in CH_3CN (800 μl). Methyl pyruvate (53 μl , 0.586 mmol) as well as TMS-triflate (106 μl , 0.586 mmol) were added. The reaction mixture was stirred at RT under argon-atmosphere. The reaction was stopped after 50 minutes when all of the starting material was consumed. The mixture was diluted with EtOAc and was brought to pH 8 by dropwise addition of triethylamine. Toluene was added and the solution was concentrated. Purification by column chromatography was done to obtain **7** and **8** (EtOAc: toluene 2.5:1 to EtOAc: MeOH 9:1).

Yield: 50.5 mg of a colourless syrup (**7**) (48.4 %, containing residual PPh_3), 33.9 mg of a white solid (**8**) (40.8 %, containing residual PPh_3)

Pure compounds were obtained after HPLC-purification (**7**: EtOAc: toluene 6:1, column: YMC 250x20, flow rate: 15 ml/min); **8**: EtOAc: EtOH 9:1, column: YMC 250x10, flow rate: 3ml/min).

2nd approach:

To a stirred solution of compound **5** (298.2 mg, 0.917 mmol) in CH_3CN (3 ml) methyl pyruvate (190 μl , 2.108 mmol) and TMS-triflate (382 μl , 2.108 mmol) were added. Stirring was continued at RT under argon-atmosphere. The reaction was stopped after 1 $\frac{3}{4}$ hours when TLC showed formation of undesired side products. The solution was concentrated. The residue was diluted with EtOAc, neutralized with Et_3N and concentrated. The crude mixture was purified by column chromatography (EtOAc: toluene 2.5:1 to EtOAc: EtOH 9:1). The resulting compounds (**7** and **8**) still showed impurities.

Yield: 198.7 mg (**7**) (53.0 %, impure), 97.0 mg (**8**) (33.1 %, impure)

Two further purifications by column chromatography (EtOAc: EtOH 10:1 to EtOAc: EtOH 9:1) led to pure, crystalline compound **8**. For complete purification of **7** one part was purified by another column chromatography (EtOAc: toluene 5:1) and the other part by HPLC (EtOAc: toluene 6:1, column: YMC 250x20, flow rate: 15ml/min).

$R_f = 0.74$ (EtOAc: EtOH 9:1, HPTLC)

$[\alpha]_D^{23} - 35.0^\circ$ (c 0.98, CHCl_3)

$^1\text{H-NMR}$ (600 MHz, CDCl_3): δ 7.41-7.39, 7.35-7.33 and 7.29-7.27 (m, 5H, OCH_2Ph), 5.76 (d, 1H, $^3J_{\text{NH},2}=9.5$ Hz, NH), 4.77 (app. s, 2H, OCH_2Ph), 4.73 (dd, 1H, $^3J_{1,2}=2.0$ Hz, $^3J_{2,3}=5.5$ Hz, H-2), 4.47 (d, 1H, $^3J_{1,2}=2.1$ Hz, H-1), 4.08 (dd, 1H, $^3J_{5,6a}=5.0$ Hz, $^2J_{6a,6b}=10.7$ Hz, H-6a), 3.84 (s, 3H, CO_2Me), 3.72 (app. t, 1H, $^3J_{3,4}=^3J_{4,5}=9.2$ Hz, H-4), 3.75 (app. t, 1H, $^3J_{5,6b}=^2J_{6a,6b}=10.7$ Hz, H-6b), 3.74 (dd, 1H, $^3J_{2,3}=5.5$ Hz, $^3J_{3,4}=8.5$ Hz, H-3), 3.42 (s, 3H, OMe), 3.38 (m, 1H, H-5), 2.03 (s, 3H, CH_3CO), 1.57 (s, 3H, Me) ppm

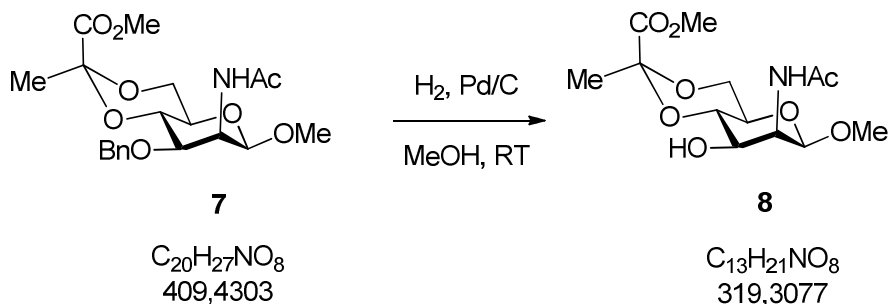
$^{13}\text{C-NMR}$ (150 MHz, CDCl_3): δ 170.49 and 170.42 (2s*, CH_3CO), 170.13 (s, MeCCO_2Me), 138.04 (s, OCH_2Ph), 100.82 (d, C-1), 99.15 (s, MeCCO_2Me), 75.81 (d, C-4), 74.52 (d, C-3), 71.44 (t, OCH_2Ph), 65.94 (d, C-5), 65.54 (t, C-6), 56.62 (q, OMe), 52.76 (q, MeCCO_2Me), 49.36 and 49.28 (2d*, C-2), 25.61 (q, MeCCO_2Me), 23.47 and 23.42 (2q*, CH_3CO) ppm

* Signal duplication was observed.

HR-MS: $[\text{M}+\text{Na}]^+$ m/z (predicted) = 432.1629, m/z (found) = 432.1627, $\Delta = 0.46$ ppm

$[\text{M}+\text{H}]^+$ m/z (predicted) = 410.1809, m/z (found) = 410.1805, $\Delta = 0.98$ ppm

4.2.8. Methyl 2-acetamido-2-deoxy-4,6-O-[1-(methoxycarbonyl)ethylidene]- β -D-mannopyranoside (**8**)



1st approach:

Compound **7** (25.1 mg, 0.061 mmol) was dissolved in dry MeOH in a flask connected to an Anschütz-extension. Pd/C (10 %, 6.7 mg, 0.063 mmol) was suspended in dry MeOH before it was added to **7**. While stirring the flask was evacuated with the water-jet pump and flushed with H₂-gas for three times. The reaction mixture was stirred further at RT under H₂-atmosphere. A second portion of Pd/C (10 %, 3.6 mg, 0.034 mmol) was added. Complete conversion was reached after 28 hours. Filtration over Celite was done without reduced pressure. The filtrate was concentrated. NMR showed that purification was not necessary.

Yield: 18.2 mg of a brownish syrup (93 %)

2nd approach:

A solution of **7** (87.0 mg, 0.212 mmol) in dry MeOH was prepared in a flask with an Anschütz-extension. Suspended Pd/C (10 %, 33.6 mg, 0.316 mmol) was added. Evacuation procedure was carried out for three times as described in the 1st approach. After 5 ½ hours of stirring at RT under H₂-gas the starting material was completely converted into compound **8** and a side product. The reaction mixture was filtered over Celite using only gravity force and the filtrate was concentrated. The product **8** was partly crystallized in a mixture of hexane and EtOAc by addition of seed crystals. The remaining impure filtrate was concentrated and purified by column chromatography (EA: MeOH 9.5:0.5).

Yield: 18.3 mg of white crystals (27.0 %), 26.4 mg of a colourless syrup (38.9 %)

R_f = 0.29 (EtOAc: EtOH 9:1, HPTLC)

Melting point: 192-195 °C

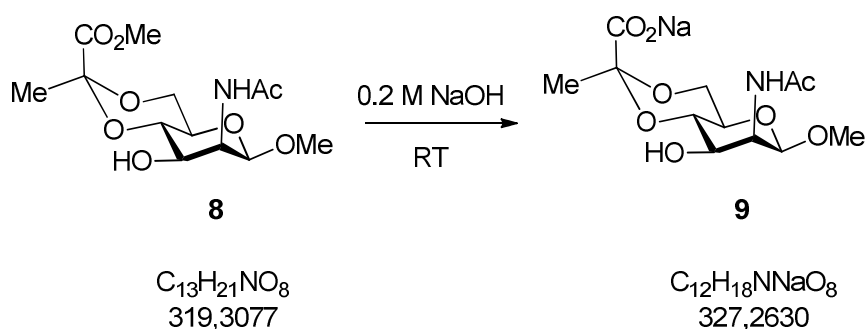
$[\alpha]_D^{20} - 49.9^\circ$ (c 0.62, MeOH)

$^1\text{H-NMR}$ (600 MHz, MeOH- d_4): δ 4.58 (d, 1H, $^3J_{1,2}=1.9$ Hz, H-1), 4.54 (dd, 1H, $^3J_{1,2}=1.7$ Hz, $^3J_{2,3}=4.7$ Hz, H-2), 3.99 (dd, 1H, $^3J_{5,6a}=5.0$ Hz, $^2J_{6a,6b}=10.5$ Hz, H-6a), 3.83 (dd, 1H, $^3J_{2,3}=4.7$ Hz, $^3J_{3,4}=9.7$ Hz, H-3), 3.83 (s, 3H, CO₂Me), 3.78 (app. t, 1H, $^3J_{5,6b}=^2J_{6a,6b}=10.5$ Hz, H-6b), 3.55 (app. t, 1H, $^3J_{3,4}=^3J_{4,5}=9.7$ Hz, H-4), 3.44 (s, 3H, OMe), 3.31 (m, 1H, H-5), 2.01 (s, 3H, CH₃CO), 1.48 (s, 3H, Me) ppm

$^{13}\text{C-NMR}$ (150 MHz, MeOH- d_4): δ 174.77 (s, CH₃CO), 172.10 (s, MeCCO₂Me), 102.60 (d, C-1), 100.70 (s, MeCCO₂Me), 76.31 (d, C-4), 71.06 (d, C-3), 68.29 (d, C-5), 65.93 (t, C-6), 57.17 (q, OMe), 54.72 (q, MeCCO₂Me), 53.17 (d, C-2), 25.92 (q, MeCCO₂Me), 22.64 (q, CH₃CO) ppm

HR-MS: $[\text{M}+\text{H}]^+$ m/z (predicted) = 320.1340, m/z (found) = 320.1340, $\Delta = 0$ ppm

4.2.9. Methyl 2-acetamido-2-deoxy-4,6-O-(1-carboxyethylidene)- β -D-mannopyranoside sodium salt (**9**)



To compound **8** (6.2 mg, 0.0194 mmol) a 0.2 M NaOH solution (1.5 ml) was added. The mixture was stirred under argon-atmosphere at RT. Reaction was stopped after 3 hours 15 minutes when complete conversion was reached. With Dowex H⁺ ion exchange resin and 0.2 M NaOH solution the pH of the reaction solution was brought to 7.5. The mixture was filtered and the filtrate was lyophilized. Product **9** was purified by size exclusion chromatography using a Biogel-P2-column and an aqueous solvent (dist. H₂O + 5 % EtOH + 8 mg/l NaCl) for elution. Purified product **9** was lyophilized.

Yield: 5.8 mg of a white solid (91.3 %)

R_f = 0.94 (CHCl₃: MeOH: H₂O 10:10:3, TLC)

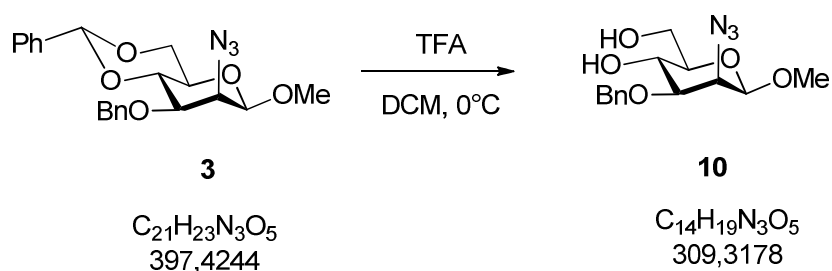
$[\alpha]_D^{20} - 34.2^\circ$ (c 0.51, H₂O)

$^1\text{H-NMR}$ (600 MHz, D_2O): δ 4.71 (d, 1H, $^3J_{1,2}=1.9$ Hz, H-1), 4.51 (dd, 1H, $^3J_{1,2}=1.7$ Hz, $^3J_{2,3}=4.6$ Hz, H-2), 4.01 (dd, 1H, $^3J_{5,6a}=5.0$ Hz, $^2J_{6a,6b}=10.6$ Hz, H-6a), 3.93 (dd, 1H, $^3J_{2,3}=4.6$ Hz, $^3J_{3,4}=10.1$ Hz, H-3), 3.70 (app. t, 1H, $^3J_{5,6b}=^2J_{6a,6b}=10.6$ Hz, H-6b), 3.58 (app. t, 1H, $^3J_{3,4}=^3J_{4,5}=9.9$ Hz, H-4), 3.45 (s, 3H, OMe), 3.40 (ddd, 1H, $^3J_{4,5}=9.8$ Hz, $^3J_{5,6a}=5.0$ Hz, $^3J_{5,6b}=10.4$ Hz, H-5), 2.02 (s, 3H, CH_3CO), 1.43 (s, 3H, Me) ppm

$^{13}\text{C-NMR}$ (150 MHz, D_2O): δ 176.36 and 176.27 (2s, MeCCO_2Na and CH_3CO), 102.65 (s, MeCCO_2Na), 101.81 (d, C-1), 72.82 (d, C-4), 70.08 (d, C-3), 67.67 (d, C-5), 64.88 (t, C-6), 58.02 (q, OMe), 54.01 (d, C-2), 25.49 (q, MeCCO_2Na), 22.80 (q, CH_3CO) ppm

HR-MS: $[\text{M}+\text{H}]^+$ m/z (predicted) = 328.1003, m/z (found) = 328.1008, Δ = 1.52 ppm

4.2.10. Methyl 2-azido-3-O-benzyl-2-deoxy- β -D-mannopyranoside (**10**)



Compound **3** (53.8 mg, 0.135 mmol) was dissolved in dry DCM (6 ml) and the solution was stirred on an ice-bath under argon-atmosphere. Trifluoroacetic acid (1.1 ml, 14.278 mmol) was added. Stirring on ice and under argon-atmosphere was continued for 35 minutes until all of the starting material was converted to product **10** and a polar side product. The reaction mixture was concentrated and co-evaporated twice with toluene. The crude residue was purified by column chromatography (EtOAc: toluene 5:1).

Yield: 27.8 mg of a colourless syrup (66.4 %)

R_f = 0.35 (EtOAc: toluene 5:1, HPTLC)

$[\alpha]_D^{23}$ – 110.1° (c 0.79, CHCl_3)

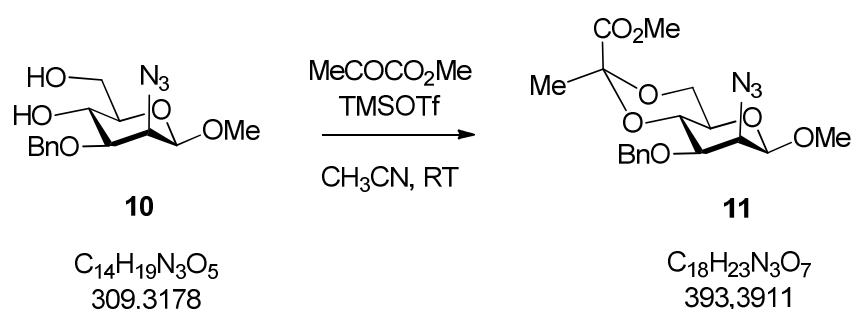
¹H-NMR (600 MHz, CDCl₃): δ 7.39-7.32 (m, 5H, OCH₂Ph), 4.76 and 4.63 (2d, 2H, ²J=11.7 Hz, OCH₂Ph), 4.44 (d, 1H, ³J_{1,2}=1.3 Hz, H-1), 3.96 (dd, 1H, ³J_{1,2}=1.2 Hz, ³J_{2,3}=3.5 Hz, H-2), 3.91 (dd, 1H, ³J_{5,6a}=3.5 Hz, ²J_{6a,6b}=11.9 Hz, H-6a), 3.87 (app. t, 1H, ³J_{3,4}=³J_{4,5}=9.4 Hz, H-4), 3.82 (dd, 1H, ³J_{5,6b}=5.1 Hz, ²J_{6a,6b}=11.9 Hz, H-6b), 3.54 (s, 3H, OMe), 3.49 (dd, 1H, ³J_{2,3}=3.5 Hz, ³J_{3,4}=9.2 Hz, H-3), 3.30 (ddd, 1H, ³J_{4,5}=9.5 Hz, ³J_{5,6a}=3.5 Hz, ³J_{5,6b}=5.1 Hz, H-5), 2.71 (s, 1H, 4-OH) ppm

¹³C-NMR (150 MHz, CDCl₃): δ 137.29 (s, OCH₂Ph), 128.90, 128.50 and 128.16 (5d, OCH₂Ph), 100.81 (d, C-1), 80.86 (d, C-3), 75.89 (d, C-5), 72.25 (t, OCH₂Ph), 67.17 (d, C-4), 62.66 (t, C-6), 61.13 (d, C-2), 57.39 (q, OMe) ppm

HR-MS: [M+Na]⁺ m/z (predicted) = 332.1217, m/z (found) = 332.1214, Δ = 0.90 ppm

[M+H]⁺ m/z (predicted) = 327.1663, m/z (found) = 327.1658, Δ = 1.53 ppm

4.2.11. Methyl 2-azido-3-O-benzyl-2-deoxy-4,6-O-[1-(methoxycarbonyl)ethylidene]-β-D-mannopyranoside (11)



Compound **10** (14.4 mg, 0.047 mmol) was stirred in CH₃CN (800 μl) under argon-atmosphere and at RT. Methyl pyruvate (10 μl, 0.107 mmol) and TMS-triflate (17 μl, 0.093 mmol) were added. Stirring under the same conditions was continued. The reaction was stopped after 1 hour when the starting material was completely converted to the product (**11**) and two side products. Two drops of triethylamine were added before the mixture was diluted with DCM and was washed once with saturated aqueous NaHCO₃-solution. The organic phase was dried with Na₂SO₄, filtered and concentrated. The residue was co-evaporated once with toluene. The crude mixture was purified by column chromatography (toluene: EtOAc 10:1 to toluene: EtOAc 1:1).

Yield: 2.2 mg of a off-white solid (12 %)

$R_f = 0.39$ (toluene: EtOAc 6:1, HPTLC)

$[\alpha]_D^{19.5} - 7.57^\circ$ (c 0.35, CHCl_3)

$^1\text{H-NMR}$ (600 MHz, CDCl_3): δ 7.43-7.30 (m, 5H, OCH_2Ph), 4.98 and 4.75 (2d, 2H, $^2J=12.4$ Hz, OCH_2Ph), 4.41 (d, 1H, $^3J_{1,2}=1.4$ Hz, H-1), 4.05 (dd, 1H, $^3J_{5,6a}=5.0$ Hz, $^2J_{6a,6b}=10.8$ Hz, H-6a), 3.90 (dd, 1H, $^3J_{1,2}=1.3$ Hz, $^3J_{2,3}=3.8$ Hz, H-2), 3.85 (s, 3H, CO_2Me), 3.83 (app. t, 1H, $^3J_{5,6b}=^2J_{6a,6b}=10.7$ Hz, H-6b), 3.80 (app. t, 1H, $^3J_{3,4}=^3J_{4,5}=9.4$ Hz, H-4), 3.63 (dd, 1H, $^3J_{2,3}=3.8$ Hz, $^3J_{3,4}=9.3$ Hz, H-3), 3.51 (s, 3H, OMe), 3.22 (ddd, 1H, $^3J_{4,5}=9.7$ Hz, $^3J_{5,6a}=5.0$ Hz, $^3J_{5,6b}=10.3$ Hz, H-5), 1.57 (s, 3H, Me) ppm

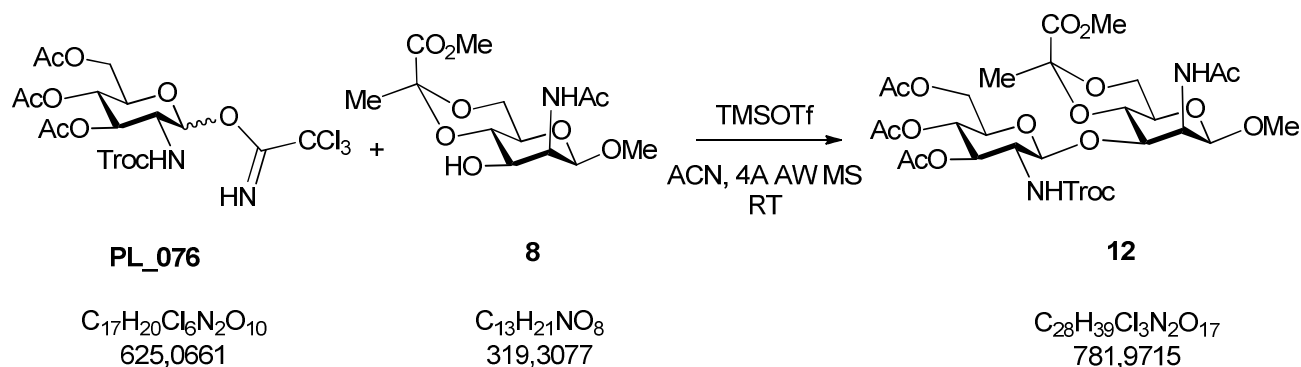
$^{13}\text{C-NMR}$ (150 MHz, CDCl_3): δ 170.18 (s, MeCCO_2Me), 138.25 (s, OCH_2Ph), 128.58 and 127.93 (5d, OCH_2Ph), 101.40 (d, C-1), 99.55 (s, MeCCO_2Me), 76.34 (d, C-3), 75.32 (d, C-4), 72.97 (t, OCH_2Ph), 67.09 (d, C-5), 65.07 (t, C-6), 63.77 (d, C-2), 57.45 (q, OMe), 53.02 (q, MeCCO_2Me), 25.72 (q, MeCCO_2Me) ppm

HR-MS: $[\text{M}+\text{Na}]^+$ m/z (predicted) = 416.1428, m/z (found) = 416.1418, $\Delta = 2.60$ ppm

$[\text{M}+\text{NH}_4]^+$ m/z (predicted) = 411.1874, m/z (found) = 411.1867, $\Delta = 1.85$ ppm

4.3. Synthesis of the Disaccharide

4.3.1. Methyl [3,4,5-tri-O-acetyl-2-deoxy-2-(2,2,2-trichloroethoxycarbonylamino)- β -D-glucopyranosyl]-(1 \rightarrow 3)-2-acetamido-2-deoxy-4,6-O-[1-(methoxycarbonyl)ethylidene]- β -D-mannopyranoside (**12**)



Acceptor **8** (38.6 mg, 0.121 mmol) was dried for several days under high vacuum. Donor **PL_076** (151.1 mg, 0.242 mmol) was dried for two hours before use. Ground powdered acid washed 4 Å molecular sieve was activated at 200 °C. **PL_076** was dissolved in dry CH₃CN (4 ml), purged with another 2 ml and both portions were added to **8**. Molecular sieves were transferred into the reaction flask and the mixture was stirred at RT under argon-atmosphere for 30 minutes. An aliquot of a 0.242 M TMS-triflate stock solution (100 µl, 0.0242 mmol) was added to start the glycosylation. Stirring under the same conditions was continued until after 1 h 45 minutes another aliquot of the TMS-triflate stock solution (100 µl, 0.0242 mmol) was added. TLC showed two products and also some side products due to hydrolysis. The reaction was stopped after 2 hours 50 minutes by adding a few drops of Et₃N. Filtration of the molecular sieve was done with Celite. Purification of the filtrate was done by column chromatography (EtOAc: toluene 6:1 to EtOAc: EtOH 4:1).

Yield: 30.2 mg of a colourless syrup (**12**) (31.9 %, impure with hydrolysis side product), 9.5 mg of a colourless syrup (side product) (20.1 %), 7.3 mg of a colourless syrup (recycled acceptor) (18.9 %)

Final purification of the product (**12**) was achieved with several HPLC runs (EtOAc: toluene 2:1, column: YMC 250x10, flow rate: 5 ml/min).

$R_f = 0.43$ (EtOAc: toluene 6:1, TLC)

$[\alpha]_D^{20} - 38.2^\circ$ (c 0.90, CHCl₃)

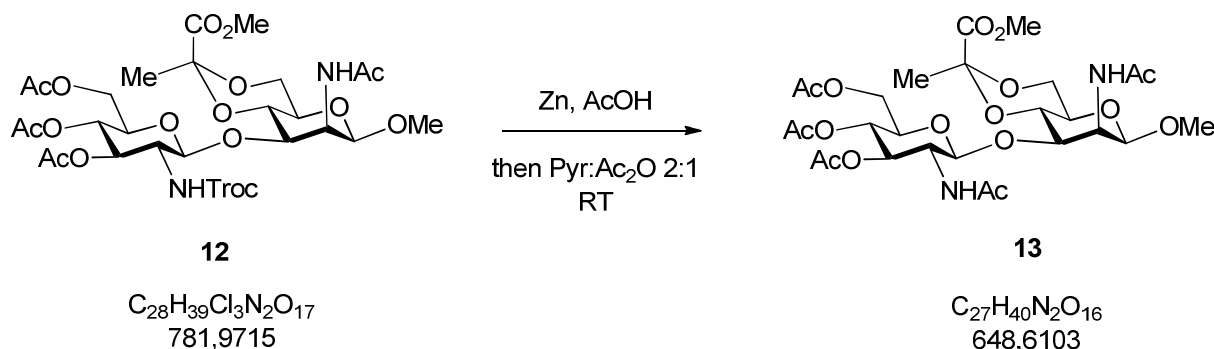
¹H-NMR (600 MHz, CDCl₃): δ 6.02 (d, 1H, ³J_{NH,2'}=8.8 Hz, NH), 5.87 (d, 1H, ³J_{NH,2}=8.2 Hz, NHCOCH₃), 5.23 (app. t, 1H, ³J_{2',3'}=³J_{3',4'}=9.8 Hz, H-3'), 5.12 (app. t, 1H, ³J_{3',4'}=³J_{4',5'}=9.6 Hz, H-4'), 5.00 (d, 1H, ³J_{1',2'}=8.4 Hz, H-1'), 4.85 and 4.59 (2d, 2H, ²J=12.1 Hz, Cl₃CCH₂), 4.64 (m, 1H, H-2), 4.50 (d, 1H, ³J_{1,2}=1.9 Hz, H-1), 4.16 (dd, 1H, ³J_{5',6a'}=4.3 Hz, ²J_{6a',6b'}=12.3 Hz, H-6a'), 4.21 (dd, 1H, ³J_{5',6b'}=2.8 Hz, ²J_{6a',6b'}=12.3 Hz, H-6b'), 4.08 (dd, 1H, ³J_{5,6a}=5.0 Hz, ²J_{6a,6b}=10.7 Hz, H-6a), 4.05 (dd, 1H, ³J_{2,3}=4.7 Hz, ³J_{3,4}=9.4 Hz, H-3), 3.87 (dt, 1H, ³J_{1',2'}=³J_{NH,2'}=8.6 Hz, ³J_{2',3'}=10.3 Hz, H-2'), 3.80 (s, 3H, CO₂Me), 3.74 (app. t, 1H, ³J_{5,6b}=²J_{6a,6b}=10.7 Hz, H-6b), 3.73 (ddd, 1H, ³J_{4',5'}=10.0 Hz, ³J_{5',6a'}=4.4 Hz, ³J_{5',6b'}=3 Hz, H-5'), 3.54 (app. t, 1H, ³J_{3,4}=³J_{4,5}=9.6 Hz, H-4), 3.46 (s, 3H, OMe), 3.38 (dt, 1H, ³J_{4,5}=³J_{5,6b}=10.1 Hz, ³J_{5,6a}=5.0 Hz, H-5), 2.09-1.98 (4s, 12H, 1xNHCOCH₃ and 3xOCOCH₃), 1.56 (s, 3H, Me) ppm

¹³C-NMR (150 MHz, CDCl₃): δ 172.43-169.65 (5s, 3xOCOCH₃, 1xNHCOCH₃ and 1xNHCOOCH₂CCl₃), 170.23 (s, MeCCO₂Me), 154.69 (s, NHCOOCH₂CCl₃), 100.90 (d, C-1), 99.55 (s, MeCCO₂Me), 96.40 (d, C-1'), 74.56 (t, NHCOOCH₂CCl₃), 73.70 (d, C-3), 73.37 (d, C-3'), 73.15 (d, C-4), 72.22 (d, C-5'), 69.09 (d, C-4'), 67.10 (d, C-5), 65.25 (t, C-6), 62.32 (t, C-6'), 57.12 (q, OMe), 55.91 (d, C-2'), 52.79 (q, MeCCO₂Me), 49.66 (d, C-2), 25.44 (q, MeCCO₂Me), 23.72-20.78 (4q, 3xOCOCH₃ and 1xNHCOCH₃) ppm

HR-MS: [M+H]⁺ m/z (predicted) = 781.1387, m/z (found) = 781.1371, Δ = 2.06 ppm

[M+Na]⁺ m/z (predicted) = 803.1207, m/z (found) = 803.1190, Δ = 2.12 ppm

4.3.2. Methyl (2-acetamido-3,4,5-tri-O-acetyl-2-deoxy- β -D-glucopyranosyl)-(1 \rightarrow 3)-2-acetamido-2-deoxy-4,6-O-[1-(methoxycarbonyl)ethylidene]- β -D-mannopyranoside (13)



Compound **12** (18.1 mg, 0.023 mmol) was dissolved in glacial acetic acid (2.0 ml) before Zn-powder (10 μm , 75.67 mg, 1.157 mmol) was added. The reaction mixture was stirred at RT under argon-atmosphere for 18 hours. As conversion was not complete another portion of Zn-powder was added. Stirring was continued for another hour. The Zn-powder was filtered over Celite and was washed with glacial acetic acid for several times. The filtrate was concentrated and co-evaporated for three times with toluene. The off-white residue was dissolved in pyridine (1.2 ml) and acetic anhydride (600 μl , 6.347 mmol) was added. Acetylation was complete after stirring for 1 hour 45 minutes at RT under argon-atmosphere. The reaction was quenched with MeOH (300 μl) and solvents were evaporated. The residue was co-evaporated twice with toluene. Purification was done by column chromatography (EtOAc: MeOH 9.5:0.5 to EtOAc: MeOH 9:1).

Yield: 12.4 mg of a white solid (82.6 %, ~12 % impurity)

R_f = 0.35 (EtOAc: MeOH 9:1, HPTLC)

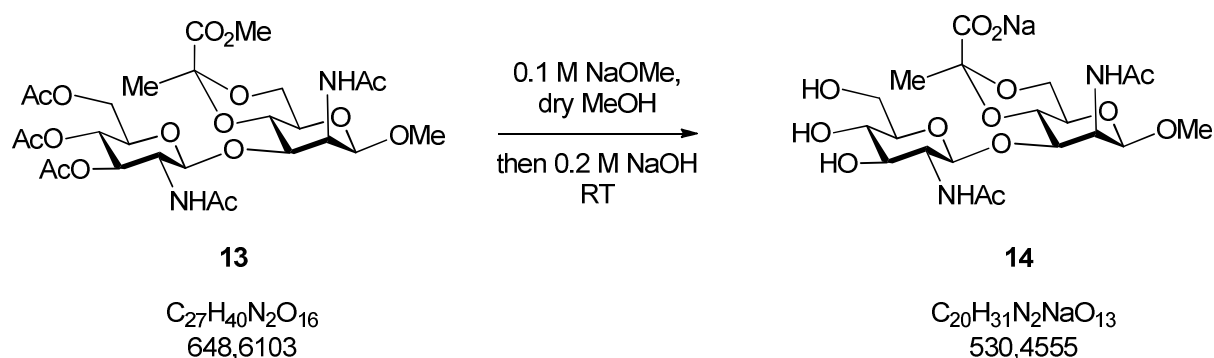
$[\alpha]_{\text{D}}^{20}$ – 53.0° (c 0.92, MeOH)

¹H-NMR (600 MHz, MeOH-*d*₄): δ 5.18 (app. t, 1H, $^3J_{2,3} = ^3J_{3,4} = 9.7$ Hz, H-3'), 5.05 (app. t, 1H, $^3J_{3,4} = ^3J_{4,5} = 9.6$ Hz, H-4'), 4.82 (d, 1H, H-1'), 4.69 (dd, 1H, $^3J_{1,2} = 1.6$ Hz, $^3J_{2,3} = 4.4$ Hz, H-2), 4.56 (d, 1H, $^3J_{1,2} = 1.7$ Hz, H-1), 4.33 (dd, 1H, $^3J_{5,6a} = 4.4$ Hz, $^2J_{6a,6b} = 12.2$ Hz, H-6a'), 4.18 (dd, 1H, $^3J_{5,6b} = 2.7$ Hz, $^2J_{6a,6b} = 12.2$ Hz, H-6b'), 4.08 (dd, 1H, $^3J_{2,3} = 4.4$ Hz, $^3J_{3,4} = 10.0$ Hz, H-3), 3.99 (dd, 1H, $^3J_{5,6a} = 5.0$ Hz, $^2J_{6a,6b} = 10.5$ Hz, H-6a), 3.96 (dd, 1H, $^3J_{1,2} = 8.2$ Hz, $^3J_{2,3} = 10.1$ Hz, H-2'), 3.82 (m, 1H, H-5'), 3.81 (s, 3H, CO₂Me), 3.80 (app. t, 1H, $^3J_{5,6b} = ^2J_{6a,6b} = 10.6$ Hz, H-6b), 3.66 (app. t, 1H, $^3J_{3,4} = ^3J_{4,5} = 9.8$ Hz, H-4), 3.44 (s, 3H, OMe), 3.35 (dt, 1H, $^3J_{4,5} = ^3J_{5,6b} = 10.0$ Hz, $^3J_{5,6a} = 4.9$ Hz, H-5), 2.06-1.98 (5s, 15H, 2xNHCOCH₃ and 3xOCOCH₃), 1.48 (s, 3H, Me) ppm; ~ 7% impurity

¹³C-NMR (150 MHz, MeOH-d₄): δ 174.45-171.30 (5s, 3xOCOCH₃ and 2xNHCOCH₃), 171.91 (s, MeCCO₂Me), 102.50 (d, C-1), 100.74 (s, MeCCO₂Me), 98.32 (d, C-1'), 75.30 (d, C-3), 74.93 (d, C-3'), 74.18 (d, C-4), 73.08 (d, C-5'), 70.24 (d, C-4'), 68.59 (d, C-5), 65.86 (t, C-6), 63.36 (t, C-6'), 57.23 (q, OMe), 55.23 (d, C-2'), 53.10 (q, MeCCO₂Me), 51.28 (d, C-2), 25.87 (q, MeCCO₂Me), 23.05-20.60 (5q, 3xOCOCH₃ and 2xNHCOCH₃) ppm

HR-MS: [M+Na]⁺ m/z (predicted) = 671.2270, m/z (found) = 671.2266, Δ = 0.62 ppm

4.3.3. Methyl (2-acetamido-2-deoxy-β-D-glucopyranosyl)-(1→3)-2-acetamido-2-deoxy-4,6-O-(1-carboxyethylidene)-β-D-mannopyranoside sodium salt (**14**)



To a solution of compound **13** (4.5 mg, 0.007 mmol, ~ 15 % impurity) in dry MeOH (2.0 ml) a 0.1 M NaOMe-solution (1.0 ml) was added. The reaction mixture was stirred at RT and was stopped after 1 hour 20 minutes when conversion was complete. The pH was brought to 7 by addition of Dowex H⁺ ion exchange resin. Filtration was done and the filtrate was concentrated in vacuo. The white residue was dried before it was treated with 0.2 M NaOH-solution (1.0 ml). The solution was stirred at RT under argon-atmosphere for 3 hours. The pH was set to 7.5 with Dowex H⁺ ion exchange resin and 0.2 M NaOH-solution. The mixture was filtered and the filtrate was lyophilized. Purification of product **14** was done by size exclusion chromatography using a Biogel-P2-column. An aqueous solvent mixture (dist. H₂O + 5 % EtOH + 8 mg/l NaCl) was used for elution. The product fractions were lyophilized.

Yield: 3.2 mg of a white solid (86.9 %, ~ 8 % impurity)

R_f = 0.32 (EtOAc: MeOH 1:1, HPTLC)

[α]_D²³ – 56.0° (c 0.37, H₂O)

¹H-NMR (600 MHz, D₂O): δ 4.63 (m, 2H, H-1 and H-2), 4.59 (d, 1H, ³J_{1,2'}=8.5 Hz, H-1'), 4.17 (dd, 1H, ³J_{2,3}=4.8 Hz, ³J_{3,4}=10.4 Hz, H-3), 3.99 (dd, 1H, ³J_{5,6a}=5.0 Hz, ²J_{6a,6b}=10.7 Hz, H-6a), 3.90 (dd, 1H, ³J_{5',6a'}=2.2 Hz, ²J_{6a',6b'}=12.4 Hz, H-6a'), 3.72 (m, 1H, H-4), 3.71 (m, 1H, H-6b), 3.70 (m, 1H, H-2'), 3.69 (m, 1H, H-6b'), 3.50 (dd, 1H, ³J_{2',3'}=10.3 Hz, ³J_{3',4'}=8.8 Hz, H-3'), 3.42 (m, 1H, H-5'), 3.43 (s, 3H, OMe), 3.39 (m, 1H, H-5), 3.38 (m, 1H, H-4'), 2.01 and 1.99 (2s, 6H, 2xNHCOCH₃), 1.43 (s, 3H, Me) ppm; ~ 8 % impurity

¹³C-NMR (150 MHz, D₂O): δ 176.09 (s, MeCCO₂Na), 175.56 and 175.12 (2s, 2xNHCOCH₃), 102.83 (s, MeCCO₂Na), 102.09 (d, C-1), 98.87 (d, C-1'), 76.78 (d, C-5'), 74.87 (d, C-3'), 74.79 (d, C-3), 73.03 (d, C-4), 70.63 (d, C-4'), 67.82 (d, C-5), 64.81 (t, C-6), 61.61 (t, C-6'), 58.06 (q, OMe), 56.14 (d, C-2'), 51.05 (d, C-2), 25.41 (q, MeCCO₂Na), 23.25 and 22.86 (2q, 2xNHCOCH₃) ppm

HR-MS: [M+H]⁺ m/z (predicted) = 531.1797, m/z (found) = 531.1796, Δ = 0.11 ppm

5. Conclusion and Outlook

Summarizing, synthetic routes for the preparation of a pyruvate-substituted monosaccharide (4,6-Pyr- β -D-ManNAcOMe) and disaccharide (β -D-GlcNAc-(1 \rightarrow 3)-4,6-Pyr- β -D-ManNAcOMe) were successfully developed within this thesis. Pyruvic acid acetal introduction at the step of the *N*-acetyl mannosamine led to satisfying results in yield and stereochemistry. In addition it was shown that glycosylation in moderate yields is possible using the pyruvate-substituted acceptor. The final disaccharide compound was useable for further experiments although containing a small percentage of an unidentified impurity.

The binding contribution of the pyruvate group in mono- and disaccharide could be shown by successful cocrystallization and STD-NMR experiments involving the truncated SpaA protein. ITC measurements revealed strong binding to the protein for the pyruvylated monosaccharide but showed very low binding affinity for the pyruvate-substituted disaccharide and the pyruvate lacking *N*-acetyl mannosamine.

For further investigations of the binding interaction with SpaA protein within cocrystallization and ITC measurements the reverse linked disaccharide (4,6-Pyr- β -D-ManNAc-(1 \rightarrow 4)- β -D-GlcNAcOMe) as well as larger oligosaccharides containing this repeating disaccharide unit should be synthesized. Additionally preparation of the corresponding mono- and disaccharide including the reduced methyl ester group should be done as these compounds would be helpful ligands for STD-NMR experiments. ITC measurements involving the native SCWP of *P. alvei* CCM 2051^T could also provide interesting information.

6. References

1. Höltje, J.-V. in *The Desk Encyclopedia of Microbiology* (eds. Schaechter, M. & Lederberg, J.) 239–250 (Elsevier Academic Press, 2004).
2. Messner, P., Schäffer, C. & Kosma, P. in *Advances in carbohydrate chemistry and biochemistry* **69**, 210–257 (Elsevier Academic Press, 2013).
3. Schäffer, C. & Messner, P. The structure of secondary cell wall polymers: how Gram-positive bacteria stick their cell walls together. *Microbiology* **151**, 643–51 (2005).
4. Sára, M. & Sleytr, U. B. S-Layer Proteins. *J. Bacteriol.* **182**, 859–868 (2000).
5. Mesnage, S., Tosi-couture, E. & Gounon, P. The Capsule and S-Layer: Two Independent and Yet Compatible Macromolecular Structures in *Bacillus anthracis*. *J. Bacteriol.* **180**, 52–58 (1998).
6. Sleytr, U. B. & Beveridge, T. J. Bacterial S-layers. *Trends Microbiol.* **7**, 253–260 (1999).
7. Sára, M. & Sleytr, U. B. Molecular sieving through S layers of *Bacillus stearothermophilus* strains. *J. Bacteriol.* **169**, 4092–4098 (1987).
8. Sleytr, U. B., Messner, P., Pum, D. & Sára, M. Crystalline Bacterial Cell Surface Layers (S Layers): From Supramolecular Cell Structure to Biomimetics and Nanotechnology. *Angew. Chem. Int. Ed.* **38**, 1034–1054 (1999).
9. Zarschler, K. *et al.* Cell surface display of chimeric glycoproteins via the S-layer of *Paenibacillus alvei*. *Carbohydr. Res.* **345**, 1422–31 (2010).
10. Kern, J. *et al.* Structure of Surface Layer Homology (SLH) Domains from *Bacillus anthracis* Surface Array Protein. *J. Biol. Chem.* **286**, 26042–26049 (2011).
11. Araki, Y. & Ito, E. Linkage Units in Cell Walls of Gram-Positive Bacteria. *Crit. Rev. Microbiol.* **17**, 121–135 (1989).
12. Schäffer, C. *et al.* A pyrophosphate bridge links the pyruvate-containing secondary cell wall polymer of *Paenibacillus alvei* CCM 2051 to muramic acid. *Glycoconj. J.* **17**, 681–690 (2000).
13. Ilk, N. *et al.* Structural and Functional Analyses of the Secondary Cell Wall Polymer of *Bacillus sphaericus* CCM 2177 That Serves as an S-Layer-Specific Anchor Structural and Functional Analyses of the Secondary Cell Wall Polymer of *Bacillus sphaericus* CCM 2177 That Serv. *J. Bacteriol.* **181**, 7643–7646 (1999).
14. Mesnage, Â. & Fontaine, T. Bacterial SLH domain proteins are non-covalently anchored to the cell surface via a conserved mechanism involving wall polysaccharide pyruvylation. *Eur. Mol. Biol. Organ.* **19**, 4473–4484 (2000).
15. Cava, F., de Pedro, M. a, Schwarz, H., Henne, A. & Berenguer, J. Binding to pyruvylated compounds as an ancestral mechanism to anchor the outer envelope in primitive bacteria. *Mol. Microbiol.* **52**, 677–690 (2004).

16. May, A., Pusztahelyi, T., Hoffmann, N., Fischer, R.-J. & Bahl, H. Mutagenesis of conserved charged amino acids in SLH domains of *Thermoanaerobacterium thermosulfurigenes* EM1 affects attachment to cell wall sacculi. *Arch. Microbiol.* **185**, 263–269 (2006).
17. Janesch, B., Messner, P. & Schäffer, C. Are the Surface Layer Homology Domains Essential for Cell Surface Display and Glycosylation of the S-Layer Protein from *Paenibacillus alvei* CCM 2051T? *J. Bacteriol.* **195**, 565–575 (2013).
18. Ziegler, T., Eckhardt, E. & Herold, G. Diastereoselective Formation of Pyruvylated Glycosides Partly Protected Sugars and Methyl Pyruvate. *Tetrahedron Lett.* **33**, 4413–4416 (1992).
19. Gorin, P. A. J. & Ishikawa, T. Configuration of pyruvic acid ketals, 4,6-O-linked to D-galactose units, in bacterial and algal polysaccharides. *Can. J. Chem.* **45**, 521–532 (1967).
20. Garegg, P. J. & Lindberg, B. Preparation and N.M.R. Studies of Pyruvic Acid and Related Acetals of Pyranosides: Configuration at the Acetal Carbon Atoms. *Carbohydr. Res.* **77**, 71–78 (1979).
21. Lipták, A. & Szabó, L. Pyruvic acetal formation from a pyruvyl thioacetal, catalyzed by methyl triflate, dimethyl(methylthio)sulfonium triflate, or nitroso tetrafluoroborate. *Carbohydr. Res.* **184**, c5–c8 (1988).
22. Collins, P. M., McKinnon, A. C. & Manro, A. An Efficient Synthesis of Sugar Pyruvic Acid Acetals. *Tetrahedron Lett.* **30**, 1399–1400 (1989).
23. Jansson, P.-E., Lindberg, J. & Widhalm, G. Syntheses and NMR Studies of Pyruvic Acid 4,6-Acetals of some Methyl Hexopyranosides. *Acta Chem. Scand.* **47**, 711–715 (1993).
24. Lipták, A. & Szabó, L. Trimethylsilyl Triflate - Catalysed Acetal Formation Between Silylated Hexopyranosides and Methyl Pyruvate. *J. Carbohydr. Chem.* **8**, 629–644 (1989).
25. Schüle, G. & Ziegler, T. Efficient convergent block synthesis of a pyruvated tetrasaccharide 5-aminopentyl glycoside related to *Streptococcus pneumoniae* type 27. *Tetrahedron* **52**, 2925–2936 (1996).
26. Ziegler, T. Rhizobial saccharides 2. Selective synthesis of both diastereomers of 4,6-O-pyruvylated D-glycopyranosides. *Tetrahedron Lett.* **35**, 6857–6860 (1994).
27. Ziegler, T. Synthesis of 5-aminopentyl mono- to tri-saccharide haptens related to the species-specific glycopeptidolipids of *Mycobacterium avium-intracellulare* serovars 8 and 21. *Carbohydr. Res.* **253**, 151–166 (1994).
28. Murphy, P. V., O'Brien, J. L., Gorey-Feret, L. J. & Smith, A. B. Synthesis of novel HIV-1 protease inhibitors based on carbohydrate scaffolds. *Tetrahedron* **59**, 2259–2271 (2003).
29. Classon, B., Garegg, P. J., Oscarson, S. & Tidén, A.-K. Synthesis of an artificial antigen that corresponds to a disaccharide repeating unit of the capsular

- polysaccharide of Haemophilus influenzae type d. A facile synthesis of methyl 2-acetamido-2-deoxy- β -D-mannopyranoside. *Carbohydr. Res.* **216**, 187–196 (1992).
30. Pétursson, S. Protecting Groups in Carbohydrate Chemistry. *J. Chem. Educ.* **74**, 1297–1303 (1997).
 31. Yoneda, Y., Kawada, T., Rosenau, T. & Kosma, P. Synthesis of methyl 4'-O-methyl-13C12-beta-D-cellobioside from 13C6-D-glucose. Part 1: reaction optimization and synthesis. *Carbohydr. Res.* **340**, 2428–35 (2005).
 32. Lindhorst, T. K. *Essentials of Carbohydrate Chemistry and Biochemistry*. (Wiley-VCH Weinheim, 2003).
 33. Qin, H. & Grindley, T. B. Improvements in the Regioselectivity of Alkylation Reactions of Stannylene Acetals. *J. Carbohydr. Chem.* **15**, 95–108 (1996).
 34. Beckmann, H. S. G. & Wittmann, V. in *Organic Azides: Syntheses and Applications* 469–490 (John Wiley & Sons: Chichester, UK, 2010).
 35. Maunier, V., Boullanger, P. & Lafont, D. A One-Pot Synthesis of Glycosyl Amides from Glycosyl Azides Using a Modified Staudinger Reaction. *J. Carbohydr. Chem.* **16**, 231–235 (1997).
 36. Bosch, I., González, A., Urpí, F. & Vilarrasa, J. On the Reaction of Acyl Chlorides and Carboxylic Anhydrides with Phosphazenes. *J. Org. Chem.* **61**, 5638–5643 (1996).
 37. Ellervik, U. & Magnusson, G. Glycosylation with N-Troc-protected glycosyl donors. *Carbohydr. Res.* **280**, 251–260 (1996).
 38. Ziegler, T. Synthesis of pyruvated saccharide fragments related to the aggregation factor of the marine sponge *Microciona prolifera*. *Liebigs Ann.* **1995**, 949–955 (1995).
 39. Zemplén, G. & Pacsu, E. Über die Verseifung acetylierter Zucker und verwandter Substanzen. *Berichte der Dtsch. Chem. Gesellschaft (A B Ser.)* **62**, 1613–1614 (1929).
 40. Al-Horani, R. A. & Desai, U. R. Electronically Rich N-Substituted Tetrahydroisoquinoline 3-Carboxylic Acid Esters: Concise Synthesis and Conformational Studies. *Tetrahedron* **68**, 2027–2040 (2012).
 41. Hu, D. X., Grice, P. & Ley, S. V. Rotamers or Diastereomers? An Overlooked NMR Solution. *J. Org. Chem.* **77**, 5198–5202 (2012).
 42. Freire, E., Mayorga, O. L. & Straume, M. Isothermal Titration Calorimetry. *Anal. Chem.* **62**, 950–959 (1990).
 43. Neuhaus, D. in *eMagRes* (John Wiley & Sons, Ltd, 2007). doi:10.1002/9780470034590.emrstm0350.pub2
 44. Viegas, A., Manso, J., Nobrega, F. L. & Cabrita, E. J. Saturation-Transfer Difference (STD) NMR: A Simple and Fast Method for Ligand Screening and Characterization of Protein Binding. *J. Chem. Educ.* **88**, 990–994 (2011).
 45. Littmann, O. & Hess, K. Syntheses in the series of the tosylsugars. *Berichte der Dtsch. Chem. Gesellschaft [Abteilung] B Abhandlungen* **67B**, 519–526 (1934).

-
46. Van der Ven, J. G. M., Wijkmans, J. C. H. M., Kamerling, J. P. & Vliegthart, J. F. G. Synthesis of three tetrasaccharides containing 3-O-methyl- D-mannose , as model compounds for xylose-containing carbohydrate chains from N-glycoproteins. *Carbohydr. Res.* **253**, 121–139 (1994).
 47. Auge, J., David, S., Guibe, L. & Jugie, G. A Nuclear-Quadrupole Resonance Study of Halogen Substituted Methyl Pyranosides-Dependence of the p-Orbital Population of an Halogen at Position 2 upon the Anomeric Configuration and a Possible Correlation with Chemical-Reactivity. *Nouveau J. Chim. J. Chem.* **4**, 481–486 (1980).
 48. Kaji, E., Lichtenthaler, F. W., Nishino, T., Yamane, A. & Zen, S. Practical syntheses of immunologically relevant β -glycosides of 2-acetamido-2-deoxy-D-mannopyranose. Methyl N-acetyl- β -D-mannosaminide, N-acetyl- β -D-mannosaminyl-(1 \rightarrow 6)-D-galactose, and methyl N-acetyl- β -D-mannosaminyl-(1 \rightarrow 4)- α -D-glucopyranoside. *Bull. Chem. Soc. Jpn.* **61**, 1291–1297 (1988).

Curriculum Vitae



Personal details

Name	Gudrun MARTINZ, BSc
Date of birth	08.06.1990
E-mail	gudrun.martinz@gmail.com

Education

Oct 2012 – Feb 2015	Master studies in chemistry, University of Vienna
Mar 2014 – Feb 2015	Master thesis at the department of organic chemistry, BOKU Vienna (group of P. Kosma) <i>Synthesis of mono- and disaccharide ligands related to the secondary cell wall polymer of Paenibacillus alvei containing pyruvate-substituted β-D mannosamine residues</i>
Oct 2008 – July 2012	Bachelor studies in chemistry, Leopold-Franzens-University of Innsbruck
June 2012	Bachelor thesis at the institute of organic chemistry, LFU Innsbruck (group of R. Micura) <i>Synthesis of ^{15}N-labeled nucleosides</i>
Sept 2000 – June 2008	Secondary school in Reutte, Tyrol Graduation with distinction

Work Experience

Oct 2014 – Feb 2015	Tutor at the department of organic chemistry, BOKU Vienna
Sept 2009	Internship at Schretter & Cie in Vils, Tyrol
Jul 2008, Jul 2010, Aug 2011	Holiday jobs at Plansee SE in Reutte, Tyrol